Semiconductor Yield Modeling Using Generalized Linear Models

by

Dana Cheree Krueger

A Dissertation Presented in Partial Fulfillment
of the Requirements for the Degree
Doctor of Philosophy

Approved March 2011 by the
Graduate Supervisory Committee:

Douglas C. Montgomery, Chair
John Fowler
Rong Pan
Michele Pfund

ARIZONA STATE UNIVERSITY

May 2011

ABSTRACT

Yield is a key process performance characteristic in the capital-intensive semiconductor fabrication process. In an industry where machines cost millions of dollars and cycle times are a number of months, predicting and optimizing yield are critical to process improvement, customer satisfaction, and financial success. Semiconductor yield modeling is essential to identifying processing issues, improving quality, and meeting customer demand in the industry. However, the complicated fabrication process, the massive amount of data collected, and the number of models available make yield modeling a complex and challenging task.

This work presents modeling strategies to forecast yield using generalized linear models (GLMs) based on defect metrology data. The research is divided into three main parts. First, the data integration and aggregation necessary for model building are described, and GLMs are constructed for yield forecasting. This technique yields results at both the die and the wafer levels, outperforms existing models found in the literature based on prediction errors, and identifies significant factors that can drive process improvement. This method also allows the nested structure of the process to be considered in the model, improving predictive capabilities and violating fewer assumptions.

To account for the random sampling typically used in fabrication, the work is extended by using generalized linear mixed models (GLMMs) and a larger dataset to show the differences between batch-specific and population-averaged models in this application and how they compare to GLMs. These

results show some additional improvements in forecasting abilities under certain conditions and show the differences between the significant effects identified in the GLM and GLMM models. The effects of link functions and sample size are also examined at the die and wafer levels.

The third part of this research describes a methodology for integrating classification and regression trees (CART) with GLMs. This technique uses the terminal nodes identified in the classification tree to add predictors to a GLM. This method enables the model to consider important interaction terms in a simpler way than with the GLM alone, and provides valuable insight into the fabrication process through the combination of the tree structure and the statistical analysis of the GLM.

DEDICATION

This work is dedicated to my husband, Chad, who has encouraged me, sacrificed with me, and loved me throughout this special season of our lives together.

ACKNOWLEDGMENTS

I would first like to thank Dr. Montgomery for teaching me, mentoring me, and believing in me. Your enduring patience and gentle encouragement have been invaluable to me, both in completing this work and in my own role as a teacher and scholar. I am also thankful for the helpful contributions from my committee members Dr. Pfund, Dr. Pan, and Dr. Fowler. Your questions and comments have made me a better researcher.

I am grateful for the support of my parents, who stood behind me as I took a leap of faith and pursued this degree. Without your encouragement, I would not dare to dream, and I wouldn't appreciate the value of taking the scenic route.

I have no words to express how grateful I am to my husband, Chad, who has sacrificed so much along with me to allow me to have time to work on this dissertation. Also, many thanks to Clara who has provided a strong and very special motivation for me to finish this race.

I am also thankful for the support of my friends and colleagues who have encouraged me through this extended process. Andrea, Shilpa, Busaba, Nat, Jing, Linda, Donita, Chwen, Diane, and many others have helped me persevere.

I would also like to acknowledge the organizations that supported me financially in this research. This work was sponsored in part by NSF and SRC (DMI-0432395). Also, the support I received through the Intel Foundation Ph.D. Fellowship and ASQ's Statistics Division's Ellis R. Ott Scholarship enabled me to continue and complete this research.

Most of all, this work would not have been possible without the Lord Jesus Christ, who called me to this degree, opened unexpected doors, carried me through many challenges, and continues to be at work in my life. Your love and faithfulness amaze me. May this work and my life glorify You.

TABLE OF CONTENTS

Page

LIST OF TABLES x

LIST OF FIGURES xii

CHAPTER

1 INTRODUCTION 1

2 LITERATURE REVIEW 6

Semiconductor Yield Modeling 8

Statistical Approaches 29

3 DATA REFINING FOR MODEL BUILDING 43

Overall Description of Data 43

Process Data 44

Defectivity Data 47

Class Probe 49

Unit Probe 50

Use of the Dataset 52

Data Refining for GLM Model Building 52

Data Integration 52

Data Aggregation 53

Managing Outliers 56

4 SEMICONDUCTOR YIELD MODELING USING GENERALIZED LINEAR MODELS 58

Introduction 58

CHAPTER Page

Model Buiding Using Logistic Regression 60

Results 61

Die-Level Logistic Regression 61

Die-Level Logistic Regression Validation 66

Wafer-Level Logistic Regression 73

Wafer-Level Logistic Regression Validation 75

Summary 80

5 SEMICONDUCTOR YIELD MODELING USING GENERALIZED

LINEAR MIXED MODELS 83

Introduction 83

Data Description 85

Model Building 85

Results 88

Die-Level Model Results 88

Die-Level Model Validation 98

Wafer-Level Model Results 103

Wafer-Level Model Validation 109

Summary 114

6 SEMICONDUCTOR YIELD MODELING INTEGRATING CART

AND GENERALIZED LINEAR MODELS 118

Introduction 118

Methodology 123

CHAPTER Page

Building Trees ... 123

Creating Models ... 129

Results ... 137

Validation ... 139

Terminal Nodes and Interactions ... 146

Summary ... 151

7 CONCLUSIONS ... 153

Limitations ... 156

Future Work ... 156

References ... 160

Appendix

A SAS CODE ... 167

Biographical Sketch ... 180

LIST OF TABLES

Table Page

2.1 Relationships between negative binomial model and other models based on values for alpha 14

3.1 Process measurements in dataset 46

3.2 Description of the layers involved in defectivity scans 48

3.3 Raw data for each defect after integration 54

3.4 Aggregated data for individual dice 55

3.5 Subset of data for analysis 55

4.1 Die-level non-nested logistic regression model results for full training data set (N=2967) 63

4.2 Comparison of link functions and outlier methods 64

4.3 Existing yield models 69

4.4 Mean squared error (MSE) and mean absolute deviation (MAD) for model comparisons at the die level using test data 71

4.5 Comparison of link functions and outlier methods (wafer-level, not nested) 75

4.6 Comparison of Pearson correlation coefficients between models and actual yields using test data 79

4.7 Mean squared error (MSE) and mean absolute deviation (MAD) for model comparisons at the wafer level 80

5.1 Models analyzed for comparisons 86

5.2 Significant fixed effects for die-level GLM models from *t*-tests 89

Table Page

5.3 Significant effects for die-level GLMM models from *t*-tests 90

5.4 Die-level significant factors for GLM models using various sample sizes 95

5.5 Die-level significant factors for GLMM batch-specif models using various sample sizes (logit link function).......................................97

5.6 Die-level significant factors for GLMM population-averaged models using various sample sizes (logit link function).............................98

5.7 Significant fixed effects for wafer-level models from *t*-tests..........104

5.8 Significant effects for wafer-level models from *t*-tests (logit link).108

6.1 Die-level predictors 125

6.2 Preliminary tree building results 127

6.3 Terminal node information for Tree 3...132

6.4 Coefficients and p-values ofr GLM models 138

6.5 Recipes and classification results for terminal nodes 1, 2, 4, 5, 7, 9, and 11 147

6.6 Recipes and classification results for terminal nodes 12, 14, 15, 16, 18, 19, 22, and 24 147

6.7 Significant interaction terms and the terminal nodes that contain both factors 151

LIST OF FIGURES

Figure Page

1.1 Semiconductor manufacturing process 2

2.1 The binary tree structure of CART 25

3.1 Cross section of semiconductor device 44

3.2 X-bar and R chart for defect densities for the device studied...........46

3.3 Sampling strategies by lot for different data types.............................. 49

3.4 A wafer map 51

3.5 Summary statistics for total defects per die.. 57

4.1. Nested structure for wafers 59

4.2. Nested structure for dice 59

4.3 Residual plots for a multiple linear regression model based on the training dataset with no outliers removed 62

4.4 Predicted vs. actual yield for die-level logistic regression models...... 68

4.5 Expected probabilities of dice passing vs. number of defects per die . 70

4.6 Mean absolute deviation (MAD) and mean squared error (MSE) results comparing GLM models with other models from the literature 72

4.7 Number of dice predicted to pass compared to actual passing dice and failing dice with defects.. 73

4.8 Predicted vs. actual yield of dice with defects 78

4.9 Wafer-level yield model predictions for the test data 78

Figure Page

4.10 Mean squared error (MSE) and mean absolute deviation (MAD) measures for the nine models from the literature and the GLM models 80

5.1 Significant wafer maps comparing 30-wafer logit models 93

5.2 Significant wafer maps comparing 168-wafer complimentary log-log models 94

5.3 Mean absolute deviation (MAD) for die-level yield models 100

5.4 Mean squared error (MSE) for die-level yield models 101

5.5 Predicted vs. actual number of passing dice on a waer for the 30-wafer models using the logit link 102

5.6 Predicted vs. actual number of passing dice on a wafer of the 168-wafer models using the logit link 103

5.7 Mean absolute deviation (MAD) for wafer-level yield models 111

5.8 Mean squared error (MSE) for wafer-level models 112

5.9 Predicted vs. actual wafer yields for wafer-level historical models Y_1-Y_9 113

5.10 Predicted vs. actual wafer yields for adjusted wafer-level GLM and GLMM models 113

6.1 Preliminary tree structures using different predictors 128

6.2 Tree 3 structure 131

6.3 CART tree showing interactions between factors 135

6.4 Bottom of CART tree showing interactions between factors 136

Figure Page

6.5 Die-level MAD and MSE for model comparisons 141

6.6 Wafer-level MAD and MSE for model comparisons 141

6.7 Wafer-level predictions for test dataset using CART alone 142

6.8 Wafer-level predictions for test dataset – Main effects only 143

6.9 Wafer-level predictions for test dataset – Main effects plus CART terminal nodes 143

6.10 Wafer-level predictions for test dataset – Main effects plus CART-selected terminal nodes 144

6.11 Wafer-level predictions for test dataset – Main effects pluc interactions from CART 145

6.12 Wafer-level predictions for test dataset – Main effects plus all two-way interactions reduced model 145

6.13 Wafer map showing the radial and quadrant regions that apply to terminal nodes 1-8 from the CART tree 149

7.1 Actual and calculated yields for wafers 159

Chapter 1

INTRODUCTION

Yield is a key process performance characteristic in the capital-intensive semiconductor fabrication process. Semiconductor yield may be defined as the fraction of total input transformed into shippable output (Cunningham, Spanos, & Voros, 1995). Hu (2009) points out that yield analysis usually has two purposes: to determine the root cause of yield loss and to build accurate models to predict yield. From a manufacturing viewpoint, it is also extremely important to predict yield impact based on in-line inspections (Nurani, Strojwas, Maly, Ouyang, Shindo, Akella, et al. (1998). In an industry where machines cost millions of dollars and cycle times are a number of months, predicting and optimizing yield are critical to process improvement, customer satisfaction, and financial success.

Since the 1960s, semiconductor yield models have been used in the planning, optimization, and control of the fabrication process (Stapper, 1989). A comprehensive review of these methods is given by Kumar, Kennedy, Gildersleeve, Albeson, Mastrangelo, and Montgomery (2006). Many of these methods focus on using defect metrology information, sometimes referred to as *defectivity* data, to predict yield. While several other measurements, such as critical dimensions and electrical tests, are taken as wafers are fabricated, defectivity data seem to be the most influential in current yield modeling practice.

Defectivity measures come from a wafer-surface scan that identifies unusual patterns such as particles, scratches, or pattern defects. These scans are performed after different layers of the wafer have completed processing (see

Figure 1). The scans are time consuming, so only a few wafers are sampled to monitor the process and to predict yield. Several types of data may be recorded for each defect, including the die the defect appears on, the size of the defect, and the location of the defect on the die. In addition, a sample of the defects is often selected for classification based on SEM images.

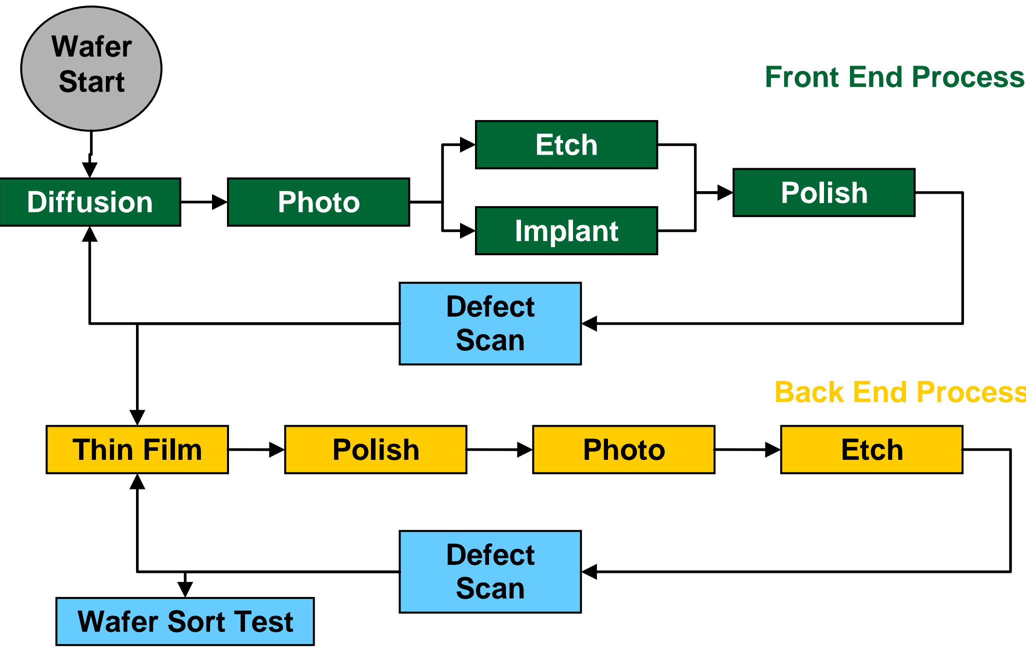

Figure 1. Semiconductor manufacturing process. The semiconductor manufacturing process involves a series of steps that are repeated for each layer. Defect scans are often done following each layer's processing, and wafer sort testing is performed when the chips have completed processing.

Another type of test is performed at *wafer sort*. At this stage, the wafers have completed the fabrication process, and each die on the wafer is tested for functionality. Dice that pass this test move on to be assembled and packaged before a final test is performed and the good product is shipped to the customer. At wafer sort, the dice are grouped into bins. Passing dice are placed into one bin,

while failing dice are separated by their failure modes into a number of different bins.

One of the challenges of working with semiconductor measurements is the size of the massive datasets available with computer-aided manufacturing. While these data record many important process parameters and test results, integrating them into a usable form is a considerable problem. Often, process data from tools are stored in one database, defectivity data in another database, and electrical and wafer sort data in yet a third database. Obtaining a dataset that contains defectivity data and the corresponding wafer sort data can require skilled knowledge of two different systems and the ability to query in both. Aggregating the data into a more useable form for model building is also a time-consuming task.

Another challenge is developing an adequate yield model. Yield models in the literature that use defect metrology data have neglected to properly account for the nested structure of the data and have assumed independence among the data. Dice are grouped together on wafers, and wafers are processed together as lots, making this assumption questionable at best. The yield models in the literature have overlooked this potential source of variation. Also, most current modeling is done at the wafer level, which loses the vast amounts of information available at the die level. In industry, many companies develop their own proprietary yield models that are not available in published literature. Some of the most common methodologies used for these models include employing classical linear regression and tree-based classification using various predictors.

Additional approaches used to predict yield and improve processing include using kill ratios (Lorenzo, Oter, Cruceta, Valtuena, Gonzalez, & Mata, 1999; Yeh, Chen, & Chen, 2007), using unified defect and parametric data (Burglund, 1996) and using process and parametric data in a hierarchical generalized linear model (GLM) (Kumar, 2006). Defectivity data have also been used to identify gross failures due to clusters of defects. Spatial filters (Wang, 2008) and tests for spatial randomness (Fellows, Mastrangelo, & White, Jr., 2009) have been developed to help identify non-random clusters. Supervised learning can also be beneficial, as shown by Skinner, Montgomery, Runger, Fowler, McCarville, Rhoads, et al. (2002) and Hu (2009), for yield models that use parametric data as predictors. Classification and regression tree (CART) techniques are recommended as a means to develop a "best path" to high-yield outputs and a path to avoid for low-yield outcomes (Skinner, et al., 2002). However, the predictive power of CART models is limited (Hu, 2009) and can have limitations due to the process parameters data not being available at the same time and due to the process and design interactions that are not considered in this approach (Bergeret & Le Gall, 2003).

The literature suggests GLMs have not been applied to model semiconductor yield from defectivity data, yet this approach is appealing because GLMs are most appropriate for response data that follow a distribution in the exponential family (i.e. binomial or Poisson) and can handle the nested data structure and the die-level data (Montgomery, Peck, & Vining, 2006).

The purpose of this dissertation is to present a modeling strategy that guides practitioners to develop die- and wafer-level GLM- or generalized linear mixed model (GLMM)-based yield models using defect metrology data. An example using real semiconductor yield data is presented that illustrates the strengths of this approach in comparison to other yield models. This work also explores the effects of outliers on GLM models and the impact of using nested models at the die level, the differences between die- and wafer- level modeling, the differences between population-averaged and batch-specific random effects modeling, and the impact of integrating CART methods with logistic regression. These GLM models can be applied to determine which process steps are significant, to identify specific wafers or locations on wafers that warrant further investigation for improvements, and to predict future yields based on intermediate data, thus fulfilling the two purposes of yield analysis mentioned by Hu (2009) with a strategy that is easy for practitioners to use and implement.

This work is organized by first presenting a review of the literature in Chapter 2 and by describing the data and the methods used to develop a useful dataset for modeling in Chapter 3. Chapter 4 shows the results of applying GLMs to model these yield data. Chapter 5 considers random effects by applying GLMM techniques and showing differences between population-averaged and batch-specific approaches. Chapter 6 discusses a methodology of integrating CART techniques with those of logistic regression for improved models. The conclusions are presented in Chapter 7 along with recommendations for future work.

Chapter 2

LITERATURE REVIEW

While there are many measures of process performance, the number one index of success in the industry is yield (J. A. Cunningham, 1990). There is some skepticism amongst practitioners when it comes to yield modeling techniques; still, their usefulness in the planning, optimization, and control of semiconductor fabrication cannot be overlooked (Stapper, 1989). As improving productivity and cost effectiveness in the industry become more critical with increasing market competition, improving productivity and cost effectiveness is vital (Nag, Maly, & Jacobs, 1998).

There are many challenges in creating a reasonable yield model. One of these is utilizing the massive datasets available with computer-aided manufacturing. Process parameters are constantly being recorded for each layer of fabrication. Defects are found and classified at each layer as well. Electrical test data and bin sort counts are also recorded, usually all in different databases. Since ownership of these data collection tools is usually segmented, the integration of the many types of data is no small task (Braun, 2002). Other challenges arise with computational complexity of the models and with ensuring the assumptions made in yield formulas accurately represent the process.

Despite the challenges, yield models have the opportunity to reap large rewards for semiconductor manufacturers. Dance & Jarvis (1992) state that implementing yield models has "made it possible for process engineers to quantify their own process sector's influence on [electrical] test yield" (p. 42).

Instead of waiting months to get final test results, the model can be used to insure process improvement. This is possible when the yield models are linked with statistical process control methods, driving process improvement (Dance & Jarvis, 1992).

Yield models are an important part of yield learning, which consists of eliminating one source of faults after another until an overwhelming portion of manufactured units function according to specification (Weber, 2004). Yield learning is especially important as new products start up. Companies must maximize yield as early as possible while still releasing a product before competitors launch. Weber (2004) states that the yield-learning rate tends to be the most significant contributor to profitability in the semiconductor industry. If the yield-learning ramp could be improved by six months, the cumulative net profit would more than double; if the yield ramp is delayed by six months, two-thirds of the profit is eliminated (Weber, 2004).

According to Nag et al. (1998), the yield learning rate depends on the relationship between particles, defects, and faults and the ease of defect localization that in turn depends on the following:

1. Size, layer and type of defect
2. Ability to analyze the IC design
3. Probability of occurrence of catastrophic events
4. The effectiveness of the corrective actions performed
5. The timing of each of the events mentioned
6. The rate of wafer movement through the process (p. 164).

Because yield models reflect the relationships between particles, defects, and faults, they are important tools in yield learning and, consequently, profitability.

Semiconductor Yield Modeling

Many different yield models have been developed and used since the 1960s. Stapper (1989) provided a history of many of these models, and Kumar, et al. (2006) also briefly discussed historical models before expanding the discussion to more recent models. In understanding the changes in yield modeling throughout the years, it is valuable to observe how yield modeling began and how it has changed to better account for the rapidly-changing semiconductor fabrication processes. This review will also demonstrate that, while advances are still being made, improved models that utilize the vast amount of data available and provide decision rules early in the process have not yet been developed.

Initial Yield Models

As Wallmark (1960) examined the effects of shrinkage in integrated circuits, he calculated yield using

$$Y_i = (1 - S/100)^N \qquad (2.1)$$

for an *N*-stage device that has shrinkage such that *S* out of every 100 stages cannot be used. Wallmark used this result in a binomial distribution to estimate yield of an integrated circuit (IC) with redundant transistors. While this model

became inappropriate in later years as the interconnect wiring evolved from repairable methods to IC methods because this yield loss was not considered in the model, Wallmark was the first to model the IC yield of circuits with fault tolerance (Stapper, 1989).

Hofstein and Heiman also examined the problems of yield and tolerance. They observed the primary failure mechanism at the time to be a faulty gate insulator, likely caused by pinholes in the oxide layer that led to a short circuit (Hofstein & Heiman, 1963). Assuming the oxide defects were randomly distributed on the surface of the silicon crystal and that the area of the pinhole was much smaller than the area of the gate electrodes, they used the Poisson model to predict yield for a device with *N* transistors,

$$Y = e^{-N(A_G D)} \tag{2.2}$$

where A_G is the active area of the gate in each transistor and *D* is the average surface density of the defects. While later work showed the assumptions used in this model to be incorrect, the relationship between defects and gate area has been useful as yield models evolve with the complexity of the process.

Murphy's Yield Model

Murphy (1964) constructed a yield model that accounted for variations in defect densities from wafer to wafer and die to die. Using *f(D)* as the normalized

distribution function of dice in defect densities, Murphy proposed the overall device yield to be

$$Y = \int_0^\infty e^{-DA} f(D) dD \tag{2.3}$$

where D is again the density of defects per unit area, and A is the susceptible area of the device. Murphy observed that distribution was bell-shaped, but due to the variation expected with the distribution from production line to production line, he used the triangular distribution as an approximation to simplify the calculations,

$$Y = \left(\frac{1 - e^{-D_0 A}}{D_0 A} \right)^2 \tag{2.4}$$

where D_0 is the mean defect density. This equation assumed that only one type of spot defect occurred. Murphy (1964) noted this limitation, knowing that the occurrence of different types of defects may or may not be independent.

The defect density distribution, *f(D),* later became known as a compounder or mixing function with the yield formula being referred to as a compound or mixed Poisson yield model (Stapper, 1989).

Seeds' Yield Formula

Seeds (1967), like Murphy, also assumed that the defect densities vary from wafer to wafer and from die to die. He used the exponential distribution to model defect densities where $f(D) = e^{-D/D_0} / D_0$ and produced the yield formula

$$Y = \frac{1}{1 + D_0 A} . \tag{2.5}$$

Seeds' method of determining yield for blocks of chips has since come to be known as the window method, where an overlay of windows is made for each set of chip multiples. The number of defect-free windows is counted and the yield determined for each window size (Stapper, 1989).

Seeds' data confirmed Murphy's predictions, but showed that Murphy's yield formula underestimated the yield due to the larger standard deviation in the triangular distribution.

Dingwall's Model

In 1968, A. G. F. Dingwall (as cited by Cunningham, 1990) presented a yield model in the form

$$Y = \left[1 + D_0 A / 3\right]^{-3} . \tag{2.6}$$

Moore's Model

Moore (as cited by Cunningham, 1990) published a yield model that he claimed was most representative of Intel's processing in the form of

$$Y = e^{-\sqrt{D_0 A}}. \tag{2.7}$$

Cunningham (1990) compares several of these models and concluded Moore's and Seeds' models can be grossly inaccurate.

Price's Model

Price (1970) criticized prior models that used an initial model that predicted yield falling off exponentially as circuit area increased, stating that this decay was less than exponential. Price argued the previous use of Boltzmann statistics, considering all spot defects to be distinguishable was inappropriate. He proposed using Bose-Einstein statistics to first derive Seeds' model and then for r independent defect-producing mechanisms having defect densities $D_1, D_2, \ldots, D_r$ modeled yield as

$$Y = \frac{(1-1/N)^r}{(1+AD_1-1/N)(1+AD_2-1/N)\cdots(1+AD_r-1/N)}. \tag{2.8}$$

Price stated the experimental measurement of defect densities due to a single defect-producing mechanism was made more tractable with this model.

While this approach was used in practice for a time, the assumption that the defects are indistinguishable was found to be inappropriate for IC fabrication. Murphy (1971) pointed out Price's error lay in confusing the highly specialized quantum mechanics terms "distinguishable" and "particle" with their everyday usage. In general, when defects are counted, they are distinguishable (Stapper, 1989). Price's model has not stood the test of time and has not been developed further.

Okabe's Model

Okabe, Nagata, and Shimada (1972) proposed a model that took into account different processing steps, assuming that critical areas and defect densities were the same for all layers. For a process with n process steps, the model had the form

$$Y = \frac{1}{(1 + D_0 A / n)^n} \tag{2.9}$$

and was derived from Murphy's model using the Erlang distribution for the compounder.

Negative Binomial Yield Model

The negative binomial yield model was the first model to consider defect clustering. This model is also derived from Murphy's but uses the gamma distribution as the compounder. This produces

$$Y = (1 + AD/\alpha)^{-\alpha} \tag{2.10}$$

where α is a parameter related to the coefficient of variation of the gamma distribution that is a rational number greater than zero (Stapper, 1989). Stapper (1976) was one of the first to consider defect clustering. The negative binomial model's parameter α was used to represent a clustering parameter. The negative binomial model has been used extensively, though when severe clustering is present, the formula becomes inadequate (Stapper, 1989).

Another concern with the negative binomial model is how α should be determined. Cunningham (1990) relates values of α to different levels of clustering and connects them to other yield models. This is shown in Table 2.

Table 2.1. *Relationships between negative binomial model and other models based on values for alpha*.

Clustering	Value of α	Yield Model
None	About 10 to ∞	Poisson
Some	4.2	Murphy
Some	3	Dingwall
Much	1	Seeds

If the company has similar, mature products, α may be determined by curve fitting for that factory environment. For different or new products, Cunningham (1990) describes a method for determining α, but the approach is not straight forward. Cunningham (1990) gives a formula for calculating α, as

$$\alpha = \frac{\bar{\lambda}}{\sigma^2 - \bar{\lambda}} \tag{2.11}$$

where $\bar{\lambda}$ is the mean of the number of defects per die, and σ^2 is the variance, but he mentions that this calculation can yield results that are quite scattered and sometimes negative. Cunningham describes how α may be determined using the defects on the wafers by using surface particle maps and an overlaid grid of different sizes. Using averages of defect densities from these grids, Cunningham (1990) proposed using

$$\alpha = \left(\bar{\lambda} / \sigma\right)^2_{avg} \frac{1}{1 - \bar{\lambda}_{avg} / \sigma^2}. \tag{2.12}$$

This approach does not always give positive values either, though, and produces different calculated values for α for the different grids.

Poisson Mixture Yield Models

Reghavachari, Srinivasan, and Sullo (1997) developed the Poisson-Rayleigh and Poisson-inverse Gaussian models furthering the expansion of Murphy's model. With the Poisson-Rayleigh model, they investigate the special case of using a Weibull distribution with $\alpha=2$. This results in the yield model

$$Y = 1 - AD_0 \exp\left[\left(AD_0\right)^2 / \pi\right] erfc\left(AD_0 / \pi^{1/2}\right) \tag{2.13}$$

Using the inverse-Gaussian distribution, Reghavachari, et al. (1997) constructed the Poisson-inverse Gaussian mixture yield model of

$$Y = L_A(A) = \exp\left(\phi\left[1 - \left(1 + \frac{2AD_0}{\phi}\right)^{1/2}\right]\right) \tag{2.14}$$

where ϕ is a shape parameter and D_0 is a scale parameter. In comparisons with other mixing distributions, such as the exponential, half Gaussian, triangular, degenerate and gamma, Reghavachari, et al. (1997) showed the Poisson-gamma (negative binomial yield model) and the Poisson-inverse Gaussian mixtures are sufficiently robust to emulate all the other models, supporting the prevalent use of the negative binomial model. Reghavachari, et al. (1997) point out the limitations of these models through a discussion on the impact of reference regions used in the models, which may be chip die areas, specific regions within wafers such as

groups of chip areas, entire wafers, or even batches of wafers. They show these models are not sufficient to completely characterize the spatial patterns of defects generated and that different specifications of such regions lead to different levels of aggregations in the spatial distribution of defects, which must be well understood to properly estimate the parameters of the model and to obtain good results.

Clustering and Critical Area Analysis

The type, size, and arrangement of defects have played a part in more recent yield models and process-improvement efforts. Nahar (1993) points out that defects may be classified into one of three categories. Point defects include oxide pinholes, isolated particles, or process-induced defects. Line defects can be scratches, step lines, or other defects that have high length-to-width ratios. Area defects are a third category and include misalignment, stains, and wafer cleaning problems. Kuo and Kim (1999) indicate it is useful to classify defects as random or nonrandom. Random defects occur by chance, such as shorts and opens or local crystal defects. Nonrandom defects include gross defects and parametric defects.

These different classifications of defects support the development of models that take into account clustering in methods different from the negative binomial model in Equation 2.10. Clusters of defects can be, in general, classified as either particle or process related, with particle-related clusters being assignable to individual machines and process-related clusters being attributable to one or

more process steps not meeting specification requirements (Hansen, Nair, & Friedman, 1997; Fellows, Mastrangelo, & White, Jr., 2009). Hansen, Nair, and Friedman (1997) developed methods for routinely monitoring wafer-map data to detect significant spatially clustered defects that are of interest in yield prediction and process improvement. White, Jr., Kundu, and Mastrangelo (2008) show how the Hough transformation can be used to automatically detect such defect clusters as stripes, horizontal and vertical scratches, and diagonal scratches at 45° and 135° from the horizontal. This technique also works well to detect defect patterns such as scratches at arbitrary angles, center defects, and edge defects, but is not useful in detecting defect clusters that cannot be so characterized, such as ring defects. Fellows, Mastrangelo, and White, Jr. (2009) compare a spatially homogeneous Bernoulli process (SHBP) and a Markov random field (MRF) for testing the randomness of defects on a wafer. Wang (2008) proposes an approach that applies a spatial filter to the defect scan data, then uses kernel eigen-decomposition of the affinity matrix for systematic components to determine the number of clusters embedded in the dataset. Spectral clustering is applied to group the data in a high-dimensional kernel space before a decision tree is used to generate the final classification results. These detections techniques have not yet been incorporated into formal yield models and are more applicable currently in process improvement and problem solving in the fab.

The size and location of defects is considered in critical area analysis. Zhou, Ross, Vickery, Metteer, Gross, and Verret (2002) discuss using critical area analysis (CAA) to help quantify how susceptible a device may be to particle

defects. The critical area of a die is described as the area where, if the center of a particle of a given size lands, the die will fail. (See Stapper, 1989, for a helpful illustration.) The probability of failure depends on the defect size, the layout feature density, and the failure modes, such as short or open (Zhou, et al., 2002). There is a unique critical area for each defect size and for each layer in the die (Nurani, et al., 1998). Yield is estimated by using a generalized Poisson-based model, given as

$$Y = \prod_{i=1}^{N} \exp - \left(\int_0^{\infty} D_i \cdot A_i^{crit}[R] \cdot f_i[R] \cdot dR \right) \qquad (2.15)$$

where i is the layer index, N is the number of layers, R is the defect radius, D is the defect density, and $A^{crit}[R], f[R]$ are the critical area and the defect size probability density functions of the defect radius, respectively (Nurani, et al., 1998).

Zhou, et al. (2002) describe the unique benefits of this approach due to it allowing factory planners to anticipate yields for a new product more precisely than the simple estimation using die area and defect density. This approach requires much information, though. The architecture of the device must be known and assessed as to what size of defects may cause faults in the various layers. The defect size distribution, while widely believed to be of $1/x^3$ type for smaller defects (Stapper, Armstrong, & Saji, 1983) is variable (Stapper & Rosner, 1995) and must be known or estimated. Scaling must be done to manipulate the critical

area as suggested by Zhou, et al. (2002). Defect types may need to be considered for different yield impacts (Nurani, et al., 1998), and all failure modes may not be considered. Thus, this modeling approach is complex and limiting.

Kill Ratios

Defect type and size can be used to determine a measure called a kill ratio which is also used in industry to estimate yield and to enable engineers to find processing problems. Kill ratios link defectivity data and unit probe data. Lorenzo, et al. (1999) define a kill ratio as bad chips with one defect divided by the sum of bad chips with one defect and good chips with one defect. Kill ratios can be used whether assuming the visual defects are randomly distributed on a wafer or assuming the presence of defect clustering (Yeh, Chen, Wu, & Chen, 2007). These ratios have been praised for their impact in providing trend charts of "dead chips," in identifying "losing layers" of processing, and in examining yield losses for a single wafer (Lorenzo, et al., 1999).

A limitation with kill ratios is they, like many of the yield models that rely only on defect data, only consider cosmetic defects while other problems can also lead to failure. They also do not consider the impact of a die having multiple defects or where the defects occur in the process. Another drawback is that as process technologies change, defect densities and their yield impact also change, so kill-ratios must be regenerated for each new product generation (Nurani, et al., 1998).

Unified Defect and Parametric Model

As the semiconductor industry moves to smaller design rules, process parameter variations now cause significant and functional yield problems (Braun, 2002). Parametric yield loss problems also dominate over defect-related yield, particularly during the early start-up phase of a new process (Berglund, 1996). This suggests both defect management and parametric control are necessary for effective yield management, rather than a single focus on defect problems. In prior models, a constant multiplier, called the area usage factor (AUF), has been used to account for parametric defects (Ham, 1978). This model is given by

$$Y = Y_0 \int f(D) e^{-AD} dD \qquad (2.16)$$

or can also be used presented using the negative-binomial model:

$$Y = Y_0 (1 + D_0 A / \alpha)^{-\alpha}. \qquad (2.17)$$

Berglund (1996) suggests the assumption of a die-size-independent area usage factor fails to accommodate the die-size dependence of the total failure area. He takes the parametric data into consideration in the formula where L is length of the die, W is width of the die, D_0 is the mean defect density and s is the defect size

$$Y = \exp\{-LWD_0\} \cdot \exp\{-D_0((L+W)s_0 + (\pi/2)s_0^2\}\,. \tag{2.18}$$

This two-parameter model is easier to use for analysis and provides good agreement with the data. It is also applicable to both point defect yield problems as well as combinations of defects, larger size defects, and parametric yield limiters (Berglund, 1996).

Hierarchical Generalized Linear Yield Model

Kumar (2006) focuses on process and parametric data to introduce the concept of using a hierarchical generalized linear model (hGLM) approach to model yield in the form of bin counts. To overcome the problems of infeasibility of using all process and test variables in a model, Kumar (2006) proposes to break the system into smaller, more manageable subprocess models, estimate the key characteristics for each subprocess, and combine all the information to estimate the higher-level key performance characteristics, such as yield. The subprocess modeling is begun by exploratory data analysis, by discussions with process experts in the industry, and by review of process reports. The relationships between the key subprocess and the in-line electrical (or parametric) test are modeled. These submodels are then combined into a metamodel that is used to estimate bin count. Kumar (2006) shows the expected value and variance of the parameters associated with the submodels and with the metamodel are unbiased when the submodels are assumed to be orthogonal to each other. These are also unbiased under the independence assumption. His results also show that the

expected bias or residual in the metamodel is reduced with each additional inclusion of an independent submodel. The use of the metamodel shows better results than using the parametric data alone to model yield.

This work was expanded by Chang (2010) to make it more general and applicable, using GLMs rather than assuming normality as Kumar (2006) did. Chang (2010) also proposed a method that does not require orthogonality, expanding the application to those beyond designed experiments and develops a model selection technique based on information criterion to find the best sub-process for the intermediate variables.

Before this hGLM method was introduced, all yield models have included defect data in their calculations. However, Kumar (2006) and Chang (2010) don't include this element in their models, relying on process data and parametric data to make the prediction. Chang (2010) indicates that defectivity data were not included in the model due to the small number of lots available that had defectivity, parametric, and process data available for the hGLM. Still, the use of the process data introduces the ability for practitioners to make decisions regarding continued processing given low yield probabilities much sooner, enabling savings of time and money (Cunningham et al., 1995).

Classification and Regression Trees (CART)

Skinner, et al. (2002) examine modeling and analysis of wafer probe data using parametric electrical tests as predictors by applying traditional statistical approaches, such as clustering and principal components and regression-based

methods, and introducing the application of classification and regression trees (CART). CART produces a decision tree built by recursive partitioning with predictor variables being used to split the data points into regions with similar responses, allowing the modeler to approximate more general response surfaces than standard regression methods (Skinner, et al., 2002). While CART did not provide a more accurate prediction than the regression methods used in the study, the model is easier to interpret and can provide a "recipe" for both high-yield and low-yield situations, which are some of its prime advantages (Skinner, et al., 2002).

Data mining has also been used in other areas of the semiconductor industry. Hu (2009) uses CART to detect the source of yield variation from electrical test parameters and equipment, and Braha and Shmilovici (2002) use data mining techniques to improve a cleaning process that removes micro-contaminants.

Data mining can be defined as an activity of extracting information from observational databases, wherein the goal is to discover hidden facts (Anderson, Hill, & Mitchell, 2002). Some of the advantages of the CART method are that this approach does not contain distribution assumptions and that these trees can handle data with fewer observations than input variables. CART is also robust to outliers and can handle missing values (Anderson, et al., 2002). It can be used effectively as an exploratory tool (Hu, 2009), which is of considerable interest when dealing with such large datasets. The goal with CART is to minimize

model deviance and to maximize node purity without over-fitting the model (Skinner, et al., 2002).

Method.

Figure 2.1 illustrates the binary tree structure used in CART. Binary recursive partitioning splits the dataset into nodes. After split 1 is done, the data are divided into two nodes, x_2 and x_3 in Figure 2.1. The data in these nodes continue to be split into subsequent nodes until terminal nodes are formed. Terminal nodes are shown by the boxes in Figure 2.1 and are denoted by T_i.

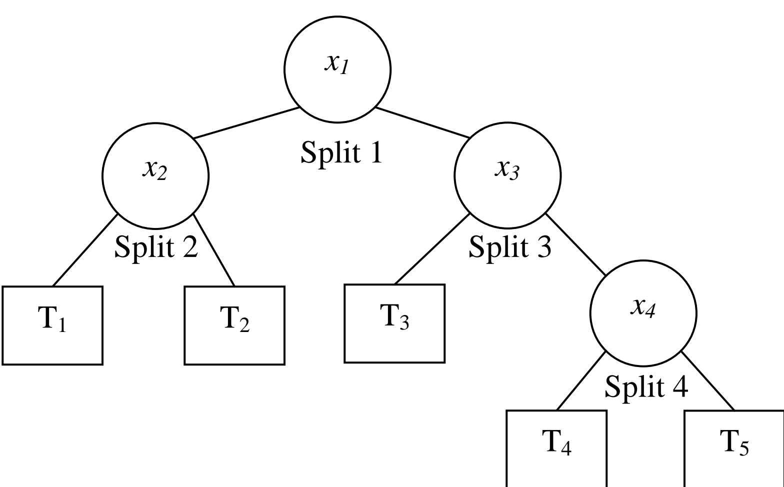

Figure 2.1. The binary tree structure of CART. This structure consists of nodes that continue to be split until terminal nodes are formed.

The entire construction of a CART decision tree revolves around three elements. These include the section of the splits, the decision of when to declare a node terminal or to continue splitting it, and the assignment of each terminal node to a class (Breiman, Friedman, Olshen, and Stone, 1984). Good splits are

defined by their purity. The impurity of a node for a classification tree can be defined as

$$i(t) = \Phi\left(p(1|t), p(2|t), ..., p(j|t)\right) \qquad (2.19)$$

where $i(t)$ is a measure of impurity of node t, $p(j/t)$ is the node proportions (e.g., the cases in node t belonging to a certain class j), and Φ is a non-negative function (Brieman, et al., 1984). The measure of node impurity by the Gini index of diversity (Brieman, et al., 1984) is defined as

$$i(t) = \sum_{j \neq i} p(i|t)\, p(j|t)\,. \qquad (2.20)$$

This Gini method is the default for CART 5.0 (CART for Windows user's guide (Version 5.0), 2002). Other splitting criteria have been developed and used and are described in depth in Brieman, et al. (1984).

Terminal nodes are created when there is no significant decrease in impurity by splitting the node. This is measured by

$$\Delta i(s,t) = i(t) - p_R i(t_R) - p_L i(t_L) \qquad (2.21)$$

where s is a candidate split, and p_R and p_L are the proportions of observations of the parent node t that go to the child node t_R and t_L, respectively (Chang & Chen, 2005). The best splitter is one that maximizes $\Delta i(s,t)$.

Once a tree is "grown," the next step is to prune the tree. This creates a sequence of simpler trees. This process begins with the saturated tree with very few observations in each terminal node and, selectively pruning upward, produces a sequence of sub-trees until the tree eventually collapses to the tree off the root node (Chang & Chen, 2005). This pruning is done to guard against overfitting (Brown, Pittard, & Park, 1996). Overfitting occurs when the decision tree constructed classifies the training examples perfectly, but fails to accurately classify new unseen instances (Braha & Shmilovici, 2002). Pruning relies on a complexity parameter which can be calculated through a cost function of the misclassification of the data and the size of the tree (Chang & Chen, 2005). To determine this cost-complexity parameter, first, the misclassification cost for a node and a tree must be determined. The node misclassification cost can be defined as

$$r(t) = 1 - p(j \mid t) \tag{2.22}$$

and the tree misclassification cost can be defined as

$$R(T) = \sum_{r \in T} r(t)\, p(t) \tag{2.23}$$

The cost-complexity measure for each subtree T, $R_\alpha(T)$, can be defined, then, as

$$R_\alpha(T) = R(T) + \alpha\,|\tilde{T}| \qquad (2.24)$$

Where $|\tilde{T}|$ is the tree complexity, which is equal to the number of terminal nodes of the subtree, and α is the complexity parameter which measures how much additional accuracy is added to the tree to warrant additional complexity (Chang & Chen, 2005). Alpha varies between 0 and 1, and by gradually increasing this parameter, the smaller $|\tilde{T}|$ becomes to minimize $R_\alpha(T)$, and a sequence of pruned subtrees is generated (Chang & Chen, 2005).

To choose the best pruned tree that avoids overfitting, cross-validation is conducted. This may be done by using techniques such as resubstitution, test sample estimation, V-fold cross validation, or N-fold cross-validation (Brieman, et al., 1984).

Other Applications.

CART has been used to model a variety of data in applications. Khoshgoftaar and Allen (2002) apply CART to predicting fault-prone software modules in embedded systems, and Khoshgoftaar and Seliya (2003) compare two CART models with other approaches for modeling software quality. Neagu and Hoerl (2005) use CART methods to define a “yellow zone” for predicting corporate defaults. Scheetz, Zhang, and Kolassa (2009) apply classification trees

to identify severe and moderate vehicular injuries, and Chang and Chen (2005) use tree-based data mining models to analyze freeway accident frequencies in Taiwan. CART is commonly applied to medical studies as well. For example, Kurt, Ture, and Kurum (2008) use CART to predict coronary heart disease, and Ture, Kurt, Kurum, and Ozdamar (2005) use this approach to predict hypertension. These two papers show how the decision tree structure of CART is similar to medical reasoning and how it can be used to complement statistical approaches such as logistic regression.

Statistical Approaches

Though many yield models have been introduced over the last five decades, there is still a need for a model that can accurately model yield for a semiconductor process for both purposes of process improvement and of forecasting yield. The assumptions made in these past models are not generally valid, and the complexity of some approaches and the data required can also be limiting factors. An approach is needed that examines the impact of a defect being located on a specific processing layer to help detect significant yield impacts for those layers. Also, these models of the past do not model yield at the die level, losing much of the information that is captured during expensive defect scans, and forcing modelers to use average defect densities across wafers or lots. The past models also do not consider the nested structure of the process, where dice are fabricated together on wafers, and wafers are processed together in lots.

In addition, interactions between various factors are not considered, such as considering the impact of having a defect on a die on multiple layers. For additional discussion of the assumptions made in yield models, see Ferris-Prabhu (1992). Statistical approaches, such as using regression techniques, offer a solution for these problems. Ordinary least squares (OLS) regression, GLMs, and GLMMs are described in this section.

Ordinary Least Squares Regression

For response data that are normally distributed, linear regression models often fit well. These models are in the form

$$y = \beta_0 + \beta_1 x_1 + ... + \beta_p x_p + \varepsilon \tag{2.25}$$

The coefficients, $\beta_0,\ \beta_1,\ \ldots\beta_p$, are estimated using the method of least squares. These models assume the residuals to be normally distributed with mean equal to zero and constant variance as well as independence between the observations. If these assumptions are violated, the model is not adequate (Montgomery, Peck & Vining, 2006).

Generalized Linear Models (GLMs)

Due to the non-normality of the pass/fail response variable for yield, techniques such as ordinary least squares regression are not adequate for semiconductor yield models. To properly model a non-normal response whose

distribution is a member of the exponential family, generalized linear models may be successfully employed. The exponential family includes the normal, Poisson, binomial, exponential, and gamma distributions.

Generalized linear models (GLMs) were introduced by Nelder and Wedderburn (1972). They combined the systematic and random (error) components of a model characterized by a dependent variable, a set of independent variables, and a linking function. The systematic component is the linear predictor part of the model, the random component is the response variable distribution (or error structure), and the link function between them defines the relationship between the mean of the *i*th observation and its linear predictor (Skinner, et al., 2002). This approach uses the maximum likelihood equations, which are solved using an iterative weighted least squares procedure (Nelder and Wedderburn, 1972). GLMs provide an alternative to data transformation methods when the assumptions of normality and constant variance are not satisfied (Montgomery, Peck, & Vining, 2006). One of the most commonly used generalized linear models is logistic regression.

Logistic regression accounts for cases that have a binomial response, such as proportion or pass/fail data. The logistic model for the mean response $E(y)$ is given by

$$E(y) = \frac{1}{1+e^{-\mathbf{x}'_i \boldsymbol{\beta}}} = \frac{1}{1+e^{-(\beta_0+\beta_1 x_1+\ldots+\beta_p x_p)}} \,. \qquad (2.26)$$

The parameters are estimated using maximum likelihood.

There are three links commonly used in logistic regression models: the logit, the probit, and the complimentary log-log links. These are expressed as

Logit $$E(y) = \frac{\exp(\mathbf{x}'\boldsymbol{\beta})}{1+\exp(\mathbf{x}'\boldsymbol{\beta})} = \frac{1}{1+\exp(-\mathbf{x}'\boldsymbol{\beta})} \quad (2.27)$$

Probit $$E(y) = \Phi(\mathbf{x}'\boldsymbol{\beta}) \quad (2.28)$$

Complimentary Log-Log $$E(y) = 1-\exp[-\exp(\mathbf{x}'\boldsymbol{\beta})]. \quad (2.29)$$

For the logit link, odds ratios are calculated that aid interpretation of the predictors. The odds ratio can be interpreted as the estimated increase in the probability of success associated with a one-unit change in the value of the predictor variable (Montgomery, Peck, & Vining, 2006). Odds ratios are calculated for each predictor by

$$\hat{O}_R = \frac{odds_{x_i+1}}{odds_{x_i}} = e^{\hat{\beta}_i} \quad (2.30)$$

where $\hat{O}_R$ is the odds ratio for the predictor variable being examined, and $\hat{\beta}_i$ is the coefficient in the model corresponding to the predictor variable. For example,

if a model predicting failing dice has $\mathbf{x}'\boldsymbol{\beta} = 2.46 + 0.985x_{defects}$, an increase of one defect will have an impact of an increased probability of failing dice of exp(0.985) = 2.678. These ratios are not calculated for the probit or complimentary log-log links.

For each of the link functions, the significance of individual regressors is determined using Wald inference, which yields *z*-statistics and *p*-values similar to the *t*-tests done in linear regression to test

$$H_0 : \beta_j = 0 \tag{2.31}$$

$$H_1 : \beta_j \neq 0 \tag{2.32}$$

.

Model adequacy is determined by goodness-of-fit tests. Three statistics are often used: the Pearson χ^2, Deviance, and the Hosmer-Lemeshow values. Deviance can also be used to evaluate possible overdispersion, which can underestimate regressors' standard errors. For more on the theory and application of logistic regression models, see McCullagh and Nelder (1989), Hosmer and Lemeshow (2000), and Myers, Montgomery, Vining, and Robinson (2010).

Logistic regression is used more often than any other member in the family of generalized linear models with wide applications to biomedical, business management, biological, and industrial problems. GLMs have also been applied to design experiments with non-normal responses (Lewis, Montgomery,

& Myers, 2001), to monitor multi-stage processes (Jearkpaporn, Borror, Runger, & Montgomery, 2007) and to analyze reliability data (Lee & Pan, 2010). Software packages such as Minitab and JMP simplify developing such models.

Generalized Linear Mixed Models (GLMMs)

One of the assumptions with GLMs is that the data are independent, suggesting the experimental run has been completely randomized. In many cases, factors in a process or experiment may be difficult or costly to change, making this randomization impractical. Observations within these groups, which may be split plots of split-plot designs or longitudinal data where an individual is tracked over time, for example, are correlated, thus violating this assumption (Robinson, Myers, and Montgomery, 2004).

Generalized linear mixed models (GLMMs) extend the GLM to include various covariance patterns, enabling the GLM to account for correlation present in random effects (Robinson, et al., 2004). The random effects models can also relate to methods of dealing with forms of missing data or with random measurement error in the explanatory variables (Agresti, 2002).

Breslow and Clayton (1993) first proposed GLMMs, and work by Wolfinger and O'Connell (1993) refined the technique. This advance has had a significant impact on research, demonstrated by the 2004 ISI Essential Science Indicator identifying Breslow and Clayton (1993) as the most cited paper in mathematics in the previous decade (Dean & Nielson, 2007). The GLMMs explicitly model variance components and can be written as a *batch-specific*

model or as a *population-averaged* model. These two approaches have different methods and scopes of inference for prediction.

Batch-specific model.

Also known as subject-specific models, batch-specific models are most useful in repeated measures studies where individual profiles of subjects across time are of interest (Myers, et al., 2010). These models produce estimates of the mean conditional on the levels of the random effects.

Similar to linear mixed models, random effects GLMs are defined by $\mathbf{y} = \boldsymbol{\mu} + \boldsymbol{\varepsilon}$, where

$$g(\boldsymbol{\mu}) = \mathbf{X}\boldsymbol{\beta} + \mathbf{Z}\boldsymbol{\gamma}. \tag{2.33}$$

Here, g is the appropriate link function, and $\boldsymbol{\gamma}$ and $\boldsymbol{\varepsilon}$ are assumed to be independent. This gives the conditional mean for the jth cluster as

$$E\left(\mathbf{y}_{n_i} \mid \boldsymbol{\gamma}_j\right) = g^{-1}\left(\boldsymbol{\eta}_j\right) = g^{-1}\left(\mathbf{X}_j\boldsymbol{\beta} + \mathbf{Z}_j\boldsymbol{\gamma}_j\right) \tag{2.34}$$

where $\mathbf{y}_{n_j}$ is the vector of responses at the jth cluster, g is the link function, $\boldsymbol{\eta}_j$ is the linear predictor, $\mathbf{X}_j$ is the $\left(n_j \times p\right)$ matrix of fixed effect model terms associate with the jth cluster, and $\boldsymbol{\beta}$ is the corresponding $\left(p \times 1\right)$ vector of fixed effect regression coefficients. For the random effect portion, $\boldsymbol{\gamma}_j$ is the $\left(q \times 1\right)$

vector of random factor levels associated with the jth cluster, and $\mathbf{Z}_j$ is the corresponding matrix of predictors for the jth cluster (Myers, et al., 2010). The jth cluster has n_j observations.

This mixed model involves some assumptions as well. The conditional response, $\mathbf{y} \mid \boldsymbol{\gamma}$, is assumed to have an exponential family distribution, and each of the random effects are assumed to be normally distributed with mean zero and the variance-covariance matrix of the vector of random effects in the jth cluster is denoted $\mathbf{G}_j$. The $\mathbf{G}_j$ is typically assumed to be the same for each cluster (Myers, et al., 2010).

Population-averaged model.

When interest is in estimating more general trends across the entire population of random effects rather than at the specific levels, a population-averaged model is more appropriate (Myers, et al., 2010). While a popular approach for estimating the marginal mean using the batch-specific models is to set $\hat{\boldsymbol{\gamma}} = 0$ since $E(\boldsymbol{\gamma}) = \mathbf{0}$, this estimate of the marginal mean will differ from that found using the population-averaged approach, and the estimated fixed effect parameters will also differ for the two approaches (Myers, et al., 2010) with the conditional effects usually being larger than the marginal effects, though the significance of the effects is usually similar (Agresti, 2002).

The marginal mean is more tedious to obtain due to the nonlinearity in GLMMs, so often approximations must be used. This is done by linearizing the

conditional mean using a first-order Taylor series expansion about $E(\boldsymbol{\eta}) = \mathbf{X}\boldsymbol{\beta}$ and gives the approximation of the unconditional process mean as

$$E(\mathbf{y}) = E[E(\mathbf{y} \mid \boldsymbol{\gamma})] \approx g^{-1}(\mathbf{X}\boldsymbol{\beta}). \tag{2.35}$$

This approximation will be exact for a linear link function and is more accurate when the variance components associated with $\boldsymbol{\delta}$ are close to zero (Myers, et al., 2010).

The population-averaged model requires that a covariance structure be defined for the error term. This is a major difference from the batch-specific approach. For split-plot designs, the correlation matrix, $\mathbf{R}$, generally has a compound symmetric structure (Robinson, et al., 2004). For a random effect such as following a subject over time in a longitudinal study, $\mathbf{R}$ may take on a first-order autoregressive (AR-1) structure.

Robinson, et al. (2004) found that in examining the application of both approaches to a split plot experiment, that when the prediction of an average across all subjects (batches, in this case) is of interest, it is better to model the unconditional expectation of the response than the conditional expectation. The population-averaged model is appealing for prediction purposes, but the quality of this model is heavily dependent on the assumption that the group of random subjects or clusters is a true representation of the whole (Robinson, et al., 2004).

Parameter estimation.

With GLMs, the independence of the data makes the log likelihood well-defined and the objective function for estimating the parameters simple to construct (SAS, 2006). This is not the case for GLMMs. The objective function may not be able to be computed due to cases:

1. where no valid joint distribution can be constructed,
2. where the dependency between the mean and the variance places constraints on the possible correlation models that simultaneously yield valid joint distributions and desired conditional distributions, or
3. where the joint distribution may be mathematically feasible but computationally impractical (SAS, 2006).

Two basic parameter estimation approaches have been suggested in the literature: to approximate the objective function and to approximate the model (SAS, 2006). Integral approximation methods approximate the log likelihood of the GLMM and use the approximated function in numerical optimization using techniques such as Laplace methods, quadrature methods, Monte Carlo integration, and Markov Chain Monte Carlo methods (SAS, 2006). The advantage of this approach is that it provides an actual objective function for optimization. This singly iterative approach has difficulty in dealing with crossed random effects, multiple subject effects, and complex marginal covariance structures (SAS, 2006).

Linearization methods are used to approximate the model, using expansions to approximate the model by one based on pseudo-data with fewer

nonlinear components (SAS, 2006). These fitting methods are usually doubly iterative. First, the GLMM is approximated by a linear mixed model based on current values of the covariance parameter estimates. The resulting linear mixed model is then fit, also using an iterative process. Upon convergence, the new parameter estimates are used to update the linearlization. The process continues until the paramenter estimates between successive linear mixed model fits change within a specified tolerance (SAS, 2006).

Linearization-based methods have the advantage of including a relatively simple form of the linearized model, allowing it to fit models for which the joint distribution is difficult or impossible to obtain (SAS, 2006). While this approach handles models with correlated errors, a large number of random effects, crossed random effects, and multiple types of subjects well, the method does not use a true objective function for the overall optimation process, and the estimates of the covariance paramenters can be potentially biased, especially for binary data (SAS, 2006). PROC GLIMMIX uses linearizations to fit GLMMs.

The default estimation technique, restricted pseudo-likelihood (RPL), is based on the work of Wolfinger and O'Connell (1993). The Pseudo-Model begins with

$$E[\mathbf{Y} \mid \boldsymbol{\gamma}] = g^{-1}(\mathbf{X}\boldsymbol{\beta} + \mathbf{Z}\boldsymbol{\gamma}) = g^{-1}(\boldsymbol{\eta}) = \boldsymbol{\mu} \qquad 2.36$$

where $\boldsymbol{\gamma} \sim N(\mathbf{0}, \mathbf{G})$ and $\text{var}[\mathbf{Y} \mid \boldsymbol{\gamma}] = \mathbf{A}^{1/2}\mathbf{R}\mathbf{A}^{1/2}$.

The first-order Taylor series of $\boldsymbol{\mu}$ about $\tilde{\boldsymbol{\beta}}$ and $\tilde{\boldsymbol{\gamma}}$ yields

$$g^{-1}(\boldsymbol{\eta}) = g^{-1}(\tilde{\boldsymbol{\eta}}) + \tilde{\boldsymbol{\Delta}}\mathbf{X}(\boldsymbol{\beta} - \tilde{\boldsymbol{\beta}}) + \tilde{\boldsymbol{\Delta}}\mathbf{Z}(\boldsymbol{\gamma} - \tilde{\boldsymbol{\gamma}}) \qquad 2.37$$

where $\tilde{\boldsymbol{\Delta}} = \left(\frac{\partial g^{-1}(\boldsymbol{\eta})}{\partial \eta}\right)_{\tilde{\beta},\tilde{\gamma}}$ is a diagonal matrix of derivatives of the conditional mean evaluated at the expansion locus (Wolfinger & O'Connell, 1993). This can also be expressed as

$$\tilde{\boldsymbol{\Delta}}^{-1}\left(\boldsymbol{\mu} - g^{-1}(\tilde{\boldsymbol{\eta}})\right) + \mathbf{X}\tilde{\boldsymbol{\beta}} + \mathbf{Z}\tilde{\boldsymbol{\gamma}} = \mathbf{X}\boldsymbol{\beta} + \mathbf{Z}\boldsymbol{\gamma} \qquad 2.38$$

The left-hand side is the expected value, conditional on $\boldsymbol{\gamma}$, of

$$\tilde{\boldsymbol{\Delta}}^{-1}\left(\mathbf{Y} - g^{-1}(\tilde{\boldsymbol{\eta}})\right) + \mathbf{X}\tilde{\boldsymbol{\beta}} + \mathbf{Z}\tilde{\boldsymbol{\gamma}} \equiv \mathbf{P} \qquad 2.39$$

and

$$\mathrm{var}[\mathbf{P} \mid \boldsymbol{\gamma}] = \tilde{\boldsymbol{\Delta}}^{-1}\mathbf{A}^{1/2}\mathbf{R}\mathbf{A}^{1/2}\tilde{\boldsymbol{\Delta}}^{-1}. \qquad 2.40$$

Thus, the model

$$\mathbf{P} = \mathbf{X}\boldsymbol{\beta} + \mathbf{Z}\boldsymbol{\gamma} + \boldsymbol{\varepsilon} \qquad 2.41$$

can be considered. This is a linear mixed model with pseudo-response $\mathbf{P}$, fixed effects $\boldsymbol{\beta}$, random effects $\boldsymbol{\gamma}$, and $\operatorname{var}[\boldsymbol{\varepsilon}] = \operatorname{var}[\mathbf{P} \mid \boldsymbol{\gamma}]$.

Now, the marginal variance in the linear mixed pseudo-model is defined as

$$\mathbf{V}(\boldsymbol{\theta}) = \mathbf{ZGZ}' + \tilde{\boldsymbol{\Delta}}\mathbf{A}^{1/2}\mathbf{RA}^{1/2}\tilde{\boldsymbol{\Delta}}^{-1} \qquad 2.42$$

where $\boldsymbol{\theta}$ is the $(q \times 1)$ parameter vector containing all unknowns in $\mathbf{G}$ and $\mathbf{R}$. Assuming the distribution of $\mathbf{P}$ is known, an objective function can be defined based on this linearized model. The restricted log pseudo-likelihood (RxPL) for $\mathbf{P}$ is

$$l_R(\boldsymbol{\theta}, \mathbf{p}) = -\frac{1}{2}\log|\mathbf{V}(\boldsymbol{\theta})| - \frac{1}{2}\mathbf{r}'\mathbf{V}(\boldsymbol{\theta})^{-1}\mathbf{r} - \frac{1}{2}\log\left|\mathbf{X}'\mathbf{V}(\boldsymbol{\theta})^{-1}\mathbf{X}\right| - \frac{f-k}{2}\log\{2\pi\} \qquad 2.43$$

With $\mathbf{r} = \mathbf{p} - \mathbf{X}\left(\mathbf{X}'\mathbf{V}^{-1}\mathbf{X}\right)^{-}\mathbf{X}'\mathbf{V}^{-1}\mathbf{p}$. f denotes the sum of the frequencies used in the analysis, and k denotes the rank of $\mathbf{X}$. The fixed effects parameters $\boldsymbol{\beta}$ are profiled from these expressions, and the parameters in $\boldsymbol{\theta}$ are estimated by optimization techniques, such as Newton-Raphson. The objective function for minimization is $-2l_R(\boldsymbol{\theta}, \mathbf{p})$. At convergence, the profiled parameters are estimated as

$$\hat{\boldsymbol{\beta}} = \left(\mathbf{X}'\mathbf{V}\left(\hat{\boldsymbol{\theta}}\right)^{-1} \mathbf{X}^{-} \mathbf{X}'\mathbf{V}\left(\hat{\boldsymbol{\theta}}\right)^{-1} \mathbf{p} \right) \qquad 2.44$$

and the random effects are predicted as

$$\hat{\boldsymbol{\gamma}} = \hat{\mathbf{G}}\mathbf{Z}'\mathbf{V}\left(\hat{\boldsymbol{\theta}}\right)^{-1} \hat{\mathbf{r}} \,. \qquad 2.45$$

Using these statistics, the pseudo-response and error weights of the linearlized model are recomputed and the objective function is minimized again until the relative change between parameter estimates at two successive iterations is sufficiently small (SAS, 2006). For more on parameter estimation, see Wolfinger and O'Connell (1993), SAS (2006), and Myers, et al. (2010).

Applications.

GLMMs have been applied widely in epidemiology (Fotouhi, 2008), but have also been used to model events such as post-earthquake fire ignitions (Davidson, 2009), electrical power outages due to severe weather events (Liu, Davidson, & Apanasovich, 2007), credit defaults (Czado & Pfluger, 2008), plant disease (Madden, Turecheck, & Nita, 2002), and workers' compensation insurance claims (Antonio & Beirlant, 2007). GLMMs can also be used in designed experiments (Robinson, et al., 2004) and robust design and analysis of signal-response systems (Gupta, Kulahci, Montgomery, & Borror, 2010). Myers, et al. (2010) and Agresti (2002) include additional examples of applications of GLMMs.

Chapter 3

DATA REFINING FOR MODEL BUILDING

The semiconductor industry is rich in data with many measurements being taken at hundreds of points throughout the fabrication process. Analyzing these data begins to become troublesome due to the amount of data available. The first step in preparing to develop any semiconductor yield model is to collect, integrate, and aggregate the data. Often, this can be the most time-consuming step in model creation. The datasets collected in computer-aided manufacturing are massive in size and complex due to the sampling strategies used that do not necessarily correspond with one another in levels of aggregation, the number of sample wafers selected for different tests, or the actual sample wafers used. This chapter describes the data that were collected from an SRC-member company that were used in the analysis provided in Chapters 4-6. The data collection, integration, and aggregation process is described in detail to aid practitioners in completing these steps in following the modeling strategies described in the following chapters.

Overall Description of Data

The device studied is a non-volatile memory chip with RAM, ROM, and flash components. It has a 32-bit microcontroller and is used in applications such as engines, tractors, printers, and basically anything that is not a personal computer. It uses communication design rule (CDR1) technology. Each 8” wafer

contains 226 dice and takes 10-12 weeks to process. A cross section of the device is provided in Figure 3.1.

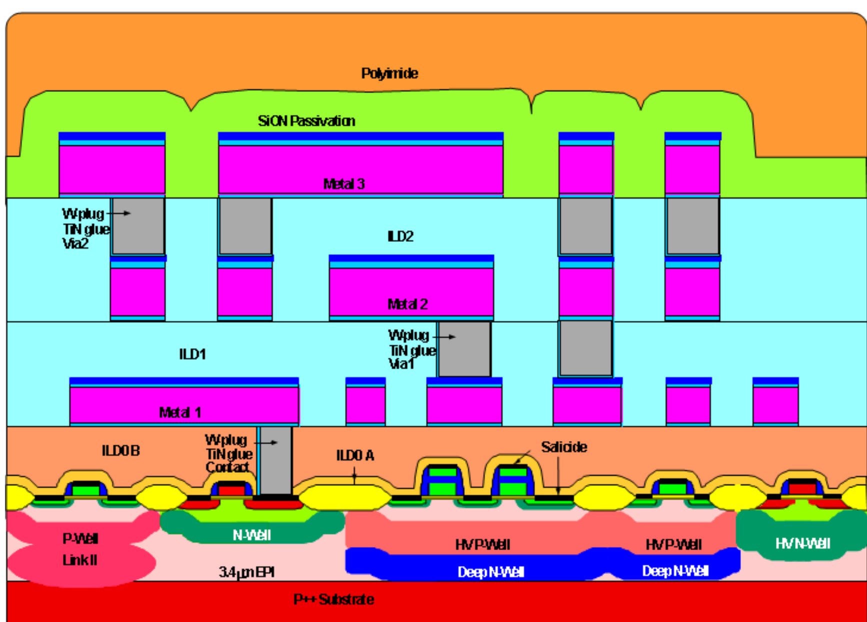

Figure 3.1. Cross section of semiconductor device from an SRC-member company. The different layers of processing are shown.

In developing a data test bed for this and future research, four areas of evaluation were considered: 1) process data, 2) defectivity data, 3) class probe, and 4) unit probe.

Process Data.

As lots move through the fabrication process, many measurements are taken at different stages to gauge how the process is performing. For example, critical dimension measurements may be taken after an etching process to ensure the correct amount of material was etched. These process measurements also measure critical dimensions and overlay for the photo processes, remaining

oxides at etch, changes in oxide thicknesses, etch endpoint times, and more. Several process parameters are recorded at each layer of fabrication.

Process data are automatically recorded in a tool, such as DataLog. Though DataLog can have data integrity issues, it is used commonly in examining process data in SPC graphs. DataLog isn't a tool often used by the device engineer. He or she relies more on the defectivity, class probe (also referred to as parametric or electrical test), and yield data. If there is a processing concern, he or she directs questions to the process owner.

Data are pulled from DataLog by using what is known as an Area – Logbook – Process or ALP. An area will usually denote the type of process and measurement. For instance, E_CD_SEM measures the critical dimensions for the etch process. The "logbook" is often a specified piece of equipment or a specified layer for the part. Often the "process" is the part name or an equipment name. Queries can be used to extract raw or summary data and can be limited by date. The process data extracted for this project are those applicable to the device of interest during the time period of April 1, 2006 through September 30, 2006. Process data are measured on two wafers from each lot after each layer of fabrication (see Figure 3.3). The data files compiled for this project include both the raw and summary data for each process parameter. This allows researchers to examine the control charts, such as the one shown in Figure 3.2 for defect density, as well as using the raw or summary data for modeling purposes. Some of the process measurements included in this data set are given in Table 3.1.

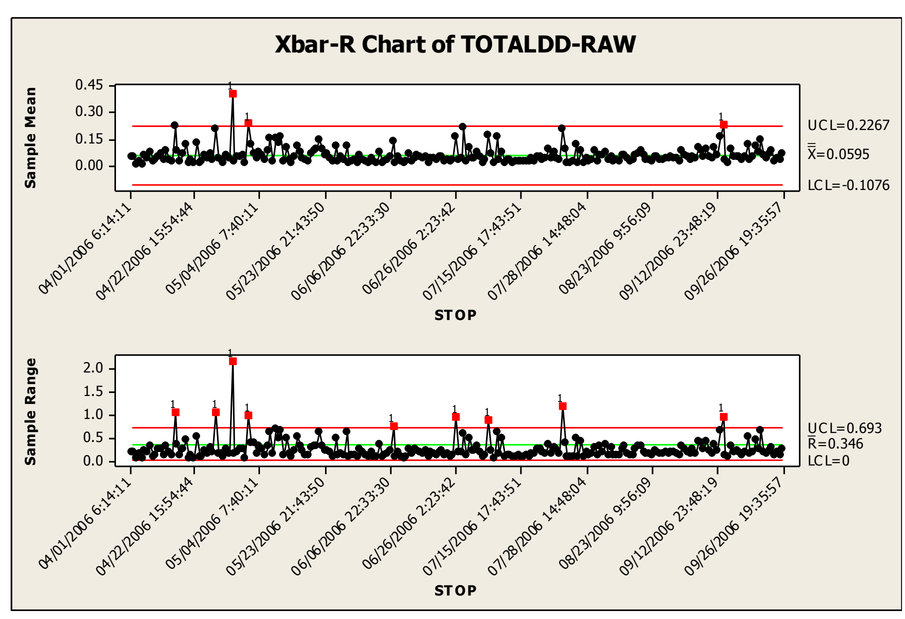

Figure 3.2. X-bar and R chart for Defect Densities for the device studied. The raw data extracted from the process allow researchers to examine the process in many different ways, including the use of control charts to detect special cause variation.

Table 3.1. *Process Measurements in Dataset*

Process	Measurements recorded
Yield	Defect counts and defect densities
Critical dimensions	CD bar CD bar delta to target
Etch	Etch endpoint time
Overlay	X offset Y offset
Oxide	Pre-oxide thickness Post-oxide thickness
Remaining oxide	Remaining oxide Damaged silicon
Diffusion thickness	Thickness Top, center, and bottom wafer ranges

Defectivity.

Defects are detected by comparative techniques using high-powered visual equipment. Defects are found by a machine comparing one die to the next and noting any differences. If there is a difference between the two die, a third dice is checked to determine which one contains the defect. These data are often used to look at significant problems with a wafer.

At the SRC-member company contributing to this project, defectivity is measured using KLA machines and is recorded in a system called KLARITY. KLARITY stores both die- and wafer-level data. However, KLARITY is not directly linked to the database that contains the unit probe data for the die. A program has been written to link the two when both types of corresponding data are needed.

The size of the defect is usually not of concern to the engineers. However, the visual images produced from selected defects are often key in determining the root causes for problems. Device engineers can access these images from their computers easily. Defects such as scratches can be easily seen at a high level, and SEM (Scanning Electron Microscope) images are also available. These images help the engineer quickly determine if the defect will cause a fatal flaw in the dice. Sometimes defects will cause a die to fail at unit probe (known as a fault), but other times (this is somewhat dependent on the location on the die and the critical area), the die will function properly regardless of the defect.

KLA data are recorded at ten layers of this device. They are given in Table 3.2.

Table 3.2. *Description of the Layers Involved in Defectivity Scans*

Layer	Description
Layer 1	Active
Layer 2	Poly 1
Layer 3	Flash
Layer 4	Flash Drain
Layer 5	Salicide
Layer 6	Contact
Layer 7	Metal 1
Layer 8	Via 1
Layer 9	Metal 2
Layer 10	Metal 3

Defectivity measures are not performed on every wafer. For this device, they are usually conducted on every tenth lot that is fabricated. From each of these test lots, two wafers (#2 and #21) are tested (see Figure 3.3). The dataset includes the wafers that had KLA data that were tested at unit probe between June 1, 2006 and September 30, 2006. This dataset includes 136 lots.

The KLA data in the dataset compiled include the lot number, wafer number, *x*- and *y*- coordinates of the die, the layer where the testing was performed, the defect number (such as the 10th defect found, etc.), the classification if the defect was classified, and the corresponding bin code from unit probe.

The process data and the defectivity data are the two types of in-line test measures available in the dataset. Toward the end of the fabrication process, class probe and bin data are collected. Figure 3.3 shows the frequency of the wafer testing for the various data types and the inconsistencies present in the sampling structure across the different data types.

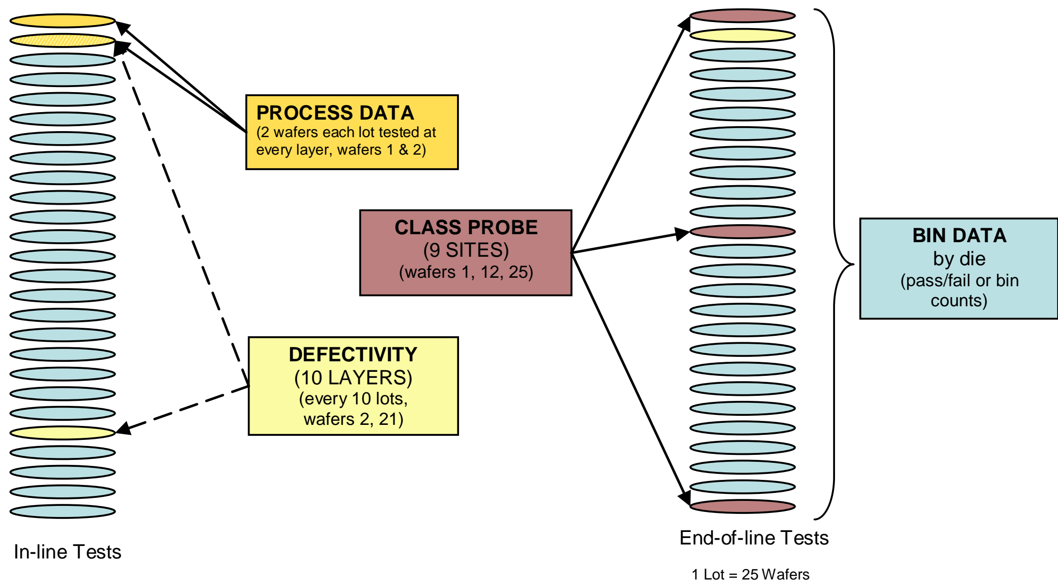

Figure 3.3. Sampling strategies by lot for different data types. Process data are taken from wafers 1 and 2 in each lot. For lots selected for defectivity scans, wafers 2 and 21 are scanned. Class probe tests are done on wafers 1, 12, and 25 for a lot, but are conducted on 9 designated sites on the wafer. Bin data are recorded for each die after wafer probe has been completed.

Class Probe.

Class probe data are recorded from electrical tests performed on the "streets" of the wafer. These tests are conducted at different reticule sites that vary from device to device. For the device studied in this research, there are 9 places where the wafers are tested for parametric data, such as L-Effective, W-Effective, and threshold voltage (VT). Due to this type of test, these data are recorded at the wafer level, not the die level.

These data are helpful to engineers in determining where in the process problems may have occurred that impact functionality of the device. There are over 400 parameters that are tested at class probe, but these are only done on

wafers 1, 12, and 25 for each lot. However, reliability tests, which include 17 or 18 parameters, are performed on 5 sites on every wafer for this device. These are stored differently in dataPOWER so device engineers as well as process engineers are able to use the information.

Some parameters are closely linked to specific processes. For instance, if a problem occurs with the L-Effective, the device engineer knows the process most likely responsible for this deviation, whereas when problems occur with W-Effective, which is formed in several different steps, it is harder to determine the root cause.

The dataset compiled includes class probe data for all wafers tested between June 1, 2006 and September 30, 2006. In addition, the company provided a list of 109 "watchdog" parameters that are more important to refine the search from the 400+ to these. The engineer also provided a list of about 40 of these "watchdog" parameters that he considers most important.

Unit Probe.

The unit probe (sometimes called wafer sort) data are needed to determine the final adequacy of the product. Testing is performed to determine if the die are good or bad. When a die fails, its failure is categorized into a specific "bin." These various bins are coded for a variety of failure modes. These failures can be viewed on a wafer map as shown in Figure 3. 4.

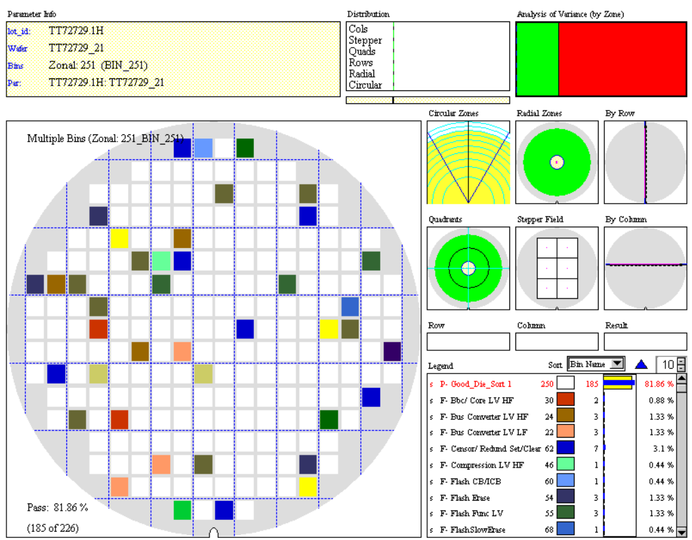

Figure 3.4. A wafer map. Different colors of dice on the wafer map indicated different failure bin assignments based on unit probe tests.

For this device, two passes of testing are required. The first pass includes all functional testing. If a wafer passes the first pass of testing, each die is classified into BIN 250, and it is baked for 72 hours before the memory is checked for retention. If a die passes this second test, it is classified as "BIN 1" and is shippable. If the wafer fails the first pass, it will be scrapped unless there are special circumstances such as the engineer hasn't readjusted the specification limits after a change. The engineer may indicate if the wafer should be retested. Hence, sometimes there are multiple sets of bin data for the same wafer. The failure limits for specific bins are kept in a specific program where the data can be easily accessed by the engineer to examine specific failures.

Use of the Dataset

As described in Chapter 1, this dissertation focuses on developing modeling strategies using GLMs to predict wafer sort outcomes at unit probe testing based on defect counts on the process layers. The other components of this dataset (class probe and process data) have been useful in furthering the work of Kumar (2006) through the work of Chang (2010) at the University of Washington. These data have been used to help further advance the methodology of hGLMs described in Chapter 2. The remainder of this chapter will describe the steps taken to refine the defect count and wafer sort data from their raw forms in the dataset to a useable form for modeling purposes.

Data Refining for GLM Model Building

Data Integration.

For GLM models that use defectivity data for predictors, the defect metrology data and the wafer sort yield data first need to be integrated by die for die-level analyses to be performed. This can be done a number of ways, including automatic or manual methods. If using software such as DataPower, these data may already be integrated and be easy to extract together. If multiple databases are used to store the various types of data recorded during the fabrication and testing process, though, running queries in both can sometimes require advanced coding expertise, especially if the location coordinates of the dice are constructed differently for different tests, specifically, defect metrology and wafer sort.

Data Aggregation.

Perhaps the most time-consuming task is taking the integrated data and aggregating them into a form that will be usable for model building. Table 3.3 contains an example of raw, integrated data extracted from a database. Rows showing dice with multiple defects on a layer are highlighted in bold text. While these integrated data contain the lot number, wafer number, layer number, die location (given in x- and y-coordinates), and the final bin assigned at wafer sort for each identified defect found during the scan, this arrangement of the data is not useful for common statistical packages such as Minitab or JMP that can create the desired models. For example, in Table 3.3, the die from Lot 1, Wafer 2, with coordinates (9, 1) has one defect on Layer 1 and three defects on Layer 2, so it is displayed on four different rows. The data need to be aggregated such that each die (or wafer for wafer-level modeling) is a row, and the total number of defects in each layer is given in a separate column with the column containing the wafer sort test result remaining. An example of the necessary aggregation is shown in Table 3.4. Here, the die from Lot 1, Wafer 2 with coordinates (9, 1) is summarized in a single row showing it had one defect detected in Layer 1 and three defects on Layer 2. Also, if using a binomial response (pass or fail), the failure bin data should be converted to reflect the appropriate binomial response rather than a specific bin number as shown in the far right column.

Table 3.3. *Raw Data for Each Defect After Integration*

Lot ID	Wafer ID	Layer ID	Die Coordinate X	Die Coordinate Y	Failure Bin Number
1	2	1	2	7	1
1	2	1	4	3	1
1	2	1	5	7	1
1	2	1	8	8	24
1	2	1	8	16	1
1	**2**	**1**	**9**	**1**	**7**
1	2	1	11	17	1
1	2	1	13	16	1
1	2	1	18	8	1
1	2	1	18	9	7
1	2	1	18	10	1
1	**2**	**2**	**1**	**9**	**1**
1	**2**	**2**	**1**	**9**	**1**
1	2	2	3	12	1
1	2	2	4	15	1
1	2	2	5	6	1
1	2	2	5	8	1
1	2	2	5	10	42
1	2	2	7	11	1
1	**2**	**2**	**9**	**1**	**7**
1	**2**	**2**	**9**	**1**	**7**
1	**2**	**2**	**9**	**1**	**7**
1	2	2	10	1	77
1	**2**	**2**	**11**	**1**	**1**
1	**2**	**2**	**11**	**1**	**1**

Defectivity measures were taken after each of ten layers in the fabrication process. These measures include a count of the number of defects found on each layer for a particular die. Die *x*- and *y*-coordinates were used to calculate radial distance from the center and also to assign a die quadrant category. An example of the types of data used for model building is shown in Table 3.5. Additional factors, such as defect size, stepper fields, indicator variables for killer or non-killer classified defects, and location of the defect within the die may also be included as predictors, but these data were not available in the dataset.

Table 3.4. *Aggregated Data for Individual Dice*

LotID	WaferID	DieX	DieY	Defects on Layer 1	Defects on Layer 2	Bin	Fail = 1
1	**2**	**1**	**9**	**0**	**2**	**1**	**0**
1	2	2	7	1	0	1	0
1	2	3	12	0	1	1	0
1	2	4	3	1	0	1	0
1	2	4	15	0	1	1	0
1	2	5	6	0	1	1	0
1	2	5	7	1	0	1	0
1	2	5	8	0	1	1	0
1	2	5	10	0	1	42	1
1	2	5	11	1	0	1	0
1	2	5	15	1	0	1	0
1	2	6	15	1	0	1	0
1	2	7	3	1	0	1	0
1	2	7	11	0	1	1	0
1	2	7	15	1	0	1	0
1	2	8	8	1	0	24	1
1	2	8	16	1	0	1	0
1	**2**	**9**	**1**	**1**	**3**	**7**	**1**
1	2	10	1	0	1	77	1
1	**2**	**11**	**1**	**0**	**2**	**1**	**0**
1	2	11	17	1	1	1	0
1	2	13	16	1	1	1	0
1	2	18	8	1	1	1	0
1	2	18	9	1	1	7	1
1	2	18	10	1	1	1	0

Table 3.5. *Subset of Data for Analysis*

Lot Number	Wafer ID	Die X	Die Y	Radial Distance	Die Quadrant	Layer 1	Layer 2	Layer 3	Layer 4	Layer 5	Layer 6	Layer 7	Layer 8	Layer 9	Layer 10	Response (Fail = 1)
1	2	2	7	7.28	3	1	0	0	0	0	0	0	0	0	0	0
1	2	2	10	7.07	2	0	0	0	0	0	1	0	0	0	0	0
1	2	2	11	7.28	2	0	0	1	0	0	0	0	0	0	0	0
1	2	2	12	7.62	2	0	0	1	0	0	0	0	0	0	0	0
1	2	3	12	6.71	2	0	1	0	0	0	0	0	0	0	0	0
1	2	4	3	7.81	3	1	0	0	0	0	0	0	0	0	0	0
1	2	5	6	5.00	3	0	1	0	0	0	0	0	0	0	0	0
1	2	5	7	4.47	3	1	0	0	0	0	0	0	0	0	0	0
1	2	5	11	4.47	2	1	0	0	0	0	0	0	0	0	0	0
1	2	5	15	7.21	2	1	0	0	0	0	0	0	0	0	0	0
1	2	6	3	6.71	3	0	0	1	0	0	0	0	0	0	0	0
1	2	6	15	6.71	2	1	0	0	0	0	0	0	0	0	0	0
1	2	7	2	7.28	3	0	0	0	1	0	0	0	0	0	0	0
1	2	7	3	6.32	3	1	0	0	0	0	0	0	0	0	0	0
1	2	7	5	4.47	3	0	0	1	0	0	0	0	0	0	0	0
1	2	7	7	2.83	3	0	0	0	0	1	0	0	0	0	0	1
1	2	7	11	2.83	2	0	1	0	0	0	0	0	0	0	0	0

Managing outliers.

With the large quantities of data available in the semiconductor industry, there is a question of which data, if any, should be removed for model building. While many algorithms exist to detect outliers, clear cutoffs for removing data are difficult to determine. Figure 3.4 illustrates the large number of possible outliers looking at the total number of defects per die. For the die-level training set, the median is 1.0, but the mean is 2.571 defects per die. Also, the third quartile is 2.0 and the maximum value is 218. This demonstrates the presence of unusual observations that may have a strong impact on model building.

To explore the effects of removing outliers, the models built in the study described in Chapter 4 were built three times from the training dataset. The distribution for the die-level training dataset showed the 97.5th percentile to be 9 total defects on a die, and the 95th percentile was 5 total defects on a die. The dice with more than 9 and more than 5 total defects were removed from the data set using a one-sided trimmed means outlier detection approach with p=0.025 and p=0.05, respectively. Hu and Sung (2004) show trimmed means to be an appropriate method for outlier detection that has higher efficiency than using median. This method unifies mean and median in a dataset. While their study uses two-sided trimmed means with p=0.15, this more conservative approach will allow the most common occurrences of defect distributions on layers to be examined while constructing useful models. No points were removed from the test dataset that was used for validation purposes described in Chapters 4, 5, and 6.

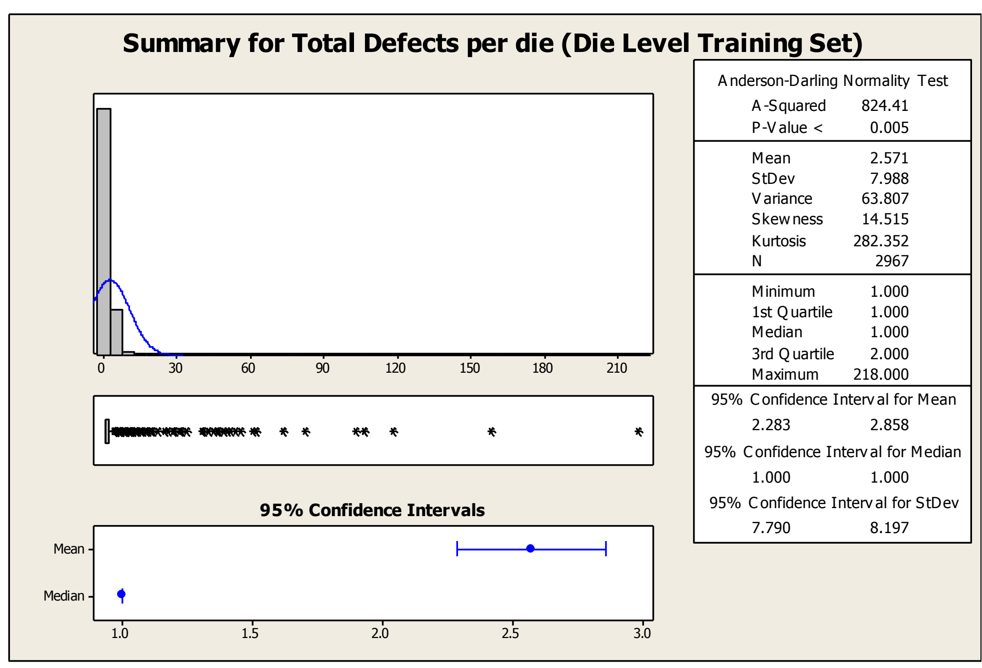

Figure 3.5. Summary statistics for total defects per die. The figure indicates a large number of outliers are present in the dataset that may have a strong influence on the model.

The collected, integrated, aggregated, and trimmed data can be used to easily develop strong prediction models for yield from defectivity data. The GLM modeling strategies of this work are described in Chapters 4-6.

Chapter 4

SEMICONDUCTOR YIELD MODELING USING GENERALIZED LINEAR MODELS

Introduction

As shown in Chapter 2, many approaches have been taken to model semiconductor yield, but these models make a number of assumptions that are not valid for the nature of the process and the data being collected. Ferris-Prabhu (1992) shows the accuracy of yield predictions depends just as much on the accuracy of the assumed average defect densities as upon the choice of yield model. Generalized linear models (GLMs), described in Chapter 2, offer a way to construct models making fewer assumptions as well as a means of modeling the data in more detail by creating die-level models that can take advantage of the raw data available, instead of relying on lot- or wafer-level summaries. This approach of die-level modeling can also consider nested effects.

In some multi-factor experiments, the levels of one factor are similar but not identical for different levels of another factor. This is called a nested (or hierarchical) design. Nested designs are often used in analyzing processes to identify the major sources of variability in the output. In a two-stage nested design, the levels of factor B are nested under the levels of factor A. That is, the levels of B are unique for each level of A. For example, for the semiconductor industry, wafers are nested within lots.

Since the dice are processed together on a wafer, and wafers are grouped together in a lot, independence from die to die cannot be assumed. To account for

this nested structure, a practitioner must include the nested variables in the model analysis. The wafers included in Lot 1 are not the same wafers included in Lot 2 and so on. This is illustrated in Figure 4.1.

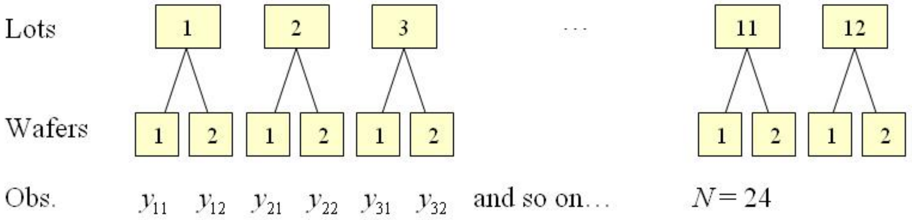

Figure 4.1. Nested structure for wafers.

At the die level, the model is a three-stage nested structure with dice (grouped by quadrants, radial sections, or other categories) nested within wafer, which is nested within lot. This assumes independence between the dice in each quadrant or other chosen grouping. This concept is illustrated in Figure 4.2.

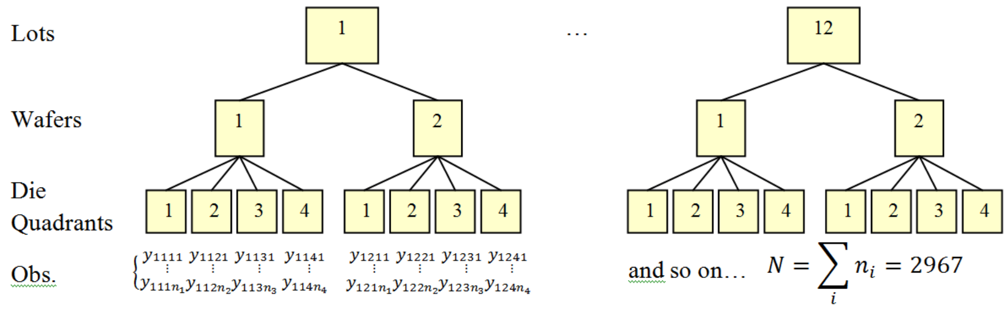

Figure 4.2. Nested structure for dice.

Model Building Using Logistic Regression

The dataset used in this phase of the research consisted of defectivity data for 36 wafers from 18 lots and the corresponding wafer sort data given for each die on those wafers that had at least one defect recorded. This included 4,413 dice. These wafers were found to be an appropriate random sample of wafers produced over time for the industrial product's dataset. In order to assess the validity of the models, the dataset of 18 lots was divided into a training dataset of 12 lots and a test dataset of 6 lots. The 12 lots used for the training dataset were chosen at random from the 18 lots. The data from these 12 selected lots were used consistently to construct the wafer- and die-level models.

Both die- and wafer-level models were developed using the training data set of 24 wafers (12 lots). For the die-level model, predictor variables included lot, wafer, radial distance, die quadrant, and the count of defects found on each of the ten layers. Non-nested and nested models were created to observe differences between the two, with the nested model created by nesting wafer within lot and die quadrant within wafer, assuming independence between the die within a die quadrant. For the wafer-level model, predictor variables included lot, wafer, and the count of defects found on each of the ten layers of the wafer. No nested models were created at the wafer level due to a lack of degrees of freedom with the current sampling structure. Minitab software was used to build these logistic regression models. Full models used all predictor variables, and reduced models were created through backward elimination using factors found to be significant at the α=0.1 level. All factors were considered to be fixed in these analyses.

Results

The results and discussion are organized primarily into examining the die-level analysis and the wafer-level analysis. Within each one, the nested structure is discussed, the significance of outliers is examined, and the different link functions used in logistic regression are compared. Validation is assessed, and a comparison to other yield models from the literature is also provided.

Die-Level Logistic Regression.

To demonstrate the problems with using standard linear regression models for this binary response, the entire training dataset (N=2967) was first analyzed using multiple linear regression. Figure 4.3 shows the residual plots for this model. The normal probability plot indicates that the errors are not normally distributed. The residuals versus the fitted values plot shows a distinct pattern, rather than showing random behavior. The histogram of the residuals again shows non-normality. These results indicate the linear model is inadequate since the assumptions for this model, including:

1. The relationship between the response and the regressors is linear, at least approximately,
2. The error term ε has zero mean,
3. The error term ε has constant variance σ^2,
4. The errors are uncorrelated, and
5. The errors are normally distributed (Montgomery, Peck, & Vining, 2006)

are violated. While this model does identify radial distance and the defect counts on Layers 4, 5, 7, 8, 9, and 10 as significant (α=0.1), the *R*-squared predicted value of 0.0% and the residual plots indicate this modeling approach should not be used.

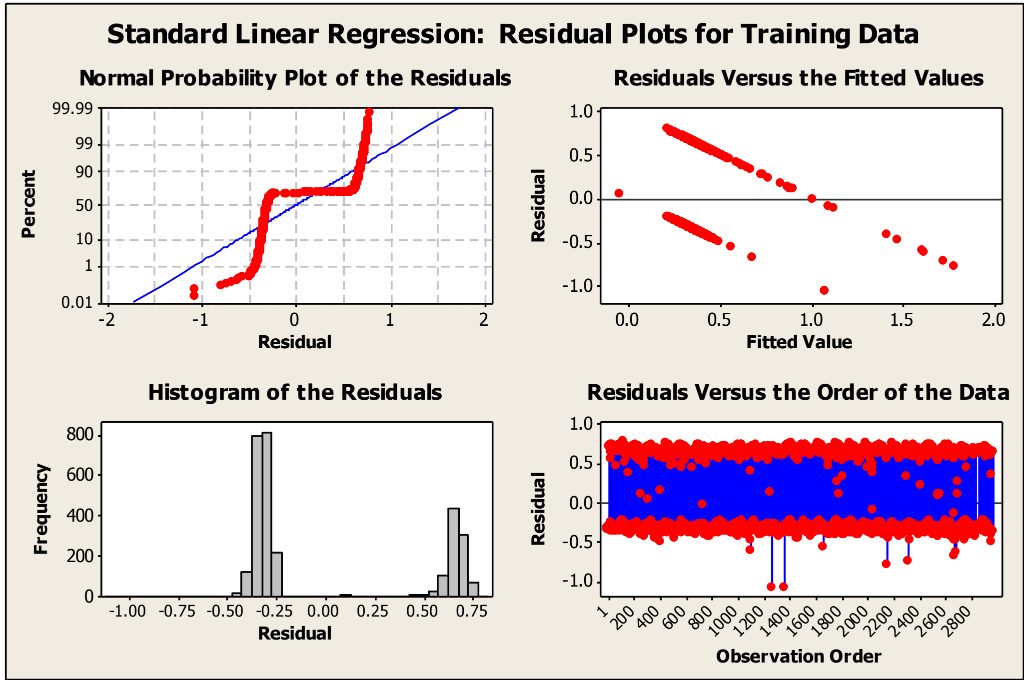

Figure 4.3. Residual plots for a multiple linear regression model based on the training dataset with no outliers removed.

Next, the die-level training data were modeled without considering the nested structure of the data using logistic regression which is more appropriate for the binomial response. The logit link was used. The results are summarized in Table 4.1. This model identifies Lots 15 and 16, Radial Distance, and Layers 4 through 10 as significant at the α=0.1 level. The Pearson method for goodness-of-fit indicates this model is not very good (*p*-value = 0.000), but the Hosmer-Lemeshow test yielding a *p*-value equal to 0.539 indicates that it may be

adequate. This model, however, assumes independence between the die, which is not valid considering the nature of the fabrication process.

Table 4.1. *Die-Level Non-Nested Logistic Regression Model Results for Full Training Data Set (N=2967)*

Significant Factors (alpha = 0.1)	*p*-value
Lot 15	0.040
Lot 16	0.010
Radial Distance	0.001
Layer 4	0.003
Layer 5	0.001
Layer 6	0.002
Layer 7	0.000
Layer 8	0.071
Layer 9	0.000
Layer 10	0.000

Next, the nested structure was modeled using the entire training dataset. This analysis gives much more information. Instead of only identifying significant lots, this model shows there to be a significant difference between Wafer 1 and Wafer 2 in Lots 4 and 16. The logit link model also shows 6 die quadrants to be significantly different from Die Quadrant 1 on the same wafer (α=0.1). This model again indicates Radial Distance is significant, and lists Layers 4 through 10 as significant predictors.

All three link functions were used to build models with the nested structure using the entire training dataset as well as with the two trimmed training datasets. These results are presented in Table 4.2. While the results were similar among the links, the probit model did not converge after 5000 iterations, and did not identify Layer 7 as significant at the 0.1 level for the full training dataset.

Also, the complimentary log-log link shows the best value for the Hosmer-Lemeshow goodness-of-fit test. It also found an additional die quadrant to be significant.

Table 4.2. *Comparison of Link Functions and Outlier Methods (Die-level, Nested)*

	All Training Set Data N=2967			**Outliers Removed (2.5% trimmed) N=2896**			**Outliers Removed (5% trimmed) N=2845**		
	Logit	**Probit**	**Complimentary Log-Log**	**Logit**	**Probit**	**Complimentary Log-Log**	**Logit**	**Probit**	**Complimentary Log-Log**
Significant Factors (□=0.10)	Wafer 2(4) Wafer 2(16) Rad. Dist. 6 Die Quadrants Layers 4-10	Wafer 2(4) Wafer 2(16) Rad. Dist. 6 Die Quadrants Layers 4-6, 8-10	Wafer 2(4) Wafer 2(16) Rad. Dist. 7 Die Quadrants Layers 4-10	Wafer 2(4) Wafer 2(16) Rad. Dist. 6 Die Quadrants Layers 2-10	Wafer 2(4) Wafer 2(16) Rad. Dist. 8 Die Quadrants Layers 2-10	Wafer 2(4) Wafer 2(14) Wafer 2(16) Rad. Dist. 7 Die Quadrants Layers 2-10	Wafer 2(4) Wafer 2(16) Rad. Dist. 7 Die Quadrants Layers 2-10	Wafer 2(4) Wafer 2(16) Rad. Dist. 8 Die Quadrants Layers 2-10	Wafer 2(4) Wafer 2(14) Wafer 2(16) Rad. Dist. 7 Die Quadrants Layers 2-10
G (p-value)	301.988 (0.000)	292.343 (0.000)	250.004 (0.000)	314.462 (0.000)	312.256 (0.000)	261.638 (0.000)	319.679 (0.000)	321.005 (0.000)	318.729 (0.000)
Pearson (p-value)	1837716 (0.000)	3143.77 (0.000)	2×10^{12} (0.000)	2930.44 (0.005)	2914.42 (0.009)	1×10^{12} (0.000)	2771.85 (0.121)	2770.59 (0.125)	2769.46 (0.128)
Deviance (p-value)	3427 (0.000)	3436.21 (0.000)	3478.56 (0.000)	3288.97 (0.000)	3291.18 (0.000)	3341.8 (0.000)	3202.48 (0.000)	3201.16 (0.000)	3203.43 (0.000)
Hosmer-Lemeshow (p-value)	8 (0.463)	8.95 (0.347)	5.1079 (0.746)	4.04 (0.853)	2.26 (0.972)	3.254 (0.917)	7.42 (0.492)	6.24 (0.620)	5.79 (0.671)
Somers' D	0.38	0.36	0.38	0.38	0.38	0.37	0.39	0.39	0.38
Notes:	Probit link did not converge within 5000 iterations.			Complimentary Log-Log link converged within 100 iterations.			Complimentary Log-Log link converged within 100 iterations.		

One disadvantage of the use of the nested model is the number of degrees of freedom required for analysis. Many more parameters are estimated using the nested structure. At the die level, the replication needed is available within the die quadrant groupings (if the practitioner is willing to assume that dice within the same quadrant are independent). In this study, for the 12 lots of training data, 107 parameters are estimated, requiring 1 degree of freedom (df) for the intercept, 11 df for lot, 12 df for wafer (1 df for every lot), 72 df for die quadrant (3 df for every lot/wafer combination), plus 1 df for every covariate added to the model (11 df total for radial distance plus defect counts from 10 layers). While this nested

approach works well for the die-level analysis with dice grouped into quadrants, there are problems when modeling the wafer level. This will be discussed in more detail with the wafer-level analysis.

Removing outliers also had an impact on the models. When all dice having more than 9 total defects were removed from the dataset, there were still 2896 dice in the training data. Using nested models, the logit, probit, and complimentary log-log link functions were compared. A summary of the results is given in Table 4.3. These results show two more layers (Layers 2 and 3) to be significant at the α=0.1 level. Also, the Pearson goodness-of-fit tests show improvement in the logit and probit models. The Hosmer-Lemeshow goodness-of-fit statistics are also improved over keeping the outliers in the dataset.

Removing 5% of the outliers (die with more than 5 total defects) left 2845 dice in the dataset. The analyses were conducted again with these data using the nested structure and all three link functions. These results are also presented in Table 4.3. These models produce the same significant factors as the model that uses 97.5% of the data with the exception of this logit model identifying an additional die quadrant as significant. The Pearson goodness-of-fit tests are improved to show these models to be adequate at the 0.05 level of significance. The Hosmer-Lemeshow statistics show lower *p*-values for these models, compared to those from the 97.5 percentile data, suggesting that this test may be more robust when including outliers.

When used for predictive purposes, the model does not need to include variables for specific lots, wafers, and die quadrants since they will not be the

same as those used in the original model. While these variables are important in identifying potential quality excursions and may aid in troubleshooting in the fabrication process, the continuous variables of radial distance and the defect counts for the layers are of most use for predicting future yield. The reduced nested logit model for the 5% trimmed training dataset that will be used for calculating expected probabilities and for validating the model can be expressed as

$$P = \frac{1}{1+e^{-\mathbf{X}'\boldsymbol{\beta}}} \tag{4.1}$$

where $\mathbf{X}'\boldsymbol{\beta}$ = -2.30820 + 0.0664864(Radial Distance) + 0.456202(Layer 2) + 0.222156(Layer 3) + 0.322290(Layer 4) + 0.322418(Layer 5) + 0.877724(Layer 6) + 0.867638(Layer 7) + 0.553416(Layer 8) + 0.947011(Layer 9) + 0.720564(Layer 10).

Die-Level Logistic Regression Validation.

The model was validated using a test dataset containing 6 lots (12 wafers) of data. No outliers were removed from this dataset, which contained 1,446 dice. The logit models built from the training dataset (5% trimmed) were used to calculate expected probabilities for these test data.

Figure 4.4 shows the predictive power of the die-level GLM models by looking at the actual and predicted number of passing dice on a wafer. In Figure 4.4(a), the non-nested die-level logistic regression model is shown for the actual

and predicted values from both the training data (5% trimmed) used to create the model and to the test data. Results from Seeds' Model (Y4) are also shown for comparison. (Seeds' Model was chosen as a baseline due its lower MAD and MSE measures, shown in Figure 4.6.) This figure shows the model fits the training data very well, but the predictive power is less with the model applied to the test data showing the predictions to underestimate the actual yield. This model significantly outperforms Seeds' model in predictive power, though.

Figure 4.4(b) is a similar chart that shows the nested, reduced die-level model applied to the training and test data. Here, the nested GLM model predicts higher values than actual for the training data, but the predicted values are very near the actual results for the test dataset, which is a demonstration of the predictive power of this approach. Again, Seeds' Model is shown for comparison.

There have been several yield models proposed in the literature that use defect count data to predict performance as described in Chapter 2. Many of these models are described in (Kumar, Kennedy, Gildersleeve, Abelson, Mastrangelo, & Montgomery, 2006) and are briefly shown in Table 4.3. In these models, the variables used are defined as:

D_0 = defects per area
D_i = defects per area from process step i
A = area of a die
A_w = area of a wafer
n=number of processing steps
α=clustering parameter

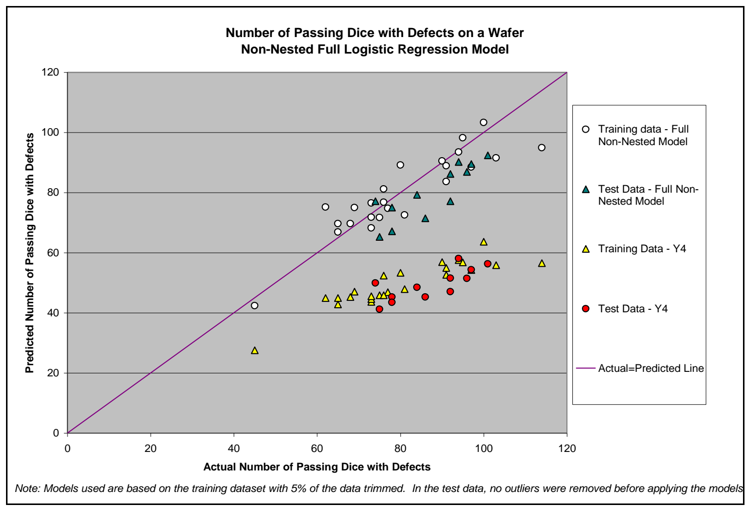

(a)

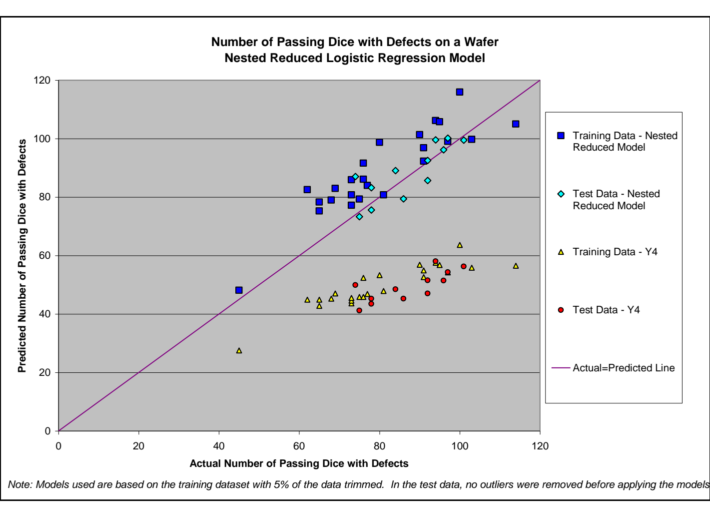

(b)

Figure 4.4. Predicted vs. actual yield for die-level logistic regression models. (a) Predicted vs. actual for non-nested full die-level logistic regression models compared to Seeds' Model (Y4). (b) Predicted vs. actual for nested die-level reduced logistic regression models compared to Seeds' Model (Y4). These charts show the predictive power of the models applied to the training data used to build them and to the test dataset. These results reflect the predicted and actual number of failing dice with defects within a wafer.

Table 4.3. *Existing Yield Models*

Popular Name	Model
Classic Poisson Model	$Y_1 = e^{-D_0 A}$
Binomial Yield Model	$Y_2 = \left[1 - A / A_w\right]^{D_0 A_w}$
Murphy's Yield Model:	$Y_3 = \left[\frac{1 - e^{-D_0 A}}{D_0 A}\right]^2$
Seeds' Yield Model:	$Y_4 = \frac{1}{1 + D_0 A}$
Dingwall's Yield Model:	$Y_5 = \left[1 + D_0 A / 3\right]^{-3}$
Moore's Yield Model:	$Y_6 = e^{-\sqrt{D_0 A}}$
Price's Yield Model:	$Y_7 = \prod_{i=1}^{n} \frac{1}{1 + D_i A}$
Price's General Model:	$Y_8 = \left(1 + D_0 A / n\right)^{-n}$
Negative Binomial Model:	$Y_9 = (1 + D_0 A / \alpha)^{-\alpha}$

In Figures 4.5 and 4.6, the die-level GLM models are compared to those from the literature. Figure 4.5 shows the expected probability for each of the nine models given in Table 4.3 at the die level. The value for the negative binomial (Y_9) clustering parameter (α) was calculated using the method proposed by Cunningham (1990) shown in Equation 2.12. This produced an average alpha value of 3.33. Figure 4.5 shows the actual performance of the die either passing (1) or failing (0). While earlier models have been formed to handle wafer-level analysis, they can be applied at the die-level to predict a yield percentage for all the dice on a wafer. The GLM model gives a range of yield probabilities that more closely reflect expected behavior without the degree of underestimation that the earlier models produce, as demonstrated in Figure 4.5. These GLM models, which consider which layer the defects are found on, can give a more precise

prediction than models that consider only the total number of defects. For a die having one, two, or three defects, the models from the literature predict much lower yields than the GLM models. Since most die have three or fewer defects (95.1% of the die in this dataset have 1, 2, or 3 defects), accurate predictions at these levels are of great importance. While it is not desirable to overestimate the yield, the magnitude of these underestimated yields can have a negative impact on decision making and may lead a manufacturer to have excess work in progress in the fab.

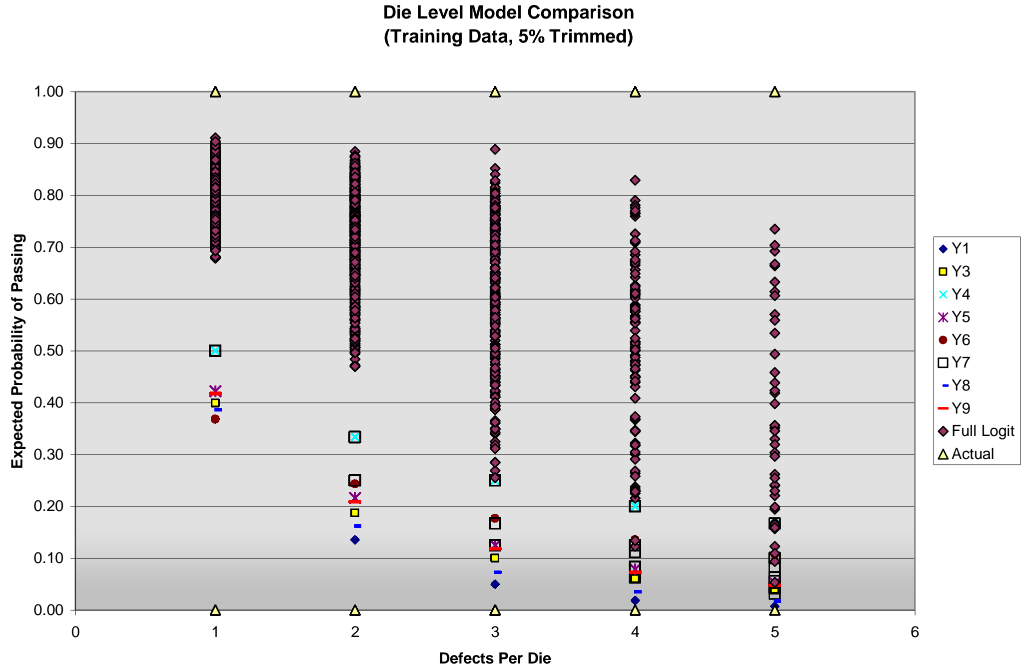

Figure. 4.5. Expected probabilities of dice passing vs. number of defects per die. This die-level model comparison illustrates the value of the die-level modeling. The GLM models predict higher yield for 1-3 defects per die and reflect a varying range based on factors beside total defect counts on a wafer. Actual results are either 0 (fail) or 1 (pass).

Additional advantages of this die-level GLM approach can also be seen when comparing the mean absolute deviation (MAD) and the mean squared error (MSE) for the models. These are shown Table 4.4 and illustrated in Figure 4.6 with the MSE and MAD values being found by applying the models to the test data and assessing how well the predicted values fit the actual results. MAD is the average of the absolute deviations for each die, and the MSE is the average of the squared errors (the actual minus predicted value) for the dice. The lower the number for either of these measures, the better the model matches the actual data. Both Seeds' Model (Y_4) and the Negative Binomial (Y_9, α=3.3) show good performance for the literature models, but the Reduced Nested Logit GLM model shows a 34.6% improvement in MSE and a 31.1% improvement in MAD over the best-performing Seeds' Model (Y_4).

Table 4.4. *Mean Squared Error (MSE) and Mean Absolute Deviation (MAD) for Model Comparisons at the Die Level Using Test Data*

	Y1	Y3	Y4	Y5	Y6	Y7	Y8	Y9	Full Nested Logit	Reduced Nested Logit	Full Non-Nested Die-Level Logit	Multiple Linear Regression
MSE	0.412	0.377	0.289	0.358	0.371	0.309	0.394	0.362	0.190	0.189	0.188	0.592
MAD	0.583	0.566	0.517	0.556	0.572	0.522	0.574	0.558	0.356	0.356	0.397	0.650

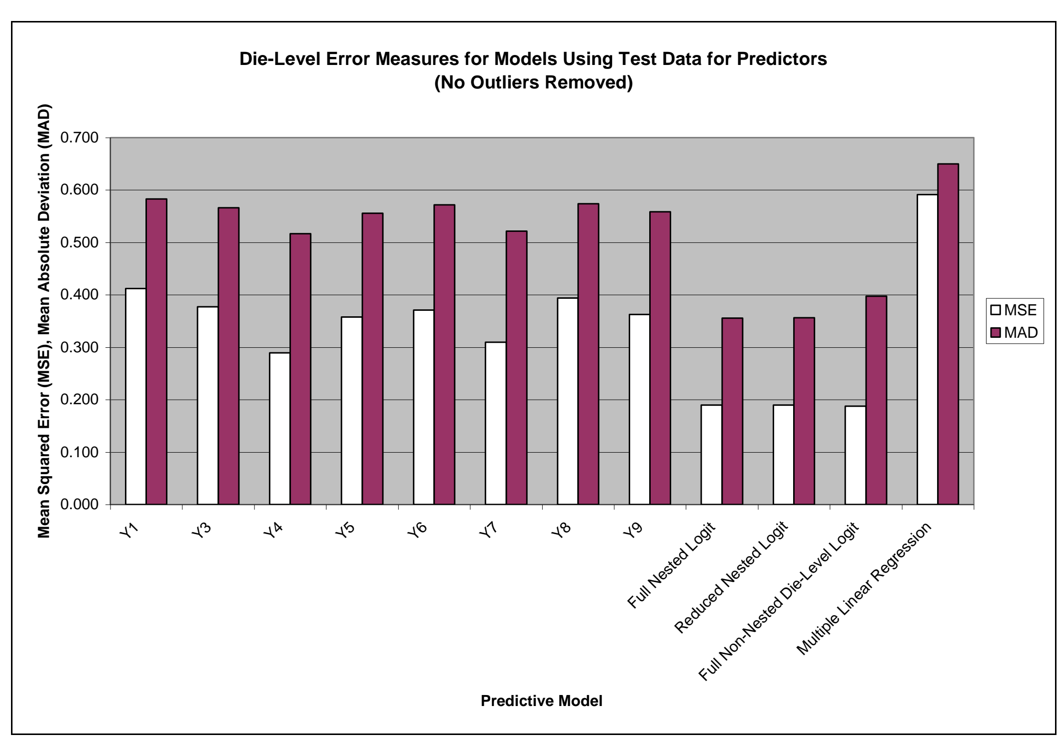

Figure 4.6. Mean Absolute Deviation (MAD) and Mean Squared Error (MSE) results comparing GLM models with other models from the literature and multiple linear regression when applied to the test dataset with no outliers removed. Lower values of MAD and MSE indicate the model is closer to the actual yield values.

The predictive power of these GLM models can also be seen by examining the predicted probabilities for the various models summed together at a high level of aggregation. Figure 4.7 shows the predicted number of passing dice for each model for the entire test dataset (1446 dice). For each model, the actual number of passing and failing dice for the 6 lots in this dataset is shown to demonstrate which models best predict the actual yield of dice that have at least one defect.

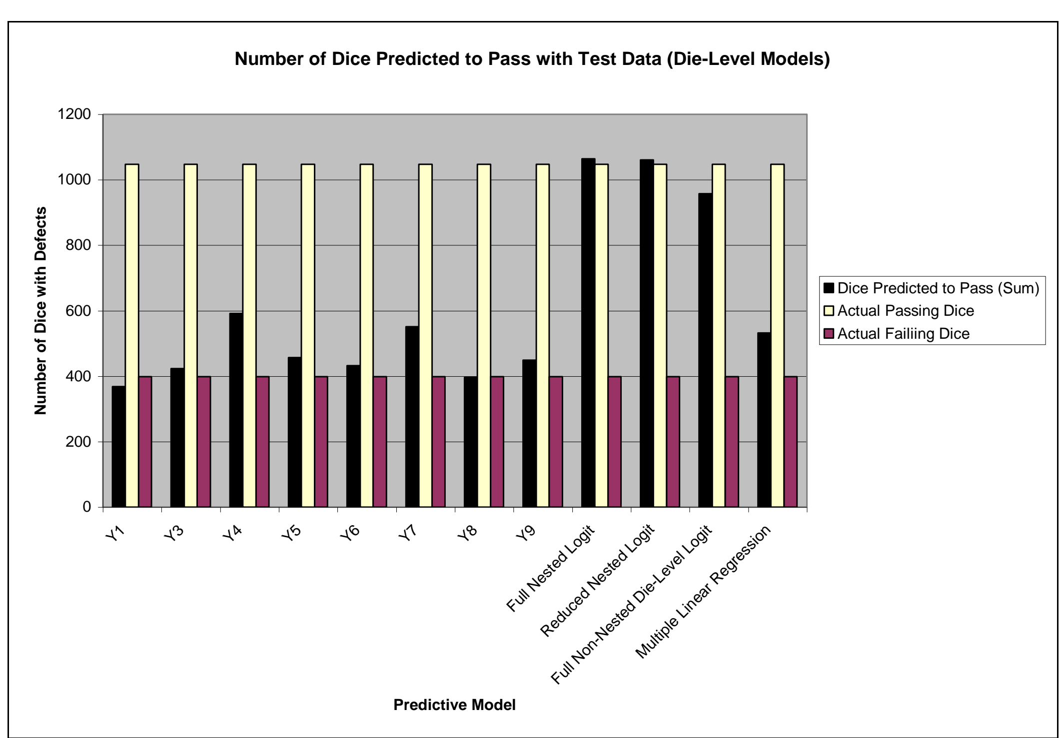

Figure 4.7. Number of dice predicted to pass compared to actual passing dice and failing dice with defects. This figure shows the expected number of passing dice for the entire test dataset (N=1,446) for various models. The die-level GLM models show the closest predictions at this level of aggregation (6 lots) as well, with the nested logit models using logistic regression showing the most accurate predictions.

Wafer-Level Logistic Regression.

Often, process data are recorded by wafer during fabrication. Measurements such as thicknesses, defect densities, critical dimensions and etch rates are recorded for sample wafers from lots. Therefore, it is useful to consider a wafer-level analysis that may correspond more easily to these other measures.

While the die-level analyses used a nested structure to account for the lack of independence between die on different wafers and lots, this approach is not available for a full model wafer-level analysis due to the sampling procedure in place (in this dataset, two wafers per lot) and the aggregation levels used. The

training dataset for the wafer level contains twelve lots (24 wafers). To utilize the nested structure for modeling, one degree of freedom is needed for estimating the constant, eleven degrees of freedom for the lots, twelve for the wafers, and ten for the product layers. Even if only the lots and wafers are considered in the nested model, the model is saturated, and goodness-of-fit statistics cannot be calculated. While adding more lots to the dataset may seem like a feasible solution to this problem, as additional lots of data are added (2 wafers each), two more parameters need to be estimated, so the full model will always be saturated. While other standard diagnostics, such as absolute deviation, can be used to evaluate the usefulness of these models in the absence of goodness-of-fit statistics, a nested model at the wafer level is not recommended as a strong approach due to the limited helpful information that it would provide given these constraints.

Non-nested models were created for the training dataset at the wafer-level using the three link functions and predictors of Lot, Wafer, and the defect counts from the ten process layers. The results are shown in Table 4.5. The logit and probit models identify Lots 6 and 8 as significantly different from Lot 1 and also indicate that Layer 8 is statistically significant. The complimentary log-log model indicates the same two lots as significant, but does not show Layer 8 to be significant at the $\alpha=0.1$ level. The goodness-of-fit tests are favorable for all three links, indicating these should be good models.

Though these models appear to be good, outliers may be impacting the results. Table 4.5 also shows the results of the models created after the dice with

more than 9 total defects (upper 2.5%) were removed from the dataset. These analyses show no lots are significantly different from Lot 1, and a different layer, Layer 9, is identified as significant (α=0.1).

Table 4.5. *Comparison of Link Functions & Outlier Methods (Wafer-level, Not-nested)*

	All Training Set Data N= 24 wafers (2967 dice)			**Outliers Removed (97.5th percentile) N= 24 wafers (2896 dice)**			**Outliers Removed (95th percentile) N= 24 wafers (2845 dice)**		
	Logit	**Probit**	**Complimentary Log-Log**	**Logit**	**Probit**	**Complimentary Log-Log**	**Logit**	**Probit**	**Complimentary Log-Log**
Significant Factors (α=0.10)	Lot 6 Lot 8 Layer 8	Lot 6 Lot 8 Layer 8	Lot 6 Lot 8	Layer 9	Layer 9	Layer 9	Layer 9	Layer 9	Layer 9
G (p-value)	52.381 (0.000)	52.368 (0.000)	52.337 (0.000)	51.402 (0.000)	51.399 (0.000)	51.392 (0.000)	51.168 (0.000)	51.158 (0.000)	51.137 (0.000)
Pearson (p-value)	0.0280972 (0.867)	0.0401750 (0.841)	0.0713576 (0.789)	0.0341 (0.853)	0.0370 (0.847)	0.0440120 (0.834)	0.0239 (0.877)	0.0334 (0.855)	0.0547531 (0.815)
Deviance (p-value)	0.0281218 (0.867)	0.0402199 (0.841)	0.0714682 (0.789)	0.0341 (0.853)	0.0370 (0.847)	0.0440098 (0.834)	0.0239 (0.877)	0.0334 (0.855)	0.0547564 (0.815)
Hosmer-Lemeshow (p-value)	0.0151858 (1.000)	0.0211868 (1.000)	0.0358298 (1.000)	0.0064 (1.000)	0.0068 (1.000)	0.0075645 (1.000)	0.0062 (1.000)	0.0086 (1.000)	0.0187298 (1.000)
Somers' D	0.16	0.16	0.16	0.16	0.16	0.16	0.16	0.16	0.16

Similar results were obtained from the training dataset with the upper 5% of the outliers removed (more than 5 total defects in a die). These results are presented in Table 4.5 as well. Goodness-of-fit measures have not improved considerably, so the wafer-level analysis seems to be more robust against outliers than the die-level study, but there are differences in which predictors are identified as significant.

Wafer-Level Logistic Regression Validation.

Since the results were similar for both of the refined datasets, the model for the training set with 5% of the outliers removed was used for validation. Since there were no significant differences between the links, the logit link was

used to form the full model using Equation 4.1 where $\mathbf{X}'\boldsymbol{\beta}$ =1.40356 - 0.027(Layer 1) + 0.00393(Layer 2) + 0.002937(Layer 3) + 0.01582(Layer 4) - 0.038756(Layer 5) + 0.0237897(Layer 6) - 0.005593(Layer 7) - 0.00848(Layer 8) - 0.041995(Layer 9) + 0.030685(Layer 10).

The reduced model for the wafer level was formed using backward elimination. Using this method, the predictors were eliminated one by one according to which had the smallest z-statistic (largest p-value). First, due to their high p-values and inability to be used in predictive modeling, Lot and Wafer were removed, followed by Layer 2, Layer 1, Layer 4, Layer 8, Layer 3, Layer 6, Layer 5, and Layer 10, respectively. A cutoff value of α=0.1 was used, as done with the previous models. This reduced model takes the form

$$P = \frac{1}{1 + e^{-(0.917234 + 0.0065599 * L7 - 0.0174814 * L9)}} \tag{4.3}$$

to predict the proportion of dice that will pass. This reduced model had p-values of 0.030, 0.027, and 0.555 for the Pearson, Deviance, and Hosmer-Lemeshow goodness-of-fit tests, respectively.

The validity of the wafer-level GLM models can be assessed in ways similar to those used for the die-level models. Figure 4.8 shows a plot of the actual yields compared to the predicted yield values for dice with defects from the wafer-level full and reduced models, the die-level nested reduced model, and Seeds' Model. As seen in the die-level plot, the GLM models are closer to the actual values than the underestimating Seeds' Model, but a good amount of variability is seen in the wafer-level results. Figure 4.8 demonstrates that the die-

level nested GLM model has the greatest and most consistent predictive power for these data.

Figure 4.9 shows the predicted yields for each model as well as the actual yield for each of the 24 wafers in the dataset. In this chart, it is clear that the models from the literature consistently underestimate the yield. While the GLM models (full logit and reduced logit) are closer to the actual yields, their behaviors are not as smooth as the other models. This can be explained both by the fact that these models take into account more specific information (the number of defects on specific layers on a die rather than the average defects per die) and by the fact that there can be other contributors to yield loss other than defect counts alone. The die-level nested reduced logit model shows very good performance to these test data, though, both in being nearest to the actual yield and in showing more stable behavior as is also shown in Figure 4.8.

The behavior of the models shown in Figure 4.9 shows varying levels of correlation to the actual yield results. To assess correlation, Pearson correlation coefficients may be calculated and compared for the different models. These results are shown in Table 4.6. The results show the models from the literature (Y1 through Y9) are significantly correlated to the actual results at the $\alpha=0.1$ level of significance. The wafer-level GLM models do not share this distinction. The highest correlation is seen with the die-level nested reduced logit GLM model with a Pearson correlation coefficient of 0.819 and a p-value of 0.001 showing this model has by far the strongest correlation to the actual results.

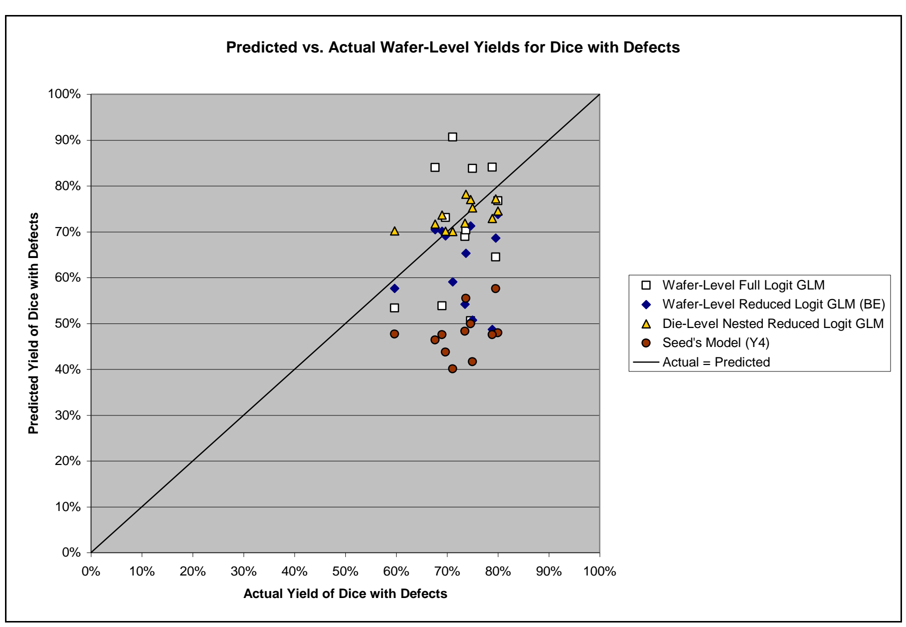

Figure 4.8. Predicted vs. Actual Yield of Dice with Defects. This figure applies the wafer-level GLM models, a die-level model, and Seed's Model to the test data (no outliers removed). While the GLM models are closer predictions than Seed's Model, the die-level model shows the best performance in terms of both accuracy and precision.

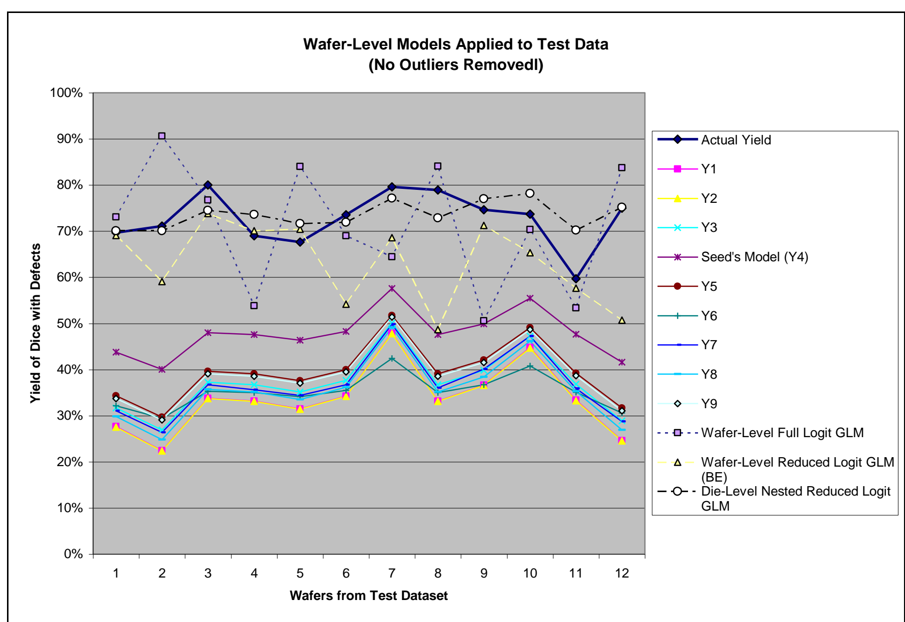

Figure 4.9. Wafer-level yield model predictions for the test data. The historical models (Y_1-Y_9) underestimate the actual yield significantly. The GLM models are nearer to the actual yield values, but the wafer-level full model GLM shows much variability. The wafer-level reduced logit GLM's stable prediction gives little value. Of the GLM models, the die-level model shows closer predictions to the actual yields as well as strong correlation to the changes from wafer to wafer.

Table 4.6. *Comparison of Pearson correlation coefficents between models and actual yields using test data*

Model	Pearson Correlation Coefficient with Actual Yields for Test Wafers	P-value
Y_1	0.498	0.099
Y_2	0.498	0.099
Y_3	0.498	0.099
Y_4	0.497	0.100
Y_5	0.498	0.100
Y_6	0.497	0.100
Y_7	0.508	0.091
Y_8	0.498	0.099
Y_9 (alpha = 3.33)	0.498	0.100
Wafer-Level Full Logit GLM	0.078	0.809
Wafer-Level Reduced Logit GLM	-0.048	0.881
Die-Level Nested Reduced Logit GLM	0.819	0.001

At the wafer level, the MSE and MAD values calculated using the test data and applying each of the 12 models are shown in Table 4.7. These are also presented graphically in Figure 4.10. The wafer-level full logit GLM model shows a 56.6% improvement over the next best model from the literature (Y_4) in terms of MSE, and 73.8% improvement in terms of MAD. Even more impressive is the die-level nested reduced logit GLM that shows a 68.9% improvement in MSE and a 90.1% improvement in MAD over Seeds' Model (Y_4).

Table 4.7. *Mean Squared Error (MSE) and Mean Absolute Deviation (MAD) for Model Comparisons at the Wafer Level (%)*

	Y1	Y2	Y3	Y4	Y5	Y6	Y7	Y8	Y9	Wafer-Level Full Logit GLM	Wafer-Level Reduced Logit GLM (BE)	Die-Level Nested Reduced Logit GLM
MAD	0.52	0.52	0.48	0.37	0.46	0.50	0.49	0.50	0.46	0.162	0.219	0.116
MSE	0.27	0.27	0.23	0.14	0.21	0.25	0.24	0.25	0.22	0.037	0.057	0.014

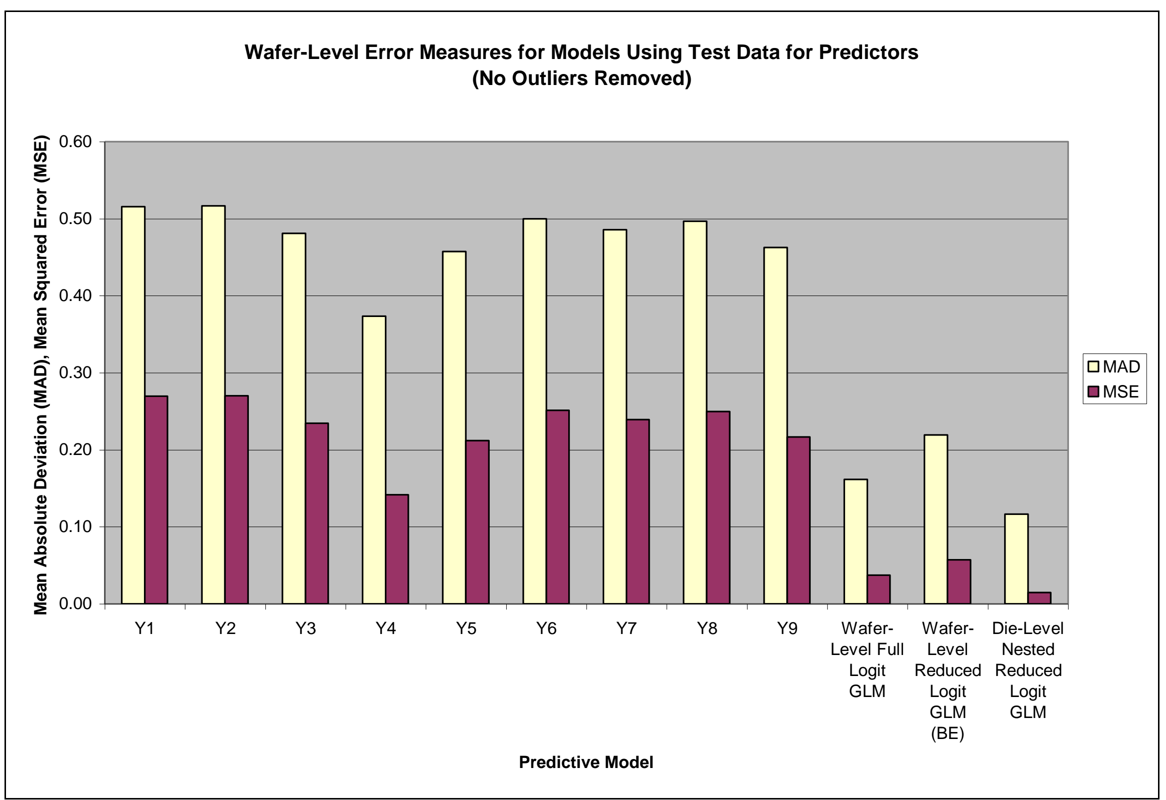

Figure 4.10. Mean Squared Error (MSE) and Mean Absolute Deviation (MAD) measures for the nine models from the literature and the GLM models. The GLM models significantly outperform previous models in these measurements of error with the best model being the die-level nested reduced logit GLM.

Summary

A number of conclusions are drawn from this phase of study. First, generalized linear models, such as logistic regression, can be used to successfully model semiconductor yield based on defect data. This empirical modeling approach can be applied to devices of various sizes and types. While this

approach does not develop a general model that can be used across different products, the simplicity of this modeling strategy makes it easy to apply to individual products to optimize yield prediction accuracy.

These generalized linear models have two primary advantages. First, the die-level models created can predict yield very well. This can be beneficial in product planning (for both the product and the process) and for yield improvement efforts for the device. While this approach is recommended primarily for application to ongoing products, the models may provide a good basis for predicting yield for new products that are similar to a device already modeled. A second advantage is in the power these models have to identify significant predictor variables. This can be helpful in diagnosing problems and finding areas of improvement that can improve quality and reduce testing time. For example, in the die-level nested GLM models, defects found in Layer 1 were not found to be significant. This suggests that defects on Layer 1 may not need to be scanned and detected for this device. Elimination of these measures for a layer can save valuable processing time and improve overall equipment effectiveness (OEE). In addition, the layers or even specific wafers that are identified as significant in the building the model can be explored in more detail to better understand their influences on yield, and any process problems may be corrected. This information can be especially helpful for processing new devices as yields usually start lower and improve as the new process is optimized. Identifying and solving process and quality issues early in a product's life cycle can help a company reduce costs.

While this modeling strategy using GLMs is shown to be very effective, a practitioner needs to carefully consider and evaluate the types of models constructed and selected for use. Wafer-level GLM analyses, while showing adequate goodness-of-fit results, can be misleading and are not as accurate at prediction as die-level models in this study. At the wafer level, very few fabrication layers are identified as significant, and the predictive power of these models is limited. Also, the nested structure cannot be used at the wafer level unless more wafers are sampled and are sorted into groups. Given constraints on scan equipment and process times, regularly testing additional wafers is not a feasible option for semiconductor manufacturers.

Die-level nested models are most effective for these data. There are not significant differences between the different link functions, even with the large sample sizes used. The nested structure provides more detailed information about significant predictors, including specific wafers and die quadrants, and it removes the need to assume independence between all dice. The nested die-level logistic regression models also show the best predictive power at both the die- and wafer-levels of aggregation.

Outliers can have a strong impact on model adequacy and on which predictors are significant for the model. The best results were obtained by removing the dice that had more than 5 total defects. (This corresponded to the top 5% of the total defects per die.) Validation testing on this model using a test dataset that included outliers proved the predictive capability of these models.

Chapter 5

SEMICONDUCTOR YIELD MODELING USING GENERALIZED LINEAR MIXED MODELS

Introduction

The results shown in Chapter 4 indicate the promise of using GLMs for semiconductor yield modeling. These fixed-effects models do not have the ability to account for the random sampling that is necessary in a fab environment, though. GLMs assume complete randomization, but commonly in practice only certain lots and/or wafers are sampled for defect scans. For the data studied in this research, only two wafers of twenty-five in every tenth lot were scanned for defects. While the nested GLM models account for the hierarchical structure of the sampling, they do not consider the nested effects as random. This suggests a violation of the GLM assumptions and indicates generalized linear mixed models (GLMMs) should be used to account for random effects such as lot and wafer.

Recall from Chapter 2 that there are two approaches when using GLMMs, the batch-specific model and the population-averaged model. The formulas for the expected values for these models are found in Equations 2.34 and 2.35 for the batch-specific and the population-averaged models, respectively. The batch-specific approach includes the random effects and provides predictions for each different random factors setting. Population-averaged models are designed to provide a more general trend across an entire population. In modeling semiconductor yield, both these approaches are appropriate for different types of applications. Batch-specific models allow estimates of slopes and/or intercepts

for each random factor setting, which can be helpful in identifying significant differences or in creating models for those specific effects (i.e. locations, patients, etc.). The population-averaged models create a marginal model that accounts for the random factors but does not provide estimates for them in the model and is used primarily for predicting across the population as a whole.

In some GLMM modeling applications, the random effects are clear. For example, a medical study may follow a particular participant over time, or a designed experiment may need to be run in split plots for hard-to-change factors. Sometimes, though, the random effects modeling may not be this straightforward. Especially with a case having multiple random effects, determining which random effects should be used in modeling and which GLMM structure is most appropriate must be carefully considered.

A modeling strategy for using GLMMs to model semiconductor yield can be useful to practitioners and may also provide guidelines that can be applied in other areas and industries as well. The advantages of this approach include being able to identify random effects, such as specific lots or wafers, that are significantly different from a baseline and to account for the random effects in the model without incorrectly assuming them to be fixed as with a GLM approach.

This research extends that from Chapter 4 by using an extended dataset to study the impact of using GLMMs, both batch-specific and population-averaged models, in various forms to model semiconductor yield. The effects of using different link functions and using different sample sizes will also be studied and discussed. This chapter is organized to first describe the dataset used in the

analysis. The model building approach is described in the next section. Next, the die-level results for the models are presented, followed by the wafer-level results and a summary.

Data Description

The data used in this phase of the research were obtained and cleaned as described in Chapter 3 and as used in Chapter 4, but this dataset is larger than the one used in Chapter 4 to advance the study. The data used in this phase included 126 lots (252 wafers) for the device described in Chapter 3. Of these, 168 wafers (84 lots) were randomly selected to be used for training the data, and 84 wafers (42 lots) were chosen for testing the models. At the die-level, 23,296 dice were used as the training dataset, after removing outliers that contained more than nine defects. The test dataset was made up of 11,240 dice. No outliers were removed from the test dataset to better assess model validity.

Model Building

Several models were constructed using the training dataset. These models were examined at both the die and wafer levels and were analyzed for comparisons at various sample sizes and using different link functions. A matrix displaying the models developed is shown in Table 5.1. The GLM models and the GLM nested models are analogous to those described in Chapter 4. As in Chapter 4, predictor variables for the die-level models included Lot, Wafer, Radial Distance, Die Quadrant, the number of layers with defects, and the count

of defects found on each of the ten layers. For GLM models, the lot and wafer factors were included as fixed effects in the model. In nested GLM models, the Wafer(Lot) nested effect was included as fixed. In the GLMM models, Lot, Wafer, or the Wafer(Lot) nested effects were included in the models as random effects. At the wafer level, Radial Distance and Die Quadrant were no longer considered as factors, and the predictors included the total number of layers with defects and defect counts for each layer as summed across the entire wafer.

Table 5.1. *Models Analyzed for Comparisons*

Models	Sample Sizes (Number of Wafers)	Links	Type of GLMM Effect
GLM	30, 168 60, 90, 120, 150	Logit, Probit, CLL Logit	None
Nested GLM	30, 168 60, 90, 120, 150	Logit, Probit, CLL Logit	None
GLM with Overdispersion	30, 168 60, 90, 120, 150	Logit, Probit, CLL Logit	None
Lot Random	30, 168 60, 90, 120, 150	Logit, Probit, CLL Logit	G and R
Lot Random with Overdispersion	30, 168 60, 90, 120, 150	Logit, Probit, CLL Logit	G
Wafer (Lot)	30, 168 60, 90, 120, 150	Logit, Probit, CLL Logit	G and R
Wafer (Lot) with Overdispersion	30, 168 60, 90, 120, 150	Logit, Probit, CLL Logit	G
Wafer Random	30, 168 60, 90, 120, 150	Logit, Probit, CLL Logit	G and R
Wafer Random with Overdispersion	30, 168 60, 90, 120, 150	Logit, Probit, CLL Logit	G

Something to consider in building these GLMM models is which degrees of freedom method to use in the analysis. The default in SAS 9.2 PROC

GLIMMIX for GLMs and GLMs with overdispersion is the RESIDUAL method. The default for random-effects models with only R-side effects and the subject option specified (population-averaged models) is the BETWITHIN method, which divides the residual degrees of freedom into between-subject and within-subject components. For G-side random effects (batch-specific models), the default method is CONTAIN, which uses the containment method. Another option for modeling is the KENWARDROGER option, which involves inflating the estimated variance-covariance matrix of the fixed and random effects and then computes Satterthwaite-type degrees of freedom from the adjustment. Sattherthwaite degrees of freedom require more computing time, and the small sample properties are not extensively studied (SAS, 2006). For the models presented in this chapter, the default degrees of freedom methods were used in SAS.

Another option in the model building requires selecting the type of the covariance structure. The default method in SAS PROC GLIMMIX for the RANDOM statement is TYPE=VC, or variance components, which uses a simple diagonal covariance matrix and models a different variance component for each random effect (SAS, 2006). For random effects that follow a subject over time, AR(1) or ARMA(1,1) may be desirable types to specify. Another option is the TYPE=CS, which specifies the compound-symmetry structure and has constant variance and constant covariance. This structure arises naturally with nested random effects, such as split-plot experiments (SAS, 2006). For the models described in this chapter, the G-side random effects (batch-specific models) used

TYPE=VC, and the R-side random effects (population-averaged) models used TYPE=CS to indicate the nested structure of the data. Examples of the SAS code used for these models are included in Appendix A.

Results

To help develop a strategy for using GLMMs in semiconductor yield modeling, many models were built in order to answer the following questions:

1. What are the differences between different GLMM modeling approaches and how do they compare to GLM models?
2. How does using different link functions affect GLMM models?
3. How does sample size impact GLMM model results?

The first question was addressed by modeling the data with different random effects and comparing them to GLM models. Logit, probit, and complimentary log-log functions (Eq. 2.27, 2.28, and 2.29, respectively) were used to compare the differences at samples sizes of 30 wafers and 168 wafers. To examine the impact of using different sample sizes on the models, subsets of the training dataset were used: 30 wafers (3797 dice), 60 wafers (7900 dice), 90 wafers (11,868 dice), 120 wafers (16,537 dice), and 150 wafers (20,872 dice). The results of the study are broken up in to die- and wafer-level results.

Die-Level Model Results

The die-level models with different link functions were very similar within the sample size used. The significant factors (α=0.1) in the models are given for

the GLM models in Table 5.2 and for the GLMM models in Table 5.3. Table 5.2 shows there are very few differences between the models formed from the logit, probit, and complimentary log-log functions. Factors that differ between the models are underlined in Table 5.2.

Table 5.2. *Significant Fixed Effects for Die-Level GLM Models from t-tests*

	30 Wafers			168 Wafers		
Model	Logit	Probit	CLL	Logit	Probit	CLL
GLM	Intercept Lots 2, 4, 6, 10, 14, 23 TotLayWithDefs RadDist L2 L6 L7 L8 L9 L10	Intercept Lots 2, 4, 6, 10, 14, 23 TotLayWithDefs RadDist L2 L3 L6 L7 L8 L9 L10	Intercept Lots 4, 6, 10, 14, 23 TotLayWithDefs RadDist L2 L6 L7 L8 L9 L10	Intercept Lots10, 11, 16, 17, 23, 24, 25, 51, 64, 77, 87, 100, 106, 111, 120, 121, 123, 134 TotLayWithDefs RadDist DieQuads 2,3 L2, L3, L4, L5, L6, L7, L8, L9, L10	Intercept Lots 10, 11, 16, 17, 23, 24, 25, 51, 64, 77, 87, 100, 106, 111, 120, 121, 123, 134 TotLayWithDefs RadDist DieQuads 2,3 L2, L3, L4, L5, L6, L7, L8, L9, L10	Intercept Lots 10, 16, 17, 23, 24, 25, 64, 77, 87, 99, 106, 120, 121, 134 TotLayWithDefs RadDist DieQuads 2,3 L2, L3, L4, L5, L6, L7, L8, L9, L10
Nested GLM	Intercept Waf 21(4) Waf 2(10) Waf21(10) Waf 2(16) Waf 2(23) Waf21(23) TotLayWithDefs RadDist DieQuad2(2) L2 L6 L7 L8 L9 L10	Intercept Waf 21(4) Waf 2(10) Waf21(10) Waf 2(16) Waf 2(23) Waf21(23) TotLayWithDefs RadDist DieQuad2(2) L2 L6 L7 L8 L9 L10	Intercept Waf 21(4) Waf 2(10) Waf21(10) Waf 2(16) Waf 2(23) Waf21(23) TotLayWithDefs RadDist DieQuad2(2) L2 L6 L7 L8 L9 L10	Intercept Waf 2(2) Waf21(4) Waf 2(6) Waf21(6) Waf 2(10) Waf21(10) Waf 2(14) Waf21(14) Waf 2(19) Waf21(20) Waf 2(23) Waf21(23) & 54 other wafers TotLayWithDefs RadDist DieQuad 2(2), 2(21) L1, L2, L3, L4, L5, L6, L7, L8, L9, L10	Intercept Waf 2(2) Waf21(4) Waf 2(6) Waf21(6) Waf 2(10) Waf21(10) Waf 2(14) Waf21(14) Waf 2(19) Waf21(20) Waf 2(23) Waf21(23) & 56 other wafers TotLayWithDefs RadDist DieQuad 2(2), 2(21), 3(21) L1, L2, L3, L4, L5, L6, L7, L8, L9, L10	Intercept Waf 2(2) Waf21(4) Waf 2(6) Waf21(6) Waf 2(10) Waf21(10) Waf 2(14) Waf21(14) Waf 2(19) Waf21(20) Waf 2(23) Waf21(23) & 61 other wafers TotLayWithDefs RadDist DieQuad 2(2), 2(21), 3(21) L2, L3, L4, L5, L6, L7, L8, L9, L10
GLM with OD	Intercept Lots 2, 4, 6, 10, 14, 23 TotLayWithDefs RadDist L2 L6 L7 L8 L9 L10	Intercept Lots 2, 4, 6, 10, 14, 23 TotLayWithDefs RadDist L2 L3 L6 L7 L8 L9 L10	Intercept Lots 4, 6, 10, 14, 23 TotLayWithDefs RadDist L2 L6 L7 L8 L9 L10	Intercept Lots 10, 11, 16, 17, 23, 24, 25, 51, 64, 77, 87, 100, 106, 120, 121, 123, 134 TotLayWithDefs RadDist DieQuad 2,3 L2, L3, L4, L5, L6, L7, L8, L9, L10	Intercept Lots 10, 11, 16, 17, 23, 24, 25, 51, 64, 77, 87, 100, 106, 120, 121, 123, 134 TotLayWithDefs RadDist DieQuad 2,3 L2, L3, L4, L5, L6, L7, L8, L9, L10	Intercept Lots 10, 16, 17, 23, 24, 25, 64, 77, 87, 99, 106, 120, 121, 134 TotLayWithDefs RadDist DieQuad 2,3 L2, L3, L4, L5, L6, L7, L8, L9, L10

Note: α=0.1

The differences between different link functions is more apparent in the GLMM models, not in the different predictors indicated as significant, but rather in the problems with the models not converging. This is shown in Table 5.3.

Table 5.3. *Significant Effects for Die-Level GLMM Models from t-tests (α=0.1)*

	30 Wafers			168 Wafers		
Model	Logit	Probit	CLL	Logit	Probit	CLL
Lot Random (G)	*Did not converge.*	*Did not converge.*	*Did not converge.*	Intercept TotLayWithDefs RadDist DieQuads 2, 3 L2, L3, L4, L5, L6, L7, L8, L9, L10 Random Lots: 10, 16, 17, 23, 24, 25, 61, 67, 77, 86, 87, 99, 120, 121, 128	*Did not converge.*	*Did not converge.*
Lot Random (G) with OD	*Did not converge.*	*Did not converge.*	*Did not converge.*	*Did not converge.*	*Did not converge.*	*Did not converge.*
Wafer (Lot) G	Intercept TotLayWithDefs RadDist L2, L3, L6, L7, L8, L9, L10 Random: 2(10), 2(11), 2(16), 2(23), 21(23)	*Did not converge.*	*Did not converge.*	*Did not converge.*	*Did not converge.*	*Did not converge.*
Wafer (Lot) G with OD	Intercept TotLayWithDefs RadDist L2, L3, L6, L7, L8, L9, L10 Random: 2(10), 2(11), 2(16), 2(23), 21(23)	*Did not converge.*	*Did not converge.*	*Did not converge.*	*Did not converge.*	Intercept TotLayWithDefs RadDist DieQuads 2,3 L2, L3, L4, L5, L6, L7, L8, L9, L10 Wafer(Lot) Random: 2(10), 2(11), 2(16), 21(17), 2(23) & 26 other wafers
Wafer G	Intercept TotLayWithDefs RadDist L2, L3, L6, L7, L8, L9, L10 *G matrix not positive definite (no WafID est)*	Intercept TotLayWithDefs RadDist L2, L3, L6, L7, L8, L9, L10 *G matrix not positive definite (no WafID est)*	Intercept TotLayWithDefs RadDist L2, L6, L7, L8, L9, L10 *G matrix not positive definite (no WafID est)*	Intercept TotLayWithDefs RadDist DieQuads 2,3 L2, L3, L4, L5, L6, L7, L8, L9, L10 *G matrix not positive definite (no WafID est)*	Intercept TotLayWithDefs RadDist DieQuads 2,3 L2, L3, L4, L5, L6, L7, L8, L9, L10 *G matrix not positive definite (no WafID est)*	Intercept TotLayWithDefs RadDist DieQuads 2,3 L2, L3, L4, L5, L6, L7, L8, L9, L10 *G matrix not positive definite (no WafID est)*
Wafer G with OD	Intercept TotLayWithDefs RadDist L2, L3, L6, L7, L8, L9, L10 *G matrix not positive definite (no WafID est)*	Intercept TotLayWithDefs RadDist L2, L3, L6, L7, L8, L9, L10 *G matrix not positive definite (no WafID est)*	Intercept TotLayWithDefs RadDist L2, L6, L7, L8, L9, L10 *G matrix not positive definite (no WafID est)*	Intercept TotLayWithDefs RadDist DieQuads 2,3 L2, L3, L4, L5, L6, L7, L8, L9, L10 *G matrix not positive definite (no WafID est)*	Intercept TotLayWithDefs RadDist DieQuads 2,3 L2, L3, L4, L5, L6, L7, L8, L9, L10 *G matrix not positive definite (no WafID est)*	Intercept TotLayWithDefs RadDist DieQuads 2,3 L2, L3, L4, L5, L6, L7, L8, L9, L10 *G matrix not positive definite (no WafID est)*
Lot Random (R)	Intercept TotLayWithDefs RadDist L2, L3, L6, L7, L8, L9, L10	Intercept TotLayWithDefs RadDist L2, L3, L6, L7, L8, L9, L10	*Did not converge.*	Intercept TotLayWithDefs RadDist DieQuads 2,3 L2, L3, L4, L5, L6, L7, L8, L9, L10	Intercept TotLayWithDefs RadDist DieQuads 2,3 L2, L3, L4, L5, L6, L7, L8, L9, L10	*Did not converge.*
Wafer(Lot) Random (R)	Intercept TotLayWithDefs RadDist L2, L3, L6, L7, L8, L9, L10	Intercept TotLayWithDefs RadDist L2, L3, L6, L7, L8, L9, L10	Intercept TotLayWithDefs RadDist L2, L3, L6, L7, L8, L9, L10	*Did not converge.*	Intercept TotLaywithDefs RadDist DieQuads 2,3 L1, L2, L3, L4, L5, L6, L7, L8, L9, L10	*Did not converge.*

For the GLMM models shown in Table 5.3, the logit link seems to work best for nested random effects in batch-specific models with smaller sample size, since it is the only link function that returned a solution with Wafer(Lot) random for 30 wafers. The complimentary log-log function was the only link function to converge with the Wafer(Lot) random effect for the 168-wafer sample size, though. At the larger sample size, at least one of the link functions gave a solution, except in the cases when Lot was a random G-side effect with overdispersion and when Wafer(Lot) was a G-side random effect. Since the significant factors are so similar between the different link functions when they do converge, if convergence is an issue, changing the link function may be the best adjustment to make first.

None of the link functions used in Table 5.3 were able to estimate random intercepts for Wafer due to the G matrix not being positive definite for the batch-specific models. The population-averaged models with Wafer as a random effect also had problems as they did not converge within reasonable computing time, even with the small samples. This may be due to only having two wafers (2 and 21) identified to compare since the Wafer(Lot) random effects, which consider each wafer individually rather than simply the position of the wafer in the lot, produced meaningful results.

In comparing the GLM models to the GLMM models, there are some interesting similarities. The same factors are identified as significant in the GLM and GLM with overdispersion as with the population-averaged models (for both

Lot and for Wafer(Lot) random) with the exception of L3 being identified as significant in all the GLMM R-side models, but only the probit link GLM model.

The GLMM batch-specific models with Wafer(Lot) as a random effect have fewer wafers identified as significant (α=0.1) than the nested GLM model, and there are also some differences between the wafers that are identified in the models. These are shown in Figure 5.1 for the 30-wafer models. Figure 5.2 shows a sample of the wafers found to be significant in the 168-wafer models by looking only at wafers identified through Lot 23 so as to be consistent with the 30-wafer models. In comparing the figures, more wafers are identified in the 168-wafer models for nested GLM structures (six wafers in the 30-wafer sample to 12 wafers in the 168-wafer sample), while the GLMM models both had five wafers identified as significant. Both Figures 5.1 and 5.2 show that the GLMM models identify significant wafers not detected by the nested GLMs that have high yields (87.17% for Lot 11, Wafer 2 and 88.94% for Lot 17, Wafer 2). The nested GLMs identify wafers as significant that the GLMMs neglect, and these wafers appear to have some potential patterns, such as edge defects on Lot 2, Wafer 2 and Lot 4, Wafer 21 and a cluster on Lot 6, Wafer 2. These patterns may be of interest to process engineers in helping detect and solve problems in the fabrication process.

As shown in examining the differences between the models created using only 30 wafers and those that used 168 wafers, sample size can play a part in modeling outcomes as well. To study this more, logit models were constructed using 30, 60, 90, 120, 150, and 168 wafers to compare the outcomes. These are shown in Tables 5.4, 5.5, and 5.6.

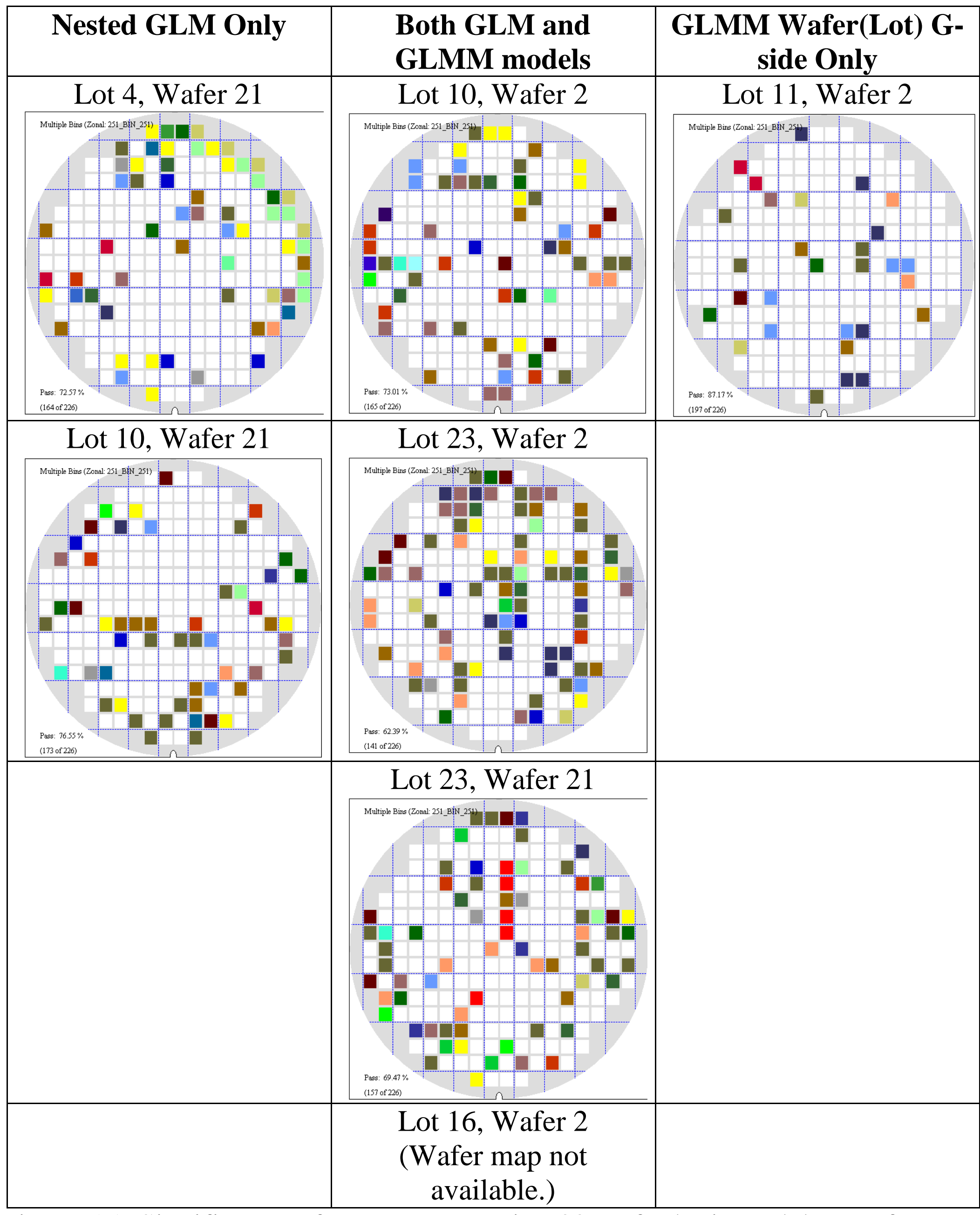

Figure 5.1. Significant wafer maps comparing 30-wafer logit models. Wafer maps for the wafers identified as significant in nested GLM models and GLMM models using Wafer(Lot) as a G-side random effect have some differences and similarities. The GLMM model seems to identify an unusually good wafer (Lot 11, Wafer 2) as well as wafers with poor yield. The nested GLM model identifies some unique wafers that may be of interest due processing problems with possible pattern defects showing (e.g. edge defects on Lot 4 Wafer 21).

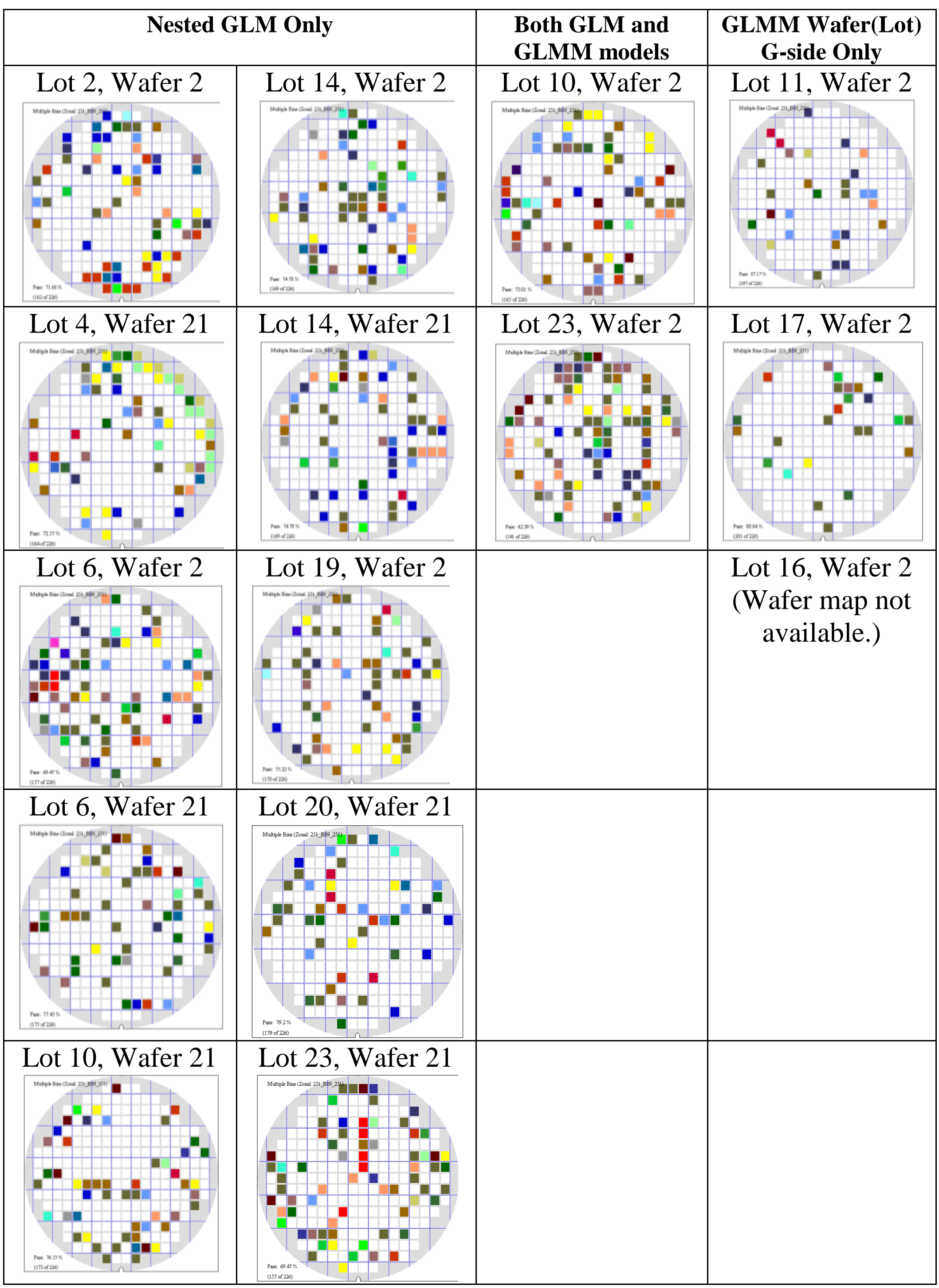

Nested GLM Only		Both GLM and GLMM models	GLMM Wafer(Lot) G-side Only
Lot 2, Wafer 2	Lot 14, Wafer 2	Lot 10, Wafer 2	Lot 11, Wafer 2
Lot 4, Wafer 21	Lot 14, Wafer 21	Lot 23, Wafer 2	Lot 17, Wafer 2
Lot 6, Wafer 2	Lot 19, Wafer 2		Lot 16, Wafer 2 (Wafer map not available.)
Lot 6, Wafer 21	Lot 20, Wafer 21		
Lot 10, Wafer 21	Lot 23, Wafer 21		

Figure 5.2. Significant wafer maps comparing 168-wafer complimentary log-log models. Again, the GLMM model identified high-yield wafers, and the nested GLMM identified some wafers that may have important patterns.

Table 5.4. *Die-level significant factors for GLM models using various sample sizes (logit link function, α=0.1)*

Model	30 Wafers	60 Wafers	90 Wafers	120 Wafers	150 Wafers	168 Wafers
GLM	Intercept Lots 2, 4, 6, 10, 14, 23 TotLayWithDef RadDist L2 L6 L7 L8 L9 L10	Intercept Lots 7, 10, 11, 16, 17, 23, 24, 25 TotLayWith Def RadDist DieQuad2 L2, L5, L6, L7, L8, L9, L10	Intercept Lots 10, 16, 17, 23, 32, 57, 60, 61, 67 TotLayWithDef RadDist DieQuad 2 L2 L6 L7 L8 L9 L10	Intercept Lots 7, 11, 16, 17, 18, 19, 20, 21, 24, 25, 26, 31, 34, 35, 39, 41, 43, 44, 46, 48, 50, 51, 64, 74, 76, 77, 87, 92, 95 TotLayWithDef RadDist DieQuads 2,3 L2, L3, L4, L5, L6, L7, L8, L9, L10	Intercept Lots 2, 4, 6, 10, 14, 19, 20, 23, 26, 29, 31, 32, 33, 37, 39, 43, 44, 47, 50, 57, 60, 61, 62, 63, 67, 68, 69, 72, 73, 75, 78, 80, 82, 86, 89, 90, 91, 95, 96, 99, 101, 107, 112, 114, 115, 116, 117, 120 TotLayWithDef RadDist DieQuads 2, 3 L2, L3, L4, L5, L6, L7, L8, L9, L10	Intercept Lots10, 11, 16, 17, 23, 24, 25, 51, 64, 77, 87, 100, 106, 111, 120, 121, 123, 134 TotLayWithDef RadDist DieQuads 2,3 L2, L3, L4, L4, L5, L6, L7, L8, L9, L10
Nested GLM	Intercept Waf 21(4) Waf 2(10) Waf21(10) Waf 2(16) Waf 2(23) Waf21(23) TotLayWithDef RadDist DieQuad2(2) L2, L6, L7, L8, L9, L10	Intercept Waf 2(7) Waf21(7) Waf 2(11) Waf 2(16) Waf 2(17) Waf21(17) Waf21(19) Waf 2(20) Waf 2(21) & 11 other wafers TotLayWith Def RadDist Die Quad2(2) L2, L5, L6, L7, L8, L9, L10	Intercept Waf 2(10) Waf 2(11) Waf 2(16) Waf 2(17) Waf21(17) Waf21(19) Waf 2(20) & 13 other wafers TotLayWithDef RadDist DieQuad 21(2) L2, L4, L6, L7, L8, L9, L10	Intercept Waf 2(10) Waf 2(11) Waf 2(16) Waf21(17) Waf 2(23) & 14 other wafers TotLayWithDef RadDist Die Quad 2(2), 21(2), 21(3) L2, L3, L4, L5, L6, L7, L8, L9, L10	Intercept Waf 2(2), Waf21(2), Waf 2(4), Waf21(4), Waf 2(6), Waf21(6), Waf 2(10), Waf21(10), Waf21(11), Waf 2(14), Waf21(14), Waf 2(19), Waf21(20), Waf21(21), Waf 2(23), Waf21(23) & 65 other wafers TotLayWithDef RadDist DieQuads 2(2), 21(2), 21(3) L1, L2, L3, L4, L5, L6, L7, L8, L9, L10	Intercept Waf 2(2) Waf21(4) Waf 2(6) Waf21(6) Waf 2(10) Waf21(10) Waf 2(14) Waf21(14) Waf 2(19) Waf21(20) Waf 2(23) Waf21(23) & 54 other wafers TotLayWithDef RadDist DieQuad 2(2), 2(21) L1, L2, L3, L4, L5, L6, L7, L8, L9, L10
GLM with OD	Intercept Lots 2, 4, 6, 10, 14, 23 TotLayWithDef RadDist L2, L6, L7, L8, L9, L10	Intercept Lots 7, 10, 11, 16, 17, 23, 24, 25, 34 TotLayWith Def RadDist DieQuad 2 L2, L5, L6, L7, L8, L9, L10	Intercept Lots 10, 16, 17, 23, 32, 57, 60, 61, 67 TotLayWithDef RadDist DieQuad2 L2, L6, L7, L8, L9, L10	Intercept Lots 7, 11, 16, 17, 18, 19, 20, 21, 24, 25, 26, 31, 34, 35, 39, 41, 43, 44, 46, 48, 50, 51, 64, 74, 76, 77, 87, 92, 95 TotLayWithDef RadDist DieQuads 2, 3 L2, L3, L4, L5, L6, L7, L8, L9, L10	Intercept Lots 2, 4, 6, 10, 14, 19, 20, 23, 26, 29, 31, 32, 33, 37, 39, 43, 44, 47, 50, 57, 60, 62, 63, 68, 69, 72, 73, 75, 78, 80, 82, 89, 90, 91, 95, 96, 101, 107, 112, 114, 115, 116, 117, 120 TotLayWithDef RadDist Die Quads 2, 3 L2, L3, L4, L5, L6, L7, L8, L9, L10	Intercept Lots 10, 11, 16, 17, 23,24, 25, 51, 64, 77, 87, 100, 106, 120, 121, 123, 134 TotLayWithDef RadDist DieQuad2,3 L2, L3, L4, L5, L6, L7, L8, L9, L10

Table 5.4 shows the GLM models constructed at the die-level for different sample sizes. As the sample size used to build the models changes, the significant factors change as well, with more significant factors being identified at the larger sample sizes. The most noticeable change in predicting significant layers comes between the 90-wafer and 120-wafer models.

Table 5.5 also shows the differences across these different sample sizes, but this table highlights the factors found to be significant in batch-specific GLMM models using the logit link function. As with the link model comparisons in Table 5.3, convergence was again an issue for these GLMM models. None of the models using a 90-wafer sample converged using the logit link. The sample sizes over 60 wafers had convergence issues for the Wafer(Lot) random effect models, and the **G**-matrix was not positive definite for any of the models using Wafer as a random effect, thus preventing any wafer position (2 or 21) from being identified as significant. Including the overdispersion parameter does not have an impact on these die-level models, suggesting there is not overdispersion present in the GLMM models, and Table 5.4 shows only very slight differences between the GLM and the GLM with overdispersion (OD) models.

Table 5.6 shows the population-averaged GLMM models using the different sample sizes and the logit link. Convergence issues again hindered drawing many conclusions. The 30-wafer model using Wafer as an R-side random effect took considerable computing time before producing the output that the model did not converge, so large sample sizes were not tried for this type of model. For the models that did converge, there seems to be very little difference between the significant fixed factors identified in the batch-specific GLMM and the population-averaged GLMM models.

Table 5.5. *Die-Level Significant Factors for GLMM Batch-Specific Models using Various Sample Sizes (logit link function, α=0.1)*

Model	30 Wafers	60 Wafers	90 Wafers	120 Wafers	150 Wafers	168 Wafers
Lot Random (G)	*Did not converge.*	Intercept TotLayWithDef RadDist DieQuad2 L2, L6, L7, L8, L9, L10 Random lots: 10, 16, 17, 23, 24, 29, 32	*Did not converge.*	*Did not converge.*	*Did not converge.*	Intercept TotLayWithDef RadDist DieQuads 2, 3 L2, L3, L4, L5, L6, L7, L8, L9, L10 Random Lots: 10, 16, 17, 23, 24, 25, 61, 67, 77, 86, 87, 99, 120, 121, 128
Lot Random (G) with OD	*Did not converge.*	Intercept TotLayWithDef DieQuad 2 L2, L6, L7, L8, L9, L10 Random lots: 10, 16, 17, 23, 24, 29, 32	*Did not converge.*	*Did not converge.*	*Did not converge.*	*Did not converge.*
Wafer (Lot) G	Intercept TotLayWithDef RadDist L2, L3, L6, L7, L8, L9, L10 Random: 2(10), 2(11), 2(16), 2(23), 21(23)	Intercept TotLayWithDef RadDist DieQuad2 L2, L6, L7, L8, L9, L10 Random: 2(10), 2(11), 2(16), 2(23), 21(23), 2(25), 2(32), 21(46)	*Did not converge.*	*Did not converge.*	*Did not converge.*	*Did not converge.*
Wafer (Lot) G with OD	Intercept TotLayWithDef RadDist L2, L3, L6, L7, L8, L9, L10 Random: 2(10), 2(11), 2(16), 2(23) 21(23)	Intercept TotLayWithDef RadDist DieQuad2 L2, L6, L7, L8, L9, L10 Random: 2(10), 2(11), 2(16), 21(17), 2(23), 21(23), 2(25), 2(32), 21(46)	*Did not converge.*	*Did not converge.*	*Did not converge.*	*Did not converge.*
Wafer G	Intercept TotLayWithDef RadDist L2,L3, L6, L7, L8, L9, L10 *G matrix not positive definite (no WafID est)*	Intercept TotLayWithDef RadDist DieQuad2 L2, L4, L6, L7, L8, L9, L10 *G matrix not positive definite (no WafID est)*	*Did not converge.*	Intercept TotLayWithDef RadDist DieQuads 2, 3 L2, L3, L4, L5, L6, L7, L8, L9, L10 *G matrix not positive definite (no WafID est)*	Intercept TotLayWithDef RadDist DieQuads 2, 3 L2, L3, L4, L5, L6, L7, L8, L9, L10 *G matrix not positive definite (no WafID est)*	Intercept TotLayWithDef RadDist DieQuads 2,3 L2, L3, L4, L5, L6, L7, L8, L9, L10 *G matrix not positive definite (no WafID est)*
Wafer G with OD	Intercept TotLayWithDef RadDist L2,L3, L6, L7, L8, L9, L10 *G matrix not positive definite (no WafID est)*	Intercept TotLayWithDef DieQuad2 L2, L4, L6, L7, L8, L9, L10 *G matrix not positive definite (no WafID est)*	*Did not converge.*	Intercept TotLayWithDef RadDist DieQuads 2, 3 L2, L3, L4, L5, L6, L7, L8, L9, L10 *G matrix not positive definite (no WafID est)*	Intercept TotLayWithDef RadDist DieQuad2, 3 L2, L3, L4, L5, L6, L7, L8, L9, L10 *G matrix not positive definite (no WafID est)*	Intercept TotLayWithDef RadDist DieQuads 2,3 L2, L3, L4, L5, L6, L7, L8, L9, L10 *G matrix not positive definite (no WafID est)*

Table 5.6. *Die-Level Significant Factors for GLMM Population-Averaged Models using Various Sample Sizes (logit link function, α=0.1)*

Model	30 Wafers	60 Wafers	90 Wafers	120 Wafers	150 Wafers	168 Wafers
Lot Random (R)	Intercept TotLayWithDef RadDist L2, L3, L6, L7, L8, L9, L10	*Did not converge.*	*Did not converge.*	*Did not converge.*	*Did not converge.*	Intercept TotLayWithDef RadDist DieQuads 2,3 L2, L3, L4, L5, L6, L7, L8, L9, L10
Wafer(Lot) Random (R)	Intercept TotLayWithDefs RadDist L2, L3, L6, L7, L8, L9, L10	*Did not converge.*	*Did not converge.*	Intercept TotLayWithDef RadDist DieQuad2 L2, L3, L4, L5, L6, L7, L8, L9, L10	*Did not converge.*	*Did not converge.*
Wafer (R)	*Did not converge.*	*(Did not try due to computing time for 30 wafers)*	*(Did not try due to computing time for 30 wafers)*	*(Did not try due to computing time for 30 wafers)*	*(Did not try due to computing time for 30 wafers)*	*(Did not try due to computing time for 30 wafers)*

Die-Level Model Validation

While one key goal of using GLM or GLMM modeling strategies may be to identfiy significant factors for understanding a process, another application is to use the models for predictive purposes. These models can be validated by testing their prediction errors and comparing them to previously published historic yield models. Several of these yield models are described in Chapter 2 and are summarized in Table 4.3. One difference between the historical yield models presented in Chapter 4 and those presented in this chapter is the value used for alpha in the negative binomial yield model (Y_9). Stapper and Rosner (1995) suggest a value of α=2 for the negative binomial model gave the best results in their work over a 16-year period, so α=2 was used in computing the negative binomial predicted values in this chapter. The GLM and GLMM models in this chapter were validated using a test dataset of 84 wafers containing 11,445 dice.

None of the dice were removed from this dataset so the models' robustness to outliers could be examined.

Figures 5.3 and 5.4 show the mean absolute deviation (MAD) and mean squared error (MSE) values for eight historical models (Y_1-Y_9) and GLM and GLMM models created with the logit link with sample sizes of 168 wafers and 30 wafers. When determining the MAD, the difference between the actual value (one for a passing die and zero for a failing die) and the predicted probability of the die to pass are calculated, then these absolute values are averaged for the test dataset. The MSE values are found by first squaring the MAD value for each die and then finding the average for the dice in the test dataset. These figures show values averaged for the entire test dataset (all data), the dice with fewer than ten defects on them, and the dice with ten or more defects on them to examine the models' predictive abilities for dice that have an unusually large number of defects on them.

The MAD values for the GLM and GLMM models in Figure 5.3 show these approaches give much better predictions than the historical models. The best results came from the nested GLM model created from 168 wafers with a value of 0.384, a 24.7% improvement over the best historical model, Seeds' model (Y_4 MAD=0.51). The GLMM models were consistent in prediction errors across models that used different random effects (Lot, Wafer, Wafer(Lot)), across the different sample sizes (30 and 168 wafers), and across the different approaches used for the GLMM (batch-specific G-side effects or population-averaged R-side effects). One interesting result is that for dice that had ten or

more defects, models built from the 30-wafer dataset produced the least amount of error. The 30-wafer GLM, GLMM with Wafer(Lot) G-side, Wafer G-side with overdispersion, Lot R-side, and Wafer(Lot) R-side models all shared the lowest MAD value of 0.302.

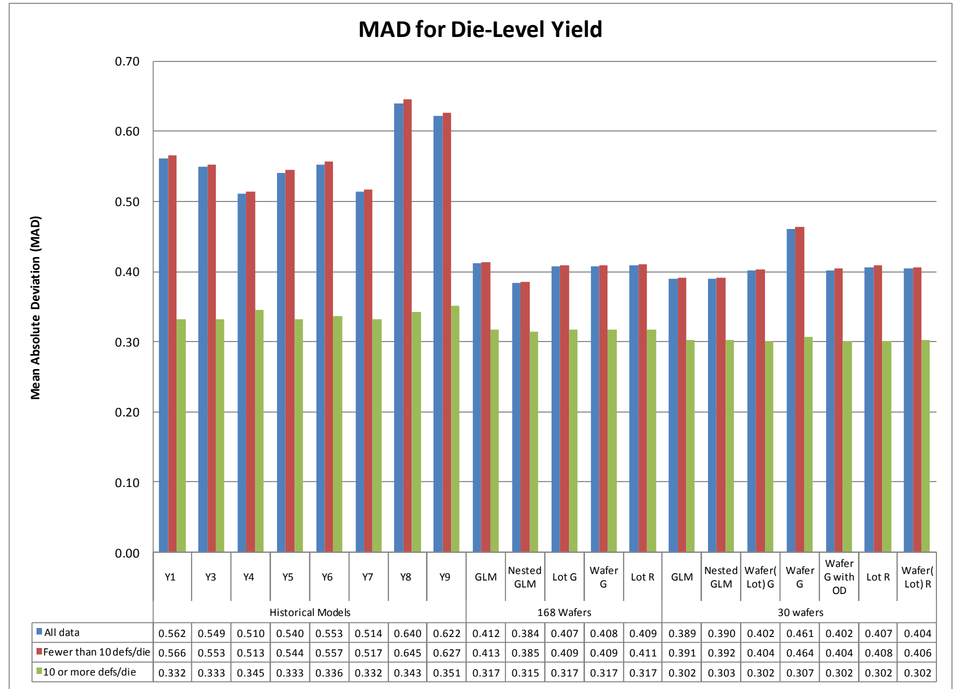

	Y1	Y3	Y4	Y5	Y6	Y7	Y8	Y9	GLM	Nested GLM	Lot G	Wafer G	Lot R	GLM	Nested GLM	Wafer(Lot) G	Wafer G	Wafer G with OD	Lot R	Wafer(Lot) R
	Historical Models								168 Wafers					30 wafers						
All data	0.562	0.549	0.510	0.540	0.553	0.514	0.640	0.622	0.412	0.384	0.407	0.408	0.409	0.389	0.390	0.402	0.461	0.402	0.407	0.404
Fewer than 10 defs/die	0.566	0.553	0.513	0.544	0.557	0.517	0.645	0.627	0.413	0.385	0.409	0.409	0.411	0.391	0.392	0.404	0.464	0.404	0.408	0.406
10 or more defs/die	0.332	0.333	0.345	0.333	0.336	0.332	0.343	0.351	0.317	0.315	0.317	0.317	0.317	0.302	0.303	0.302	0.307	0.302	0.302	0.302

Figure 5.3. Mean absolute deviation (MAD) for die-level yield models. The MAD for the GLM and GLMM models significantly outperforms the historical models.

Figure 5.4 shows the MSE values for the same models and supports similar conclusions. The best performing historical model (Y_4) has a MSE value of 0.287. The best performing GLM and GLMM models come from the 168-wafer dataset, where the GLM, Lot G-side, Wafer G-side, and Lot R-side all have MSE values of 0.205, which is a 28.6% improvement over the Y_4 model. Since larger deviations have more weight in MSE values after being squared, these results show that the predictive power of the GLMM models from larger sample

sizes can be just as strong as GLM models and even stronger than nested GLM models.

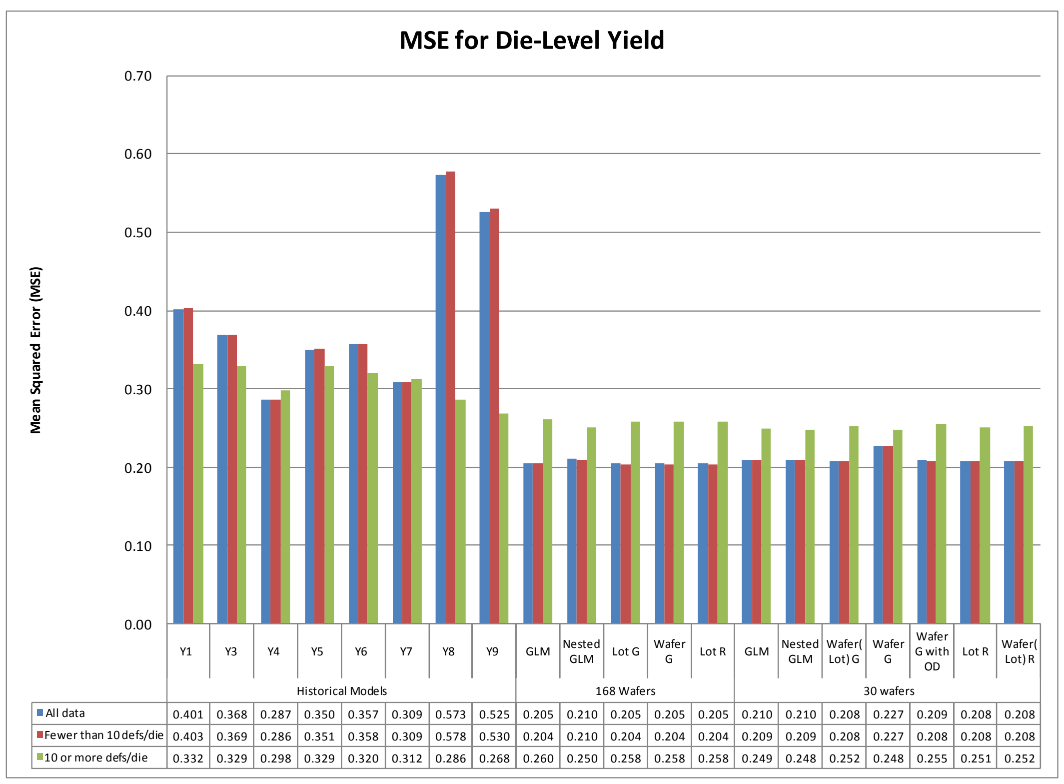

	Y1	Y3	Y4	Y5	Y6	Y7	Y8	Y9	GLM	Nested GLM	Lot G	Wafer G	Lot R	GLM	Nested GLM	Wafer(Lot) G	Wafer G	Wafer G with OD	Lot R	Wafer(Lot) R
	Historical Models								168 Wafers					30 wafers						
All data	0.401	0.368	0.287	0.350	0.357	0.309	0.573	0.525	0.205	0.210	0.205	0.205	0.205	0.210	0.210	0.208	0.227	0.209	0.208	0.208
Fewer than 10 defs/die	0.403	0.369	0.286	0.351	0.358	0.309	0.578	0.530	0.204	0.210	0.204	0.204	0.204	0.209	0.209	0.208	0.227	0.208	0.208	0.208
10 or more defs/die	0.332	0.329	0.298	0.329	0.320	0.312	0.286	0.268	0.260	0.250	0.258	0.258	0.258	0.249	0.248	0.252	0.248	0.255	0.251	0.252

Figure 5.4. Mean squared error (MSE) for die-level yield models. The MSE for GLM and GLMM models significantly outperforms the historical models.

Another way the model results can be compared is by looking at the number of dice predicted to pass on a wafer compared to the actual number of passing dice. Figures 5.5 and 5.6 show these results plotted for the 30-wafer and 168-wafer models using the logit link and compared to the actual values in the test dataset. For the 30-wafer models shown in Figure 5.5, the GLM and GLMM models all show much better predictions than Seeds' Model (Y_4), which is included for comparison. The GLMM model using Wafer as a G-side random effect gave predictions consistently lower than normal, but the addition of the

overdispersion factor to this model improved the performance to be much closer to the actual values and more in line with the other GLMM models. From this figure, the GLM and nested GLM models appear to give higher predicted values than the GLMM models.

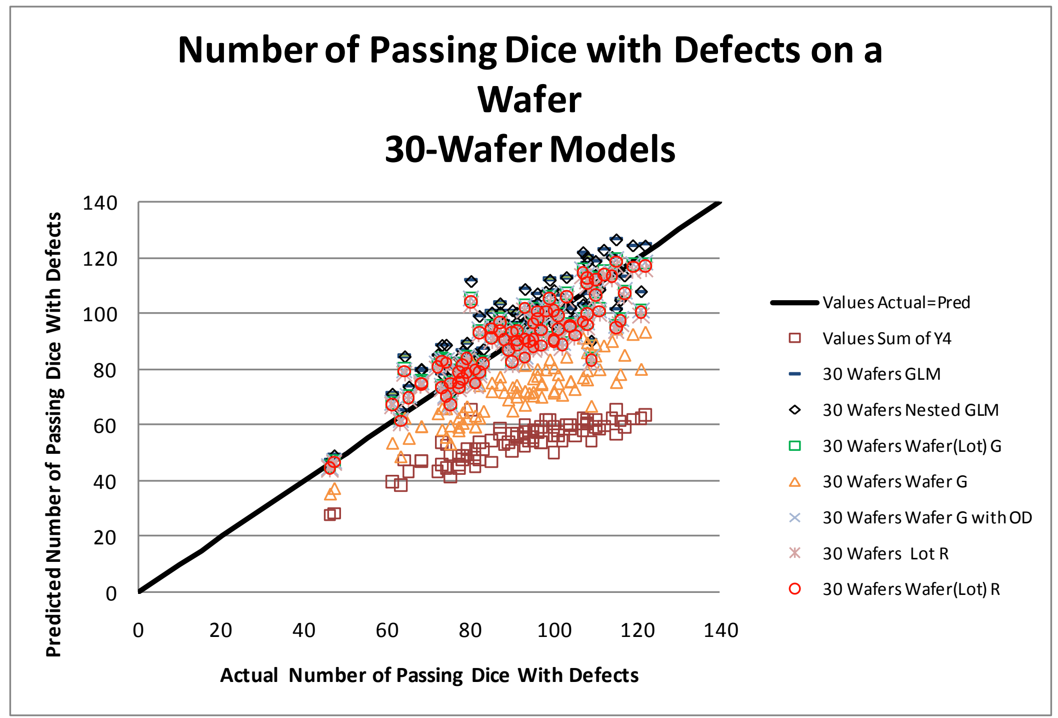

Figure 5.5. Predicted vs. actual number of passing dice on a wafer for the 30-wafer models using the logit link. Seeds' model (Y_4) is shown for comparison.

Figure 5.6 shows a similar chart for the models created with the 168-wafer training dataset. Again, the GLM and GLMM models clearly provide better predictions than the best historical model, Y_4, for these data. With this larger sample size, the Wafer G-side random effect model does not underestimate as it did for the smaller sample size. This shows at larger sample sizes, the model is robust even when the **G** matrix is not positive definite. Also, in this figure the overestimation by the nested GLM model is more apparent. These figures show

the predictive power of the GLMM models, both batch-specific and population-averaged, is strong and outperforms historical models, such as Seeds' model.

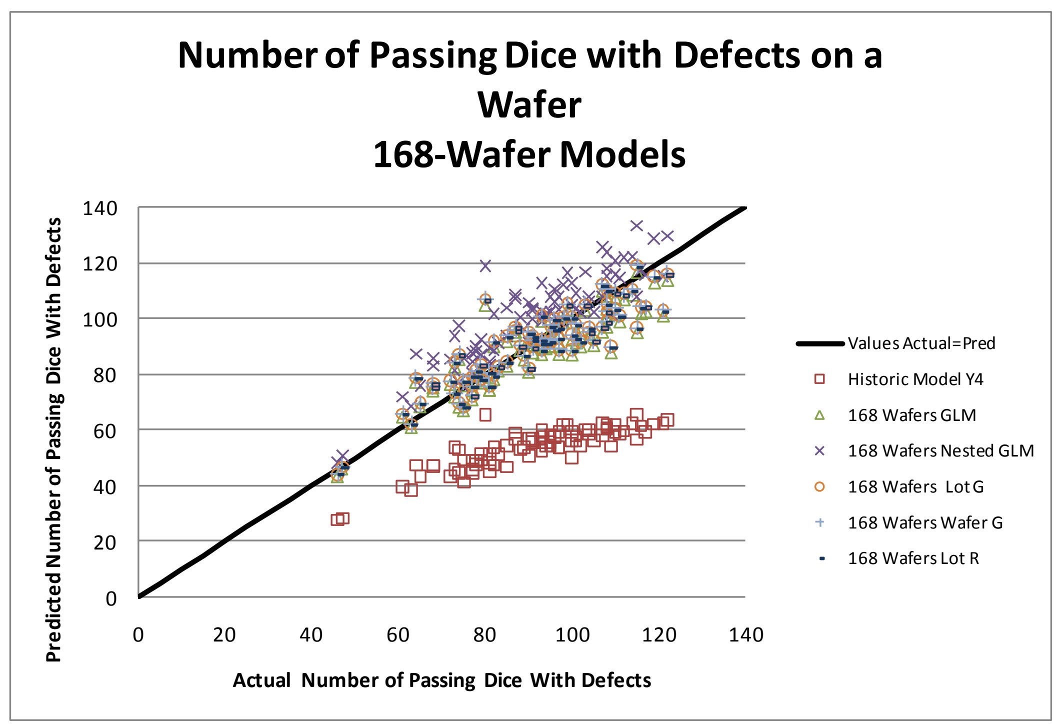

Figure 5.6. Predicted vs. actual number of passing dice on a wafer for the 168-wafer models using the logit link. Seeds' model (Y_4) is shown for comparison.

Wafer-Level Model Results

Wafer-level analyses may be beneficial as well, and studying the different levels of aggregation in this research helps determine the advantages of both approaches. At the wafer level, the nested GLM models cannot be constructed, as in Chapter 4, due to a lack of degrees of freedom with the particular nested structure and sampling used. With this exception, all the models in Table 5.1 were run at the wafer level to study the effects of sample size and link functions as well as the differences between the GLM and various GLMM models. The

significant factors for the wafer-level models comparing link functions for 30-wafer and 168-wafer datasets are summarized in Table 5.7.

Table 5.7. *Significant Fixed Effects for Wafer-Level Models from t-tests (α=0.1)*

	30 Wafers			168 Wafers		
Model	Logit	Probit	CLL	Logit	Probit	CLL
GLM	None	None	None	None	None	None
Nested GLM WafID(LotNo)	*(Not enough df)*	*(Not enough df)*	*(Not enough df)*	*(Not enough df)*	*(Not enough df)*	*(Not enough df)*
GLM with OD	TotLayWith Defs	TotLayWith Defs	None	Intercept Lots 16, 17, 23, 24, 25, 87 L9 L10	Intercept Lots 16, 17, 23, 24, 25, 87 L9 L10	Intercept Lots 17, 23, 24, 87, 120 L9 L10
Lot Random (G)	None *G-matrix not pos. def.*	None *G-matrix not pos. def.*	None *G-matrix not pos. def.*	None *G-matrix not pos. def.*	None *G-matrix not pos. def.*	None *G-matrix not pos. def.*
Lot Random (G) with OD	Intercept TotLayWith Defs L1, L6, L9, L10 Random lots: 4, 10, 17, 19	Intercept TotLayWith Defs L1, L6, L8, L9, L10 Random lots: 4, 10, 17, 19	TotLayWith Defs L1, L6, L8, L9, L10 Random lots: 4, 10, 17, 19	Intercept L2, L9, L10 Random lots: 24	Intercept L2, L9, L10 Random lots: 24	Intercept L2, L9, L10 Random lots: 24
Wafer(Lot) G	(No p-values produced) *G-matrix not pos. def.*	(No p-values produced) *G-matrix not pos. def.*	(No p-values produced) *G-matrix not pos. def.*	(No p-values produced) *G-matrix not pos. def.*	(No p-values produced) *G-matrix not pos. def.*	(No p-values produced) *G-matrix not pos. def.*
Wafer(Lot) G with OD	(No p-values produced) *G-matrix not pos. def.*	(No p-values produced) *G-matrix not pos. def.*	(No p-values produced)	*Did not converge.*	*Did not converge.*	(No p-values produced) *G-matrix not pos. def.*
Wafer G	None *G-matrix not pos. def.*	None *G-matrix not pos. def.*	None *G-matrix not pos. def.*	None *G-matrix not pos. def.*	None *G-matrix not pos. def.*	None *G-matrix not pos. def.*
Wafer G with OD	TotLayWith Defs L1, L4, L7, L8, L9, L10 Random wafers: none	TotLayWith Defs L1, L4, L7, L8, L9, L10 Random wafers: none	TotLayWith Defs L1, L4, L7, L8, L9, L10 Random wafers: none	Intercept L2, L9, L10 *G-matrix not pos. def.*	Intercept L2, L9, L10 *G-matrix not pos. def.*	L2, L9, L10 *G-matrix not pos. def.*
Lot Random (R)	Intercept TotLayWith Defs L1, L6, L9, L10	Intercept TotLayWith Defs L1, L6, L9, L10	TotLayWith Defs L1, L6, L8, L9, L10	Intercept L2, L9, L10	Intercept L2, L9, L10	Intercept L2, L9, L10
Wafer(Lot) Random (R)	TotLayWith Defs L1, L4, L7, L8, L9, L10	TotLayWith Defs L1, L4, L7, L8, L9, L10	TotLayWith Defs L1, L4, L7, L8, L9, L10	Intercept L2, L9, L10	Intercept L2, L9, L10	Intercept L2, L9, L10
Wafer (R)	TotLayWith Defs L1, L4, L7, L8, L9, L10	TotLayWith Defs L1, L4, L7, L8, L9, L10	TotLayWith Defs L1, L4, L7, L8, L9, L10	*Did not converge.*	*Did not converge.*	L2, L4, L9, L10

There are several interesting differences to observe in these model comparisons. First, at the wafer level, neither the GLM model nor the batch-specific GLMM models identified any effects as significant unless the overdispersion parameter was included in the model. Also, the GLM model with overdispersion for the 30-wafer models only identified at most one significant factor. From a process improvement standpoint, this is a limitation of the GLM models at small sample sizes. At larger sample size (168 wafers), the GLM models were able to identify more significant factors, but they did not identify Layer 2 as significant like the GLMM models for the 168-wafer dataset did. They did, though, identify more lots as significant (considering them as fixed effects) than the batch-specific GLMM did.

As shown in Table 5.7, there are very few differences in significant factors across link functions at either the small or the large sample size. There are not as many convergence problems with these wafer-level models as there were with the die-level models, which enable better understanding of the differences between the links. These wafer-level data suggest the complimentary log-log link seems to work better than the probit or logit links for the large sample size of 168 wafers in delivering a solution.

There are also some interesting similarities and differences in comparing the GLMM models. In comparing the batch-specific (including the overdispersion parameter) and the population-averaged GLMM models, the same predictive factors were identified as statistically significant in both types of GLMM for random effects of Lot and of Wafer. The batch-specific model was

able to identify specific significant lots. This suggest there is some robustness in model selection since choosing either the batch-specific or the population-averaged approach delivered the same results in terms of identifying the same significant fixed effects. For the 30-wafer models, there were differences in the results between the GLMM models that used only Lot as a random effect and those that used Wafer or Wafer(Lot) as a random effect. These differences are not seen in the 168-wafer models, with the exception of the complimentary log-log link with Wafer as an R-side random effect identifying an additional significant layer (L4). This consistency suggests that at large sample sizes, the choice of the random effect used in the model may not be critical to obtaining useful results.

The GLMM models in Table 5.7 that included Wafer(Lot) or Wafer as random G-side effects had problems with the **G** matrix not being positive definite (except for the 30-wafer models that included Wafer as a G-side random effect and included an overdispersion parameter). The wafer-level population-averaged GLMM models did not not have as many convergence issues as the die-level models did, though two of the links did not converge for the 168-wafer models using Wafer as an R-side random effect. None of the die-level models converged using Wafer as an R-side random effect, so the ability to obtain results for this model at the wafer level is an important difference to consider.

Since the nested GLM model cannot be assessed at the wafer level, it was interesting to see these results show that the nested Wafer(Lot) random effect could produce results for the population-averaged model. Also, these results were

the same as both the batch-specific models (with overdispersion) and the population-averaged models that considered Wafer alone random for the 30-wafer models.

To better understand the impact of sample size in the wafer-level models, the same GLM and GLMM models were constructed for samples of 30, 60, 90, 120, 150, and 168 wafers using the logit link function. These models are summarized in Table 5.8, which shows the significant factors identified for model (α=0.1). As in Table 5.7, the results show that for all of the sample sizes used, the models did not identify significant factors for GLM and GLMM batch-specific models that did not include an overdispersion parameter. Also, the batch-specific models with Wafer(Lot) as a random effect did not produce results, even when the overdispersion parameter was included.

One important question is: what is an appropriate sample size for these wafer-level models? In looking at the significant factors identified for each model across the different sample sizes, these results show that the results seem to stabilize at 150 wafers with there being no differences between the 150-wafer and 168-wafer GLMM models' significant effects. Note that this is not the case for the GLM model. A sample size of 150 wafers may be too large, though, for population-averaged models including Wafer as a random effect. For this type of model, no results were returned for datasets including 120 or more wafers. It is also of interest to see at what sample size the indifference between the GLMM models begins. At 90 wafers, all of the converging GLMM models (batch-specific with overdispersion and population-averaged) identify the intercept, L9,

Table 5.8. *Significant Effects for Wafer-Level Models from t-tests (logit link, α=0.1)*

Model	30 Wafers	60 Wafers	90 Wafers	120 Wafers	150 Wafers	168 Wafers
GLM	None	None	None	None	None	None
Nested GLM	*(Not enough df)*	*(Not enough df)*	*(Not enough df)*	*(Not enough df)*	*(Not enough df)*	*(Not enough df)*
GLM with OD	TotLayWithDefs	L6	Intercept	Intercept Lots 16, 24, 25, 87	Intercept Lots 10, 14, 23 57, 61, 67, 114, 120 L2, L9, L10	Intercept Lots 16, 17, 23, 24, 25, 87 L9, L10
Lot Random (G)	None *G-matrix not pos. def.*	None *G-matrix not pos. def.*	None *G-matrix not pos. def.*	None *G-matrix not pos. def.*	None *G-matrix not pos. def.*	None *G-matrix not pos. def.*
Lot Random (G) with OD	Intercept TotLayWithDefs L1, L6, L9, L10 Random lots: 4, 10, 17, 19	Intercept L8, L10 Random lots: None	Intercept L9, L10 Random lots: None	Intercept L2, L9 Random lots: None	Intercept L2, L9, L10 Random lots: 24, 120	Intercept L2, L9, L10 Random lots: 24
Wafer(Lot) Random (G)	(No p-values produced) *G-matrix not pos. def.*	(No p-values produced) *G-matrix not pos. def.*	(No p-values produced) *G-matrix not pos. def.*	(No p-values produced) *G-matrix not pos. def.*	(No p-values produced) *G-matrix not pos. def.*	(No p-values produced) *G-matrix not pos. def.*
Wafer(Lot) Random (G) with OD	(No p-values produced) *G-matrix not pos. def.*	*Did not converge.*	*Did not converge.*	*Did not converge.*	*Did not converge.*	*Did not converge.*
Wafer Random (G)	None *G-matrix not pos. def.*	None *G-matrix not pos. def.*	None *G-matrix not pos. def.*	None *G-matrix not pos. def.*	None *G-matrix not pos. def.*	None *G-matrix not pos. def.*
Wafer Random (G) with OD	TotLayWithDefs L1, L4, L7, L8, L9, L10 Random wafers: none	L10 *G-matrix not pos. def.*	Intercept L9, L10 *G-matrix not pos. def.*	Intercept L4, L9 *G-matrix not pos. def.*	Intercept L2, L9, L10 *G-matrix not pos. def.*	Intercept L2, L9, L10 *G-matrix not pos. def.*
Lot Random (R)	Intercept TotLayWithDefs L1, L6, L9, L10	Intercept L8, L10	Intercept L9, L10	Intercept L2, L9	Intercept L2, L9, L10	Intercept L2, L9, L10
Wafer(Lot) Random (R)	TotLayWithDefs L1, L4, L7, L8, L9, L10	Intercept L8, L10	Intercept L9, L10	Intercept L4, L9	Intercept L2, L9, L10	Intercept L2, L9, L10
Wafer Random (R)	TotLayWithDefs L1, L4, L7, L8, L9, L10	L8, L10	Intercept L9, L10	*Stopped because of infinite objective function.*	*Stopped because of infinite objective function.*	*Did not converge.*

and L10 as significant. There are some slight differences for the 120-wafer models with the models using Lot as a random effect identifying the intercept, L2, and L9 as significant while the Wafer (G-side) and Wafer(Lot) (R-side) models show the intercept, L2, and L9 to be significant. Any differences between significant factors across different types of GLMM models appear to be resolved for models containing 150 wafers or more.

Wafer-Level Model Validation

As with the die-level models, MAD and MSE can help compare the predictive power of the GLM and GLMM models compared to the historical models. At the wafer-level, these comparisons were made using the models developed for the 30-wafer and 168-wafer datasets. Adjusted models were also considered. These adjusted wafer-level models took the wafer-level GLM or GLMM and adjusted the forecasted yield from predicting that of the entire wafer to instead forecast the yield for only the defective dice. For example, the wafer-level GLMM prediction may be 75% yield for a wafer. This prediction, however, is really modeling the proportion of dice that have defects and pass, not a proportion of all the dice on the wafer. The adjusted models take this into account and assume that all non-defective dice will pass. To illustrate this, consider a wafer (Lot 8, Wafer 2 in the training dataset) that has 226 total dice on the wafer, 154 of them with detectable defects on at least one layer. Of these defective dice, 101 of them pass. The wafer-level GLM predicts 63.7% yield. The adjusted yield is found simply by taking:

$$\text{Adjusted model yield} = \frac{\text{Predicted number of passing defective dice} + \text{number of non-defective dice}}{\text{Total dice on the wafer}}$$

$$= \frac{0.637 * 154 + (226 - 154)}{226} = 75.26\%.$$

The actual yield for this wafer is 76.11% (172 passing dice), so the adjusted yield gives a much more accurate forecast and is fitting, considering the data used to build the GLM and GLMM models is based only on dice containing defects.

Die-level models were also included in these comparisons by summing the prediction probabilities for all the dice on a wafer to predict how many dice on the wafer would pass. These values were also adjusted while assuming non-defective dice will pass. For example, for Lot 8, Wafer 2, the die-level nested GLM predicted probabilities sum to 106.38 for the wafer. The adjustment simply takes:

$$\frac{106.38 + (226 - 154)}{226} = 78.9\%.$$

Figure 5.7 displays the mean absolute deviation (MAD) values for the historical yield models Y_1-Y_9, the wafer-level GLM and GLMM models from both the 30-wafer and 168-wafer datasets, the adjusted wafer-level models, and the adjusted die-level models. These values are calculated using the actual yields from the wafers in the test dataset (84 wafers). The chart shows that all the GLM and GLMM models signficantly outperform the historical models. The best of the previously published models is Y_4, Seeds' model, with a MAD value of 0.336 and an MSE value of 0.1205. Figure 5.7 shows a number of interesting relationships between the models. First, wafer-level GLM and GLMM models from the larger sample size (168 wafers) are very consistent in their prediction errors, regardless of the form of the model. This is not the case for the 30-wafer models, where

much more variation can be observed. For the non-adjusted wafer-level models, the GLM shows the lowest MAD (0.144 for 168 wafers and 0.174 for 30 wafers), but for the adjusted wafer-level models, the lowest errors come from the batch-specific GLMM with Lot and overdispersion random (MAD=0.048 for the 168-wafer model and 0.093 for the 30-wafer model) and the population-averaged model with Lot random (MAD=0.048 for the 168-wafer model and 0.092 for 30-wafer model), outperforming the GLM slightly.

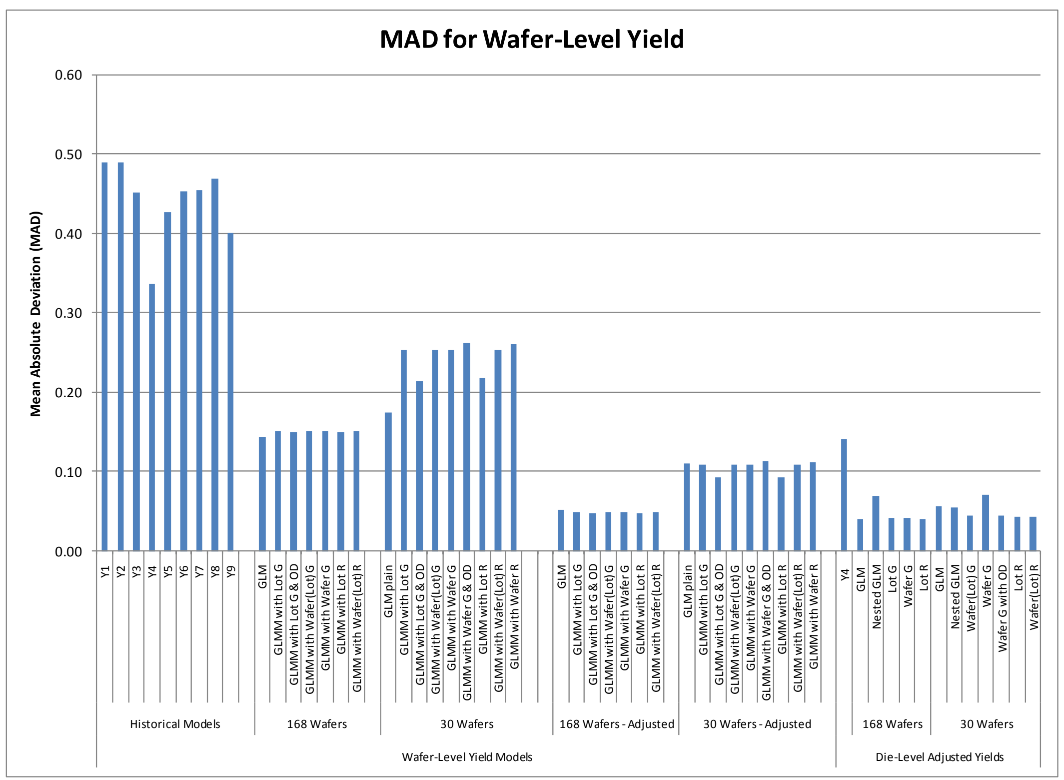

Figure 5.7. Mean absolute deviation (MAD) for wafer-level yield models. The MAD for the GLM and GLMM models significantly outperforms the historical models with the lowest values coming from the die-level adjusted GLM models.

The die-level adjusted models are also consistent across model type for the larger 168-wafer sample size, with the exception of the nested GLM having a higher MAD. At the 30-wafer sample size, the GLMM models, with the

exception of the GLMM with Wafer as a G-side random effect, give better predictions than the GLM or nested GLM models.

The lowest MAD value comes from the die-level adjusted GLM model from 168 wafers (0.040), but as Figure 5.7 shows, adjusted wafer-level models from a large sample (168 wafers) are nearly as accurate (within 1% yield) and are simpler to obtain for a wafer-level prediction purposes.

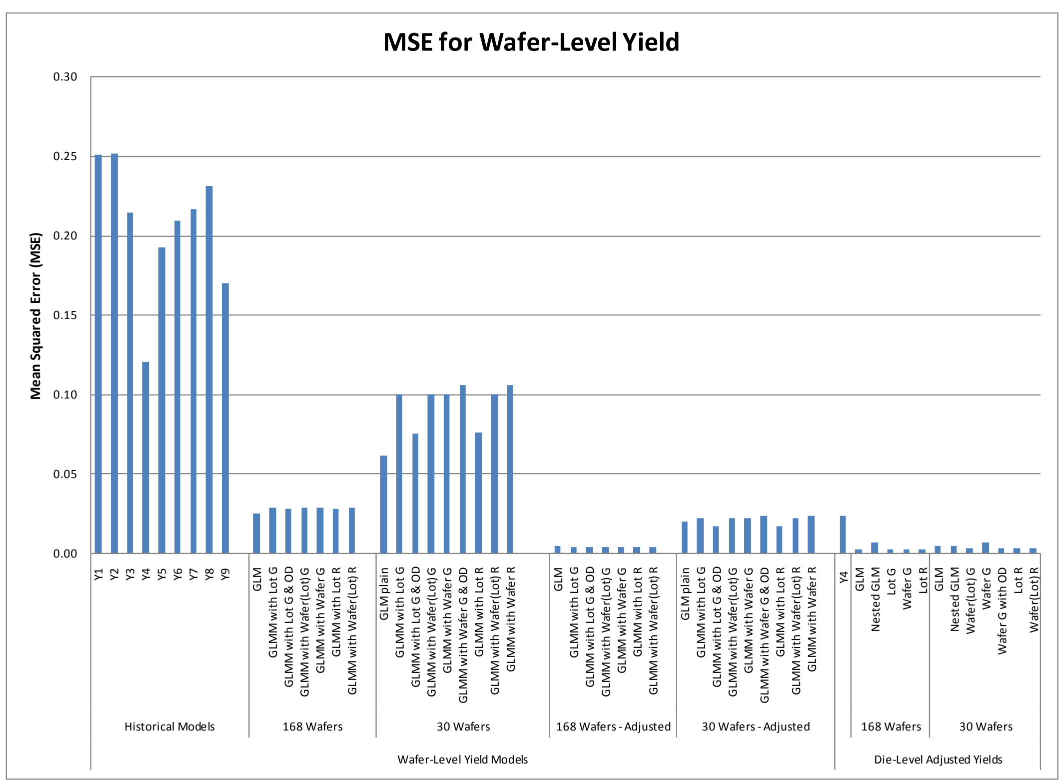

Figure 5.8. Mean squared error (MSE) for wafer-level yield models. The MSE for the GLM and GLMM models significantly outperforms the historical models with the lowest values coming from the die-level adjusted GLM models.

The mean squared errors for the models, shown in Figure 5.8, also support these conclusions. Again, the GLM and GLMM models significantly outperform the historical models, with the models coming from a larger dataset (168 wafers) being more accurate and consistent across model type than those created from the

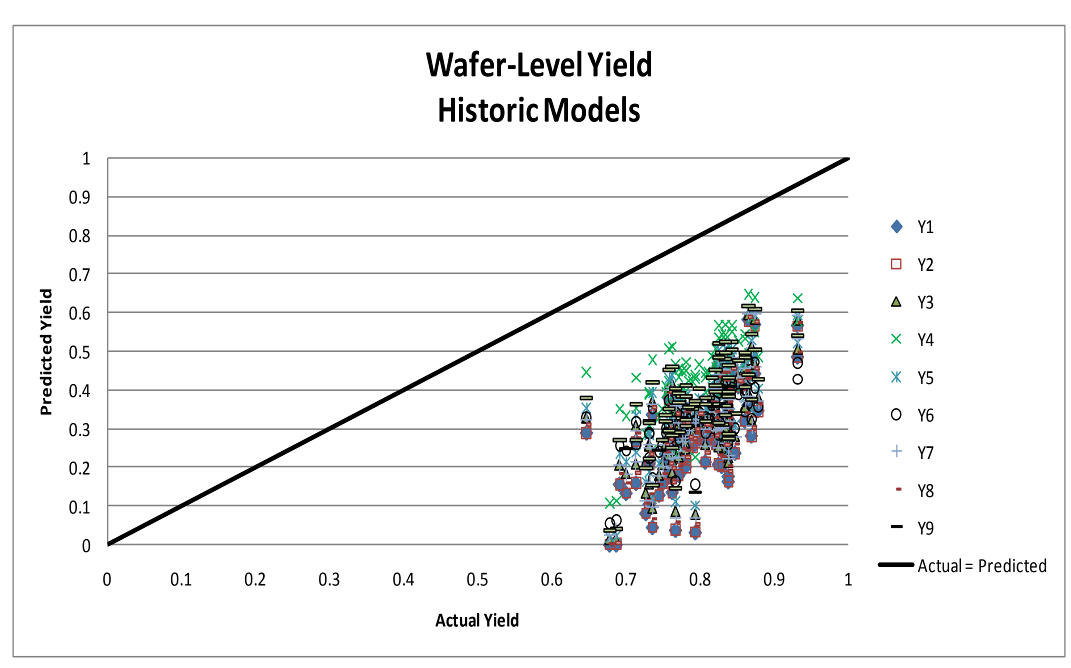

Figure 5.9. Predicted vs. actual wafer yields for wafer-level historical models Y_1-Y_9. The historical models significantly underestimate the actual yield.

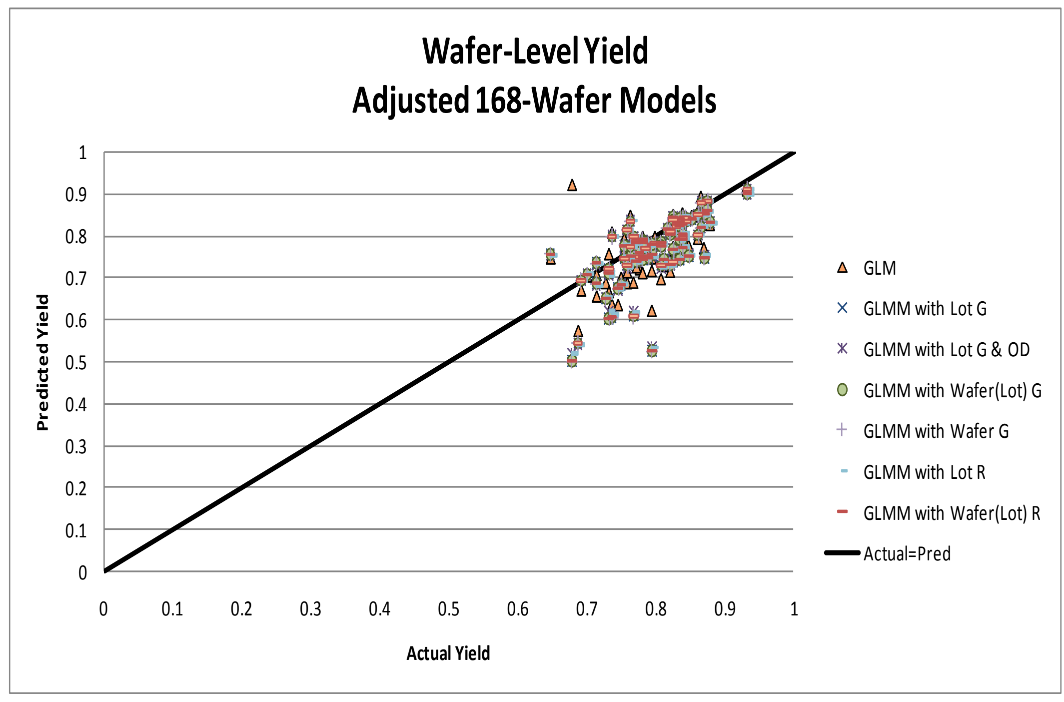

Figure 5.10. Predicted vs. actual wafer yields for adjusted wafer-level GLM and GLMM models. These models all give very similar predictions and are much nearer the actual yield values than the historical models shown in Figure 5.9.

30-wafer dataset. Again, the die-level adjusted models give the lowest values (MSE=0.0026 for the 168-wafer die-level adjusted GLM), but the adjusted wafer-level results from the 168-wafer dataset perform nearly as well (MSE=0.0042 for GLMM with Lot (G) and overdispersion and for GLMM with Lot (R)).

The predictive power of these models compared to the models of the past can also be shown by looking at the actual and predicted yields for the wafers in the test dataset. Figures 5.9 shows the actual and predicted values using the historic models Y1-Y9. Similar to the results seen at the die-level, these models severely underestimate the actual wafer yield. Figure 5.10 shows the adjusted wafer-level GLM and GLMM models' predicted values plotted against the actual wafer yield for the 168-wafer dataset. As shown in the MAD and MSE charts, there is very little difference between these models in terms of predicted values, and all these models are very near the actual yield values for the wafers in the test dataset.

Summary

Using GLMMs is a clear extension of using GLMs to model semiconductor yield, given the random sampling that is inherent in the fabrication process. This study compared many different GLMM approaches to GLM models using different link functions and sample sizes. The results in this study can guide a practitioner in using GLMMs as a modeling strategy to forecast semiconductor yield and as a process improvement tool for identifying critical layers that are most sensitive to defects and specific lots and wafers that may need further investigation.

One limitation of the study was the lack of convergence in many of the models examined. This may be due to the degrees of freedom method used. Preliminary models using the Sattherwaite degrees of freedom method (ddfm) for wafer-level models did not have as many problems with convergence, so using this method or the Kenward-Rogers approach, both available in PROC GLIMMIX in SAS, may provide more conclusive results when the default settings do not.

The results from this research can provide a meaningful modeling strategy for yield modeling or other applications, but the approach depends on the researcher's objectives. Different information is provided by the models at different levels of aggregation and through the different model types.

For a focus on process improvement, the die-level models described here can be very helpful in identifying significant process layers impacted by defects and in distinguishing important wafers or lots for further investigation. The GLMM models include high-yield wafers in those found to be significant, while the GLM models identify more wafers and tend to identify more low-yield wafers as significant. Some of the wafers identified by the GLM model appear to have some pattern defects, so this identification, either done at the end of the line as with this study or earlier in the fabrication process, may be helpful in detecting processing issues that can be resolved to boost yield on future wafers. Conversely, the high-yield wafers identified by the GLMM model may be helpful in studying optimal operating conditions that can be replicated in future fabrication. Also, at the die level GLM models identified a much larger number

of lots or wafers as significant compared to the GLMM models. This additional detection may lead to some false alarms in process improvement efforts, meaning some of the wafers or lots identified may actually be different from the baseline due to random effects rather than systematic problems.

Due to the convergence issues, it is not clear if one link function consistently outperforms the others at the die level, but there were very few differences between the results using different link functions when they all provided results. The die-level models did give the best predictions of wafer yield in terms of MAD and MSE, even for the small 30-wafer sample size. This suggests that if only a small dataset is available for modeling, die-level models should be used to predict wafer yield.

For a focus on wafer-level predictions that have little error and are robust as to model type, adjusted wafer-level models from large sample datasets can work very well. Sample sizes over 150 wafers seem to work best for wafer-level modeling, and the complimentary log-log link seems to work best for generating results at this larger sample size.

The wafer-level GLM and GLMM models all identified fewer significant factors than the die-level models, with the 150-wafer models selecting only L2, L9, and L10 as significant. These differences between the die- and wafer-level modeling may make a strong difference in detecting problems, and since the die-level models take advantage of more complete and specific information, the die-level models are most useful for process and yield improvement efforts.

The GLM and GLMM models significantly outperformed the models of the past in terms of prediction error. GLMM models offer a modeling approach that accounts for the random factors in a system without violating the assumptions of the model. This work shows that the GLMM models do this while providing additional insight into the process and maintaining or even improving prediction power compared to using GLMs.

Chapter 6

SEMICONDUCTOR YIELD MODELING INTEGRATING CART AND GENERALIZED LINEAR MODELS

Introduction

The approach used in building classification and regression trees (CART) is described in Chapter 2 and in full detail by Brieman, et al. (1984). Recall the main steps involved in CART are (1) building the tree through binary recursive partitioning by minimizing the impurity of the nodes, (2) pruning the tree using a cost-complexity parameter, and (3) selecting the best tree to avoid overfitting by using cross-validation techniques. This approach has shown promise in a variety of applications.

Many articles have been published that compare the use of classification trees with other approaches such as logistic regression. Costanza and Paccaud (2004) compare the use of linear regression, logistic regression, classification trees, and regression trees to predict occurrences of dyslipidemia. Skinner, et al. (2002) compare the use of cluster analysis, principal components, ordinary least squares regression, logistic regression, and CART to determine the cause of low yield wafers from unit probe testing. Chang and Chen (2005) consider CART models and negative binomial regression models to analyze freeway accident frequency. Khoshgoftaar and Seliya (2003) use CART-least squares, CART-least absolute deviation, S-PLUS, multiple linear regression, artificial neural networks, and case-based reasoning and compare these modeling techniques applied to

predicting software quality. Predicting essential hypertension was studied by Ture, et al. (2005) as they applied CART, Quick, Unbiased, Efficient Statistical Tree (QUEST), logistic regression, Flexible Discriminant Analysis (FDA), Multivariate Addititve Regression Splines (MARS), Multi-Layer Perceptron (MLP) and Radial Basis Function (RBF) neural networks to compare the models. These studies demonstrate the value of CART for handling large datasets that do not fit the assumptions required for more traditional statistical techniques.

CART's tree structure is easy for users to interpret and understand. If sufficient data are available to form the model, good predictions can be achieved using CART. The CART approach also is beneficial as a supplemental tool to other modeling techniques that provides a different type of information through the trees that are generated, including a "recipe" for groups such as high yield. Limitations mentioned include the limited predictive power of CART and the need for large datasets to construct meaningful models.

Some work has also been done to integrate CART or decision trees with other techniques to build new modeling approaches. Choi and Lee (2010) develop a method for selecting retaining wall systems to prevent failures. While previous studies in this area have used machine-learning techniques, the training datasets had to be very large to produce adequate prediction values. These large amounts of data are not feasible in the excavation area, so Choi and Lee (2010) demonstrate a different approach. They first use a series of logistic regression to determine significant factors, reduce multicollinearity, and adjust certain outcome groups. Next, the derived explanatory variables were examined against general

findings documented in the literature and were reviewed by process experts (Choi & Lee, 2010). The third step of the process was to develop these explanatory variables into a binary decision tree based on their impact on outcomes. Threshold values at each node were determined using ROC curves. The resulting decision tree showed high prediction rates (82.6% for retaining walls), which was much improved over using a data-mining algorithm along that produced a decision tree with accuracy of 58.7% (Choi & Lee, 2010).

Chandra, et al. (2009) use a variety of approaches to determine important factors and prediction accuracy for survival of dotcom companies, also called "click-and-mortar" corporations. They compare using multilayer perceptrons (MLP), CART, support vector machines (SVM), random forest (RF), and logistic regression (LR) to their dataset of 24 financial ratios for 240 dotcom companies. They compared both full and reduced (10 of the 24 financial ratios determined from *t*-tests) models and also explored the use of *ensembling* and *boosting* to improve the accuracy of the method. *Ensembling*, which aims to exploit each constituent model's unique features to capture different patterns in the dataset (Chandra, et al., 2009), was used to combine the results from RF, CART, and SVM by majority voting. For the dotcom data, Chandra, et al. (2009) found this ensembling approach did not improve the accuracy of the model compared to the individual classifying methods. *Boosting* focuses on producing a series of classifiers and attempts to produce new classifiers that are better able to predict examples for which the current ensemble's performance is not adequate (Chandra, et al., 2009). This is a more hierarchical approach where the misclassified

samples from using one approach, such as RF, are then modeled using another approach, such as CART. Any samples that are still misclassified by the second step (CART) are modeled using yet as third approach, such as MLP. Chandra, et al. (2009) found that this technique of boosting using RF+SVM+MLP to give the most accurate predictions.

Kuhnert, Do, and McClure (2000) consider combining CART, multivariate adaptive regression splines (MARS), and logistic regression to improve on logistic regression modeling by using the variable importance rankings from CART to aid in identifying important variables and also in visualizing each variable's contribution to the response being modeled. As they apply their approach to motor vehicle accident data, they show how using these approaches together can improve understanding of significant factors (risk factors such as seat belts and speeding), interactions (age and experience), and groups of special interest (middle-aged "rural" drivers). The approach of modeling with all three methods first contributed to a stronger logistic regression model by using the age*experience interaction identified by MARS and creating two logistic regression models after splitting the data into groups determined by CART (splitting by age < 27.5 years and age > 27.5 years), which allowed for better interpretation of the interaction (Kuhnert, et al., 2000).

Fu (2004) took a similar approach by using loglinear models and CART together to examine occurrences of low birth weight and preterm birth. The use of both CART and loglinear models produced more information about potential

relationships between the variables than using either approach alone. Using these methods jointly produced the benefits of both, including the odds ratios and ability to deal with multiple responses simultaneously for the loglinear model and the strength of being able to be used for predictive classification from the CART model. These methods are complementary for data analysis (Fu, 2004).

These integrated techniques show promise but do not fully explore the ways CART can be used with GLMs. For semiconductor yield modeling using defectivity data, Krueger, Montgomery, and Mastrangelo (2011) found die-level GLM models to best outperform yield models of the past (also described in Chapter 4), but interaction terms between the process layers were not considered. This is also the case for the GLMM models described in Chapter 5. Considering all the two-way interaction terms in the model would require an additional 45 predictor variables, significantly adding to the complexity of the model. Additional interactions may be present as well. CART's tree structure classifies each data point into a terminal node that is reached by following a series of splitting nodes. These terminal nodes form groups that may be statistically significant (as mentioned in Skinner, et al., 2002) and can be detected as such using a GLM. These groups may be of particular interest in developing "recipes" for reproducing those outcomes. Also, the CART tree can quickly identify which interactions may be of most interest to include in the GLM as predictors.

The purpose of this chapter is to describe a methodology that integrates CART and GLMs in a way that enhances the modeling results and interpretation

for process improvement and outcome prediction. An example using semiconductor yield data is provided to demonstrate the benefits of this integrated approach. This chapter is organized to first describe the methodology, then discuss the results, and summarize the findings.

Methodology

This integrated approach includes two main components: first, building decision trees using a method such as CART to determine terminal nodes and important interaction terms in the dataset and, second, building a GLM model using the factors in the dataset as well as indicator variables from the terminal nodes of the classification trees. The approach is described in detail and demonstrated through an example using semiconductor yield data.

Building Trees

Often in exploratory data mining, prior knowledge of the data may not exist. While a process owner may understand the important process factors and logical interactions, sometimes this information is unknown, such as for a new product or process or when only limited previous analyses have been performed.

Recall from Chapter 2 that nodes are split to minimize impurity based on a given method. The Gini splitting method is a well-known and commonly used standard splitting rule (see Equation 2.20). Other possible splitting criteria include symmetric Gini, entropy, class probability, twoing, and ordered twoing (CART for Windows User's Guide, Version 5.0, 2002).

An Example from Semiconductor Yield Modeling.

For the die-level data, the dataset included 18 possible predictors. These are shown and described in Table 6.1. Dice with more than nine defects were removed as outliers based on the results described in Chapter 4, leaving a training dataset of 23,296 dice that were used to build the trees. The number of defects on layers is found from a wafer scan performed after certain processing steps have been completed as described in Chapter 3. Krueger, et al. (2011) found the die-level data to be most accurate in GLM predictions for semiconductor yield modeling of this type, so the die-level data, rather than wafer-level data are used in this modeling approach.

Classification trees may be built in a number of different ways, and several options can be specified in the CART 5.0 software from Salford Systems based on methods developed by Breiman, Friedman, Olshen, and Stone (1984). To begin the tree building, this step is assumed to be exploratory in nature, without detailed prior knowledge. Due to the binary nature of the data, classification trees were chosen for the modeling. Case weights, prior probabilities, and misclassification costs were not specified for the dataset. Since the dataset of 23,296 records was well over 3,000 records, 10-fold cross-validation was selected to evaluate the performance of the results. The Gini splitting rule is the default splitting technique, and was selected for this work, though since "Favor even splits" was set to zero and a unit cost matrix used, the Gini, symmetric Gini, twoing, and ordered twoing splitting methods will produce

identical results. These splitting rules provide the greatest variety of differences for multilevel targets (CART for Windows User's Guide (Version 5.0), 2002). For these binomial data, the splitting rule choice is not as critical. Gini splitting works to produce small nodes with only one target class prevailing and works best for binary responses.

Table 6.1. *Die-Level Predictors*

Predictor	Variable Description	Predictor	Variable Description
Lot	Classification variable (84 levels in training data) that indicates which sampled lot the data are from.	Wafer	Classification variable (2 levels) that indicates which sampled wafer the data are from.
Die X	*x*-coordinate for the die.	Die Y	*y*-coordinate for the die.
Die Quadrant	From the (x,y) coordinates, dice were assigned a quadrant.	Radial Distance	From the (x,y) coordinates, a radial distance was calculated.
Total Layers with Defects	A count of the number of layers that contain at least one defect.	Total Defects per Die	A count of the total defects present on the die.
L1	Number of defects detected on Layer 1.	L2	Number of defects detected on Layer 2.
L3	Number of defects detected on Layer 3.	L4	Number of defects detected on Layer 4.
L5	Number of defects detected on Layer 5.	L6	Number of defects detected on Layer 6.
L7	Number of defects detected on Layer 7.	L8	Number of defects detected on Layer 8.
L9	Number of defects detected on Layer 9.	L10	Number of defects detected on Layer 10.

First, trees were built with different combinations of predictor variables to assess which tree would be best for use in GLM model building. Four trees were built with the die-level training dataset. These four trees are outlined in Table 6.2 and are shown in Figure 6.1. Table 6.2 includes the predictors for each tree, the number of important predictors determined by CART, the number of terminal nodes, the percentage of terminal nodes that were identified as nodes that outperformed the root node, and the percent of predicted class that was correct. In looking at the predictions, the column for 0 (Fail) indicates the percentage of actual failing dice that were predicted to fail. The column for 1 (Pass) indicates the percentage of actual passing dice that were predicted to pass. For example, in the dataset, there are 7,819 failing dice and 15,477 passing dice. Tree 3 predicts that 5,044 of the actual failing dice will fail and that 2,775 of them will pass (64.51% predicted class correct). Tree 3 also predicts 9,322 of the actual passing dice will pass and 6,155 of them will fail (60.23%).

Tree 1 used all of the available predictors from the dataset. Lot and Wafer were deemed unimportant by CART with variable scores (out of 100) of 0. Lot and Wafer were removed from the list of predictors for building Tree 2. Tree 2 found one of the device layers with defects (L8) to be unimportant (variable score of 0), but each of the device layers are of interest in the initial tree building for modeling.

To try a simpler tree, the *x*- and *y*-coordinates (Die X and Die Y) were not included as predictors in Tree 3. The use of the die coordinates in Tree 1 did not seem to help the model as only one split came from Die Y and none from Die X.

Die Y had a variable score of 2.33 and a Die X variable score of 0.34 for Tree 1. Tree 2 had 4 spits using Die X and 1 split using Die Y. Die X had a variable score of 4.89, and Die Y had a variable score of 3.21 for Tree 2. Since these coordinates were used to determine the Die Quadrant and Radial Distance predictors for each die, which give a better positional indicator (i.e. identifying center or edge defects), it was reasonable to drop these coordinates as predictors in developing Tree 3. These were also the predictors used in the GLM models developed by Krueger, et al. (2011) with the exception of including Total Defects per Die.

Table 6.2. *Preliminary Tree Building Results*

Preliminary Tree	Predictors Included	Number of Important Predictors	Number of Terminal Nodes	Percentage of Terminal Nodes that Outperform Root Node	Percent Predicted Class Correct	
					0 (Fail)	1 (Pass)
1	Lot, Wafer, Die X, Die Y, Radial Distance, Die Quadrant, Total Layers with Defects, , L1-L10, Total Defects on Die	16	23	12/23 = 52.2%	61.96%	65.58%
2	Lot, Wafer, Radial Distance, Die Quadrant, Total Layers with Defects, L1-L10, Total Defects on Die	14	24	12/24 = 50%	61.44%	63.57%
3	Radial Distance, Die Quadrant, Total Layers with Defects, L1-L10, Total Defects on Die	13	25	13/25 = 52%	64.51%	60.23%
4	Radial Distance, Die Quadrant, Total Layers with Defects, L1-L10	13	53	20/53 = 37.7%	64.06%	62.12%

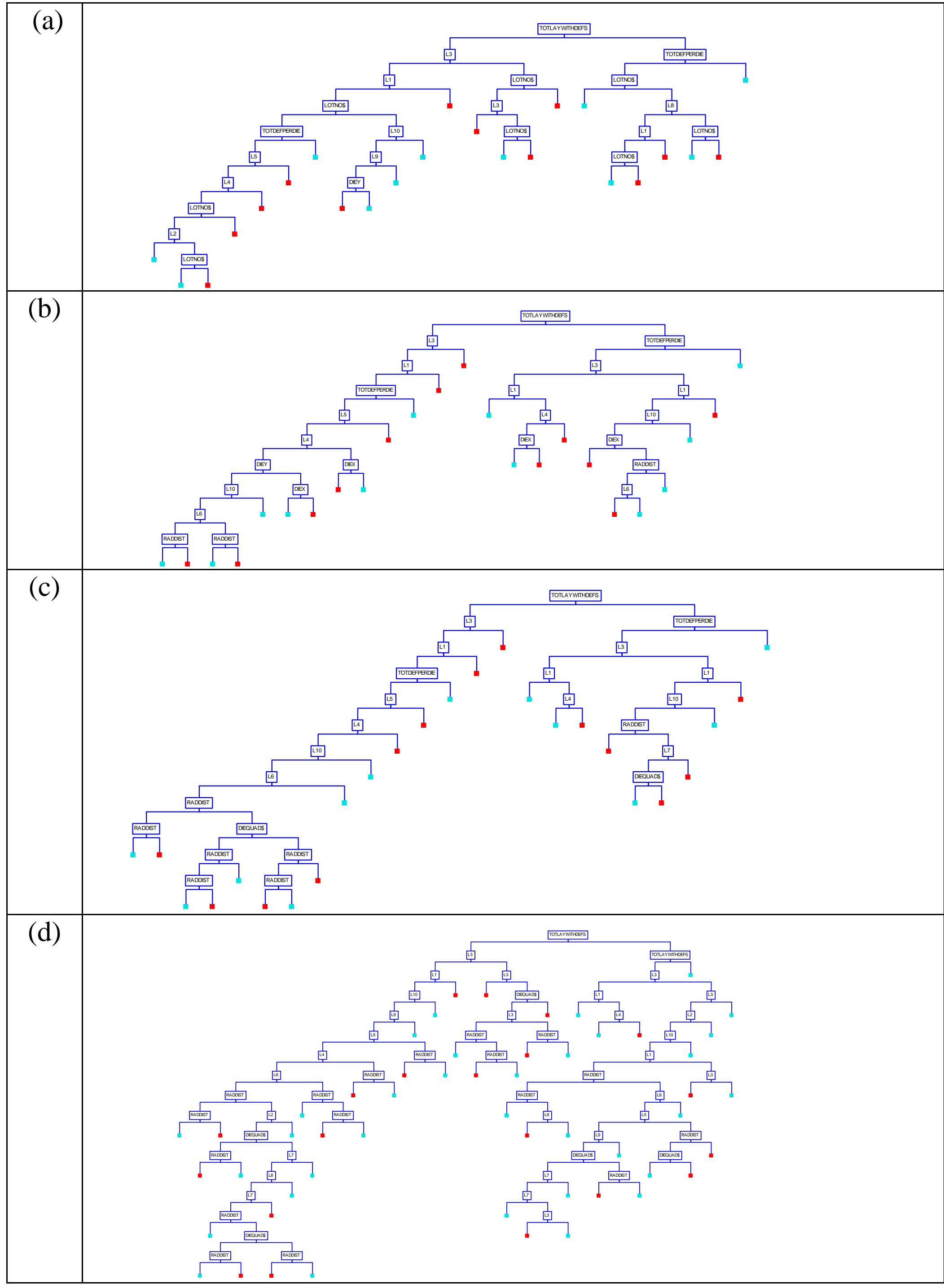

Figure 6.1. Preliminary tree structures using different predictors. These figures show the variables used for splitting and indicate if a node is better than the root node (dark red) or not as good as the root node (light blue). (a) Corresponds to Tree 1 in Table 6.2 with 18 predictors and 23 terminal nodes. (b) Corresponds to Tree 2 in Table 6.2 with 16 predictors and 24 terminal nodes. (c) Corresponds to Tree 3 in Table 6.2 with 14 predictors and 25 terminal nodes. (d) Corresponds to Tree 4 in Table 6.2 with 13 predictors and 53 terminal nodes.

Tree 4, shown in Figure 6.1(d), used the same predictors as Tree 3, except Total Defects per Die was removed as a predictor. This change had a strong impact on the tree, creating 53 terminal nodes and a much more complex structure than the other trees.

From these four trees, Tree 3 was chosen to be the best. This tree includes the predictors used in Krueger, et al. (2011), plus the "Total Defects per Die" count. The inclusion of "Total Defects per Die" simplifies the tree considerably from what is seen in Tree 4. Also, of Trees 1 through 3, Tree 3 has the largest number of nodes that are identified as being better than the root node with only a small increase in the number of terminal nodes needed. The details of Tree 3 are shown in Figure 6.2. The information displayed included the splitting values for nodes, the tree structure, and the number of passing, failing, and total dice in each terminal node. Each terminal node also includes a bar at the bottom that indicates the proportion of passing dice in the node. In the bars, the royal blue (black) portion is the proportion of passing dice, and the red (gray) portion is the proportion of failing dice.

Creating Models

Once the appropriate tree has been selected, the information from the tree can be used in developing a generalized linear model. This can be done in different ways. When the goals of the study may include learning about certain groups (such as high-yield or low-yield, high-risk or low-risk) to determine a "recipe" for achieving or avoiding these outcomes, the terminal nodes from

CART are quite helpful. These terminal nodes can be used as indicator variables that give information about important interactions for these groups that are then included in the GLM. The use of indicator variables is well described in Chapter 8 of Montgomery, Peck, and Vining (2006). This approach can determine which terminal nodes are statistically significant and help the user by providing a better understanding of the important factors and interactions for those particular groups.

Another approach is to use the CART-constructed tree to identify important two-way interactions more quickly by looking at the splits and implementing these interaction terms into the GLM model as predictors. This can simplify model building if a large number of factors and interactions are part of the dataset by letting the modeler avoid having to include all the interaction terms and then reducing the model through backward elimination or other techniques.

Reduced models, using the terminal nodes or the interaction terms from the CART tree, can be developed to achieve parsimony using backward elimination techniques. Using this approach, factors are eliminated one-by-one from the model on the basis of their *p*-values, starting with the highest p-values, and proceeding until all the factors in the model have the desired level of significance. Forward selection and step-wise regression may also be used (Montgomery, Peck, & Vining, 2006).

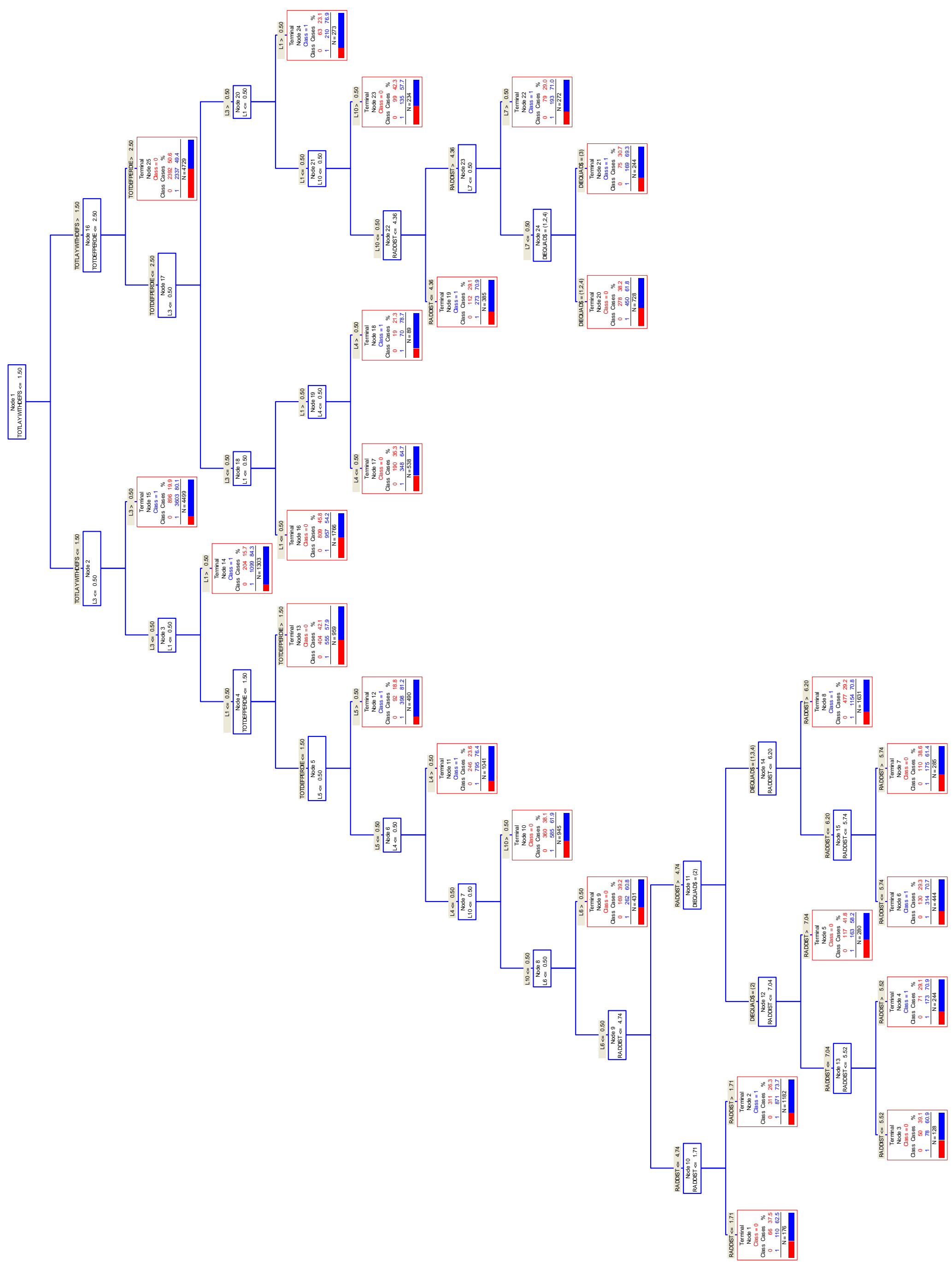

FIGURE 6.2. Tree 3 structure. These details include splitting criteria and terminal node data including the number of dice in each class and the percent of the total dice in that node. The bar at the bottom of each terminal node shows the proportion of failing dice red (gray) and the number of passing dice royal blue (black) in the node.

Table 6.3. *Terminal Node Information for Tree 3*

Terminal Node	Number of Dice (Total)	Number of Failing Dice	Number of Passing Dice	Probability Passing
1	176	66	110	0.625
2	1182	311	871	0.737
3	128	50	78	0.609
4	244	71	172	0.709
5	280	117	163	0.582
6	444	130	314	0.707
7	265	110	175	0.614
8	1631	477	1154	0.708
9	431	169	262	0.608
10	945	360	585	0.619
11	1041	246	795	0.764
12	490	92	398	0.812
13	959	404	555	0.579
14	1303	204	1099	0.843
15	4499	896	3603	0.801
16	1766	809	957	0.542
17	538	190	348	0.647
18	89	19	70	0.787
19	385	112	273	0.709
20	728	278	450	0.618
21	244	75	169	0.693
22	272	79	193	0.710
23	234	99	135	0.577
24	273	63	210	0.769
25	4729	2392	2337	0.494

An Example from Semiconductor Yield Modeling.

Once the best tree is chosen for the semiconductor data, indicator variables may be used to show which terminal node in the tree each die fits into. For Tree 3, there are 25 terminal nodes. Each die will fall into one of the terminal nodes. For example, a die having defects on more than one layer and a total number of defects greater than 2 will be in Terminal Node 25. Dice that have defects on only one layer and have at least one defect in Layer 3 will be classified into

Terminal Node 15. Indicator variables can be quickly constructed in Excel by using the splitting criteria and "If" statements to give values of "1" for the terminal node a row of data falls into and a value of "0" for all other terminal nodes. For 25 terminal nodes, 24 indicator variables are used for a full model.

GLM models can be constructed by adding these indicator variables as predictors in the model. Several models were constructed using SAS 9.2 and PROC GLIMMIX (see Appendix A for SAS code) to compare various approaches. These GLM models included full and reduced logit models with only the main effects used as predictors, full and reduced models using the main effects and the terminal node indicator variables as predictors, full and reduced models using the main effects and the terminal nodes identified by CART as outperforming the root node (red nodes) as predictors, a reduced model from using the main effects and the interactions identified in the CART tree for the predictors, and a reduced model using the main effects and all two-way interactions in the model as predictors. The terms used in these models are shown in more detail in Table 6.4.

The models constructed using only the main effects are similar to those described in Chapter 4 but are built using this larger dataset. The models built with the terminal nodes develop a model that is adjusted by the coefficient for the terminal node a row of data falls into, giving the resulting models a form that resembles having different intercepts for a line. The significant terminal nodes can be determined by reducing the model through backward selection or another method.

CART also provides information that describes each terminal node as being a better or worse classifier than the root node. (Recall this percentage was used to help select the best tree in Table 6.2.) Nodes that outperform the root node are marked in different shades of red on the resulting tree while nodes that do not outperform the root node are marked in blue. These selected terminal nodes may also be of interest in model building, and reduced models can again be formed from these predictors. All of the models described to this point were reduced through backward elimination using the *t*-test values and a level of significance of α=0.1 since the *F*-test and *t*-test *p*-values are the same for the GLM with only the main effects, and the models with terminal nodes included did not produce *F*-values.

While the use of terminal nodes themselves give an increased understanding into significant groupings and interactions that pertain to them, more general modeling can be done with the interaction terms from the CART tree. By following the various branches of the tree, different interaction terms can be quickly identified. For example, Figure 6.3 shows L1 branching off an L3 node in two places, indicating a possibly significant interaction between these two factors. This branching occurs near the root node, suggesting this interaction term (L1*L3) may be one of the strongest for these data. Including this interaction term in the GLM model can confirm this through the *t*-test and *F*-test results. Another example of finding possible interactions from the CART tree is shown in Figure 6.4, which shows in more detail the bottom, left-hand side of the tree and the relevant interactions. This figure shows interactions L5* L4, L4* L10,

L10*L6, L6*RadDist, and RadDist*DieQuad that may be significant. These interaction terms, along with RadDist*L10, L1*L4, RadDist*L7, and L7*DieQuad found in other parts of the tree were included one of the models that was then reduced through backward elimination using the *F*-test values and a level of significance of α=0.1.

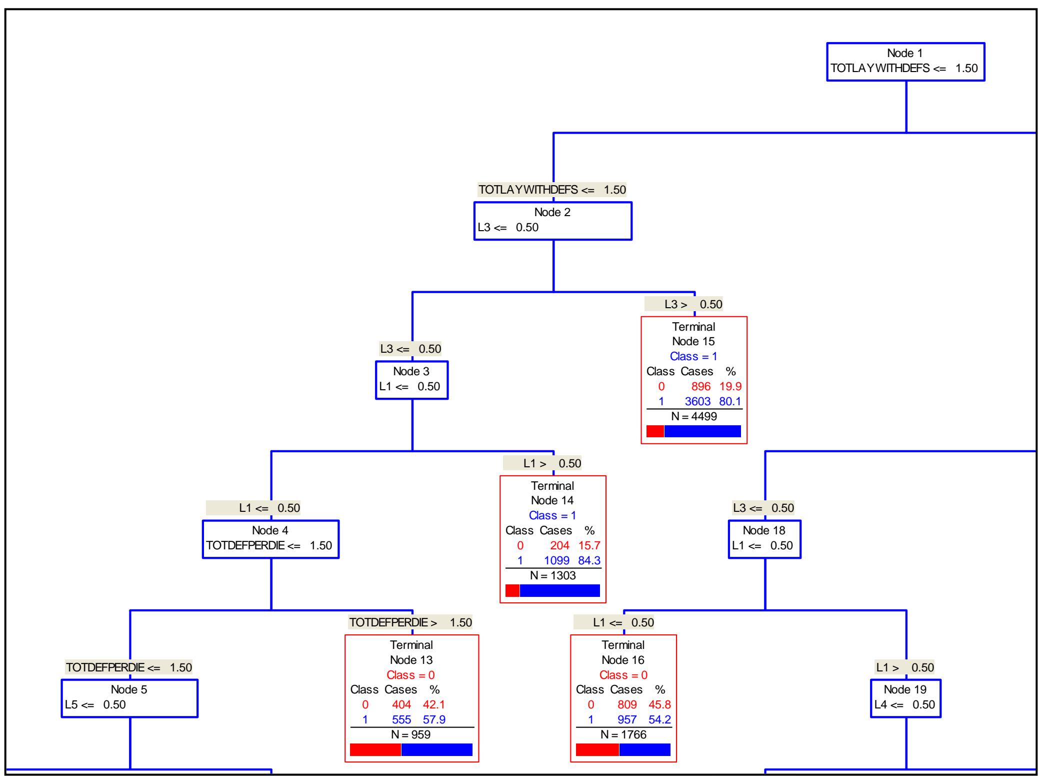

Figure 6.3. CART tree showing interactions between factors. Here, near the root node, a connection is seen between L3 and L1 in two places on the tree. The position of this interaction and its repetition indicate that it may be a significant interaction term that should be included in the model.

Another model was built by first including all two-way interactions between the main effects and then reducing the model by backward elimination. There were 66 two-way interactions included with the 12 factors considered (L1-L10, RadDist, and DieQuad). The total layers with defects (TotLaywithDefs) and

the total defects per die (TotDefPerDie) were not used in creating interaction terms due to multicollinearity. Reduced models were constructed by removing factors and interactions one at a time based on the *F*-values with a level of significance of α=0.1. The terms contained in the reduced model are shown in Table 6.4.

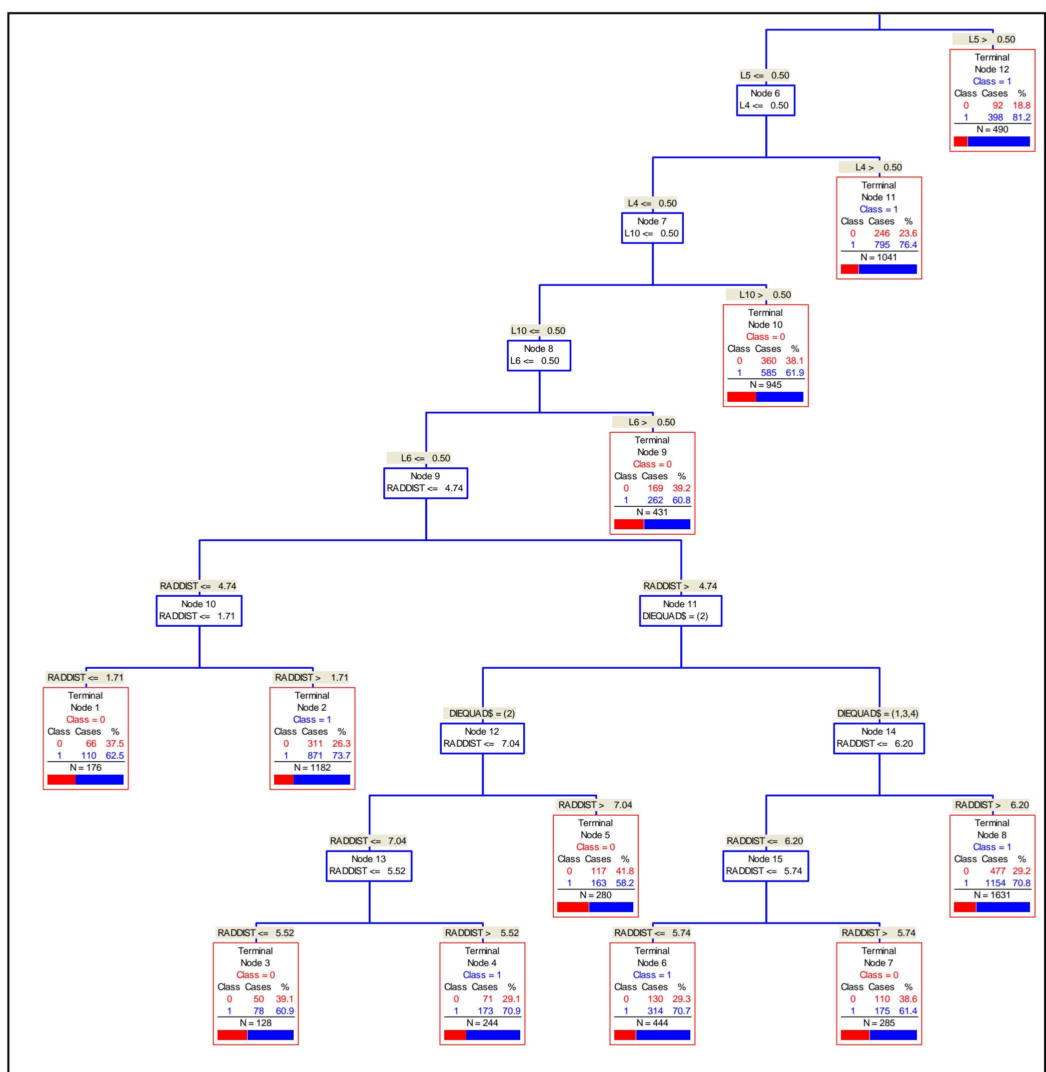

Figure 6.4. Bottom of CART tree showing interactions between factors. Here, near the bottom of the tree, more interactions are shown. These include interactions between L5 and L4, L4 and L10, L10 and L6, L6 and RadDist, and RadDist and DieQuad.

All of the models were built using the logit link in PROC GLIMMIX. Though PROC GLIMMIX is designed to analyze GLMMs, if no random effects are specified, SAS runs in GLM mode and provides the same analysis as PROC GENMOD.

Results

Table 6.4 displays the model coefficients and *p*-values for significant factors and interactions obtained from the *t*-tests for the different models using a level of significance of 0.1. There are some interesting differences between the models. In considering the reduced models, the models with only the main effects or the main effects with the terminal nodes from CART included eliminate Layer 1 as significant while the models containing interaction terms retain Layer 1. The reduced models using the CART terminal nodes eliminate radial distance as a significant predictor, suggesting that this location parameter is important only in connection with the other variables as described through the terminal node recipes. Radial distance is included as a splitting factor in terminal nodes 1-8 and 19-22, several of which are included in the reduced models containing terminal nodes. The reduced model from including all the possible two-way interactions deems Layer 8 as insignificant, but interactions between Layers 8 and Layer 1, Layer 2, and Radial Distance are significant in the model. The reduced model using interactions taken from the CART tree indicated 11 interactions to be significant, matching with 11 of the 21 identified through backward elimination from the model that examined all two-way interactions.

Table 6.4. *Coefficients and p-values for GLM Models*

Models	Main Effects Only		Main Effects Only - Reduced		All Terminal Nodes from CART		All Terminal Nodes from CART - Reduced		Red Nodes from CART		Red Nodes from CART - Reduced		Interactions from CART - Reduced		All Interactions - Reduced	
Predictors	Coefficient	P-value	Coefficient	P-value	Coefficient	P-value	Coefficient	P-value	Coefficient	P-value	Coefficient	P-value	Coefficient	P-value	Coefficient	P-value
Intercept	1.656	<.0001	1.654	<.0001	1.253	<.0001	1.225	<.0001	1.068	<.0001	1.008	<.0001	1.781	<.0001	1.611	<.0001
TotalLayWithDefs	-0.248	<.0001	-0.236	<.0001	-0.174	0.0001	-0.189	<.0001	-0.133	<.0001	-0.143	<.0001	-0.234	<.0001	-0.228	<.0001
RadDist	-0.017	0.0244	-0.016	0.0269	-0.013	0.1206			-0.010	0.1986			-0.043	<.0001	-0.006	0.714*
DieQuad1	-0.047	0.2479	-0.048	0.2401	-0.050	0.2236	-0.050	0.2218	-0.049	0.2296	-0.050	0.2284	-0.043	0.2972	0.341	0.0127
DieQuad2	-0.190	<.0001	-0.191	<.0001	-0.177	<.0001	-0.182	<.0001	-0.182	<.0001	-0.176	<.0001	-0.187	<.0001	0.353	0.0069
DieQuad3	0.089	0.0283	0.088	0.0293	0.091	0.0285	0.105	0.0093	0.083	0.044	0.090	0.0279	0.093	0.0218	0.280	0.0214
DieQuad4	0.000	.	0.000	.	0.000	.	0.000	.	0.000	.	0.000	.	0.000	.	0.000	.
L1	0.035	0.2289			-0.035	0.303			-0.008	0.7989			0.093	0.0054	0.121	0.0011
L2	-0.299	<.0001	-0.307	<.0001	-0.180	<.0001	-0.185	<.0001	-0.177	<.0001	-0.172	<.0001	-0.306	<.0001	-0.408	<.0001
L3	-0.074	<.0001	-0.079	<.0001	-0.125	<.0001	-0.128	<.0001	-0.106	<.0001	-0.105	<.0001	-0.060	0.0003	-0.069	<.0001
L4	-0.193	<.0001	-0.202	<.0001	-0.113	0.009	-0.119	0.0027	-0.108	0.0078	-0.100	0.0113	-0.174	<.0001	-0.227	<.0001
L5	-0.086	0.0376	-0.094	0.021	-0.038	0.399			-0.033	0.4513					-0.294	0.0225
L6	-0.423	<.0001	-0.431	<.0001	-0.278	<.0001	-0.286	<.0001	-0.291	<.0001	-0.286	<.0001	-1.302	<.0001	-1.346	<.0001
L7	-0.265	<.0001	-0.273	<.0001	-0.159	<.0001	-0.169	<.0001	-0.159	<.0001	-0.155	<.0001	-0.545	<.0001	-0.594	<.0001
L8	-0.246	<.0001	-0.251	<.0001	-0.162	<.0001	-0.166	<.0001	-0.155	<.0001	-0.149	<.0001	-0.255	<.0001		
L9	-0.468	<.0001	-0.477	<.0001	-0.336	<.0001	-0.343	<.0001	-0.335	<.0001	-0.331	<.0001	-0.472	<.0001	-0.881	<.0001
L10	-0.633	<.0001	-0.643	<.0001	-0.464	<.0001	-0.483	<.0001	-0.426	<.0001	-0.420	<.0001	-0.902	<.0001	-1.007	<.0001
Tnode1					-0.337	0.0651	-0.306	0.0549								
Tnode2					0.243	0.0281	0.245	0.0009	0.377	<.0001	0.405	<.0001				
Tnode3					-0.173	0.3926										
Tnode4					0.279	0.0967	0.251	0.0887	0.407	0.0058	0.403	0.0062				
Tnode5					-0.241	0.1142	-0.285	0.027								
Tnode6					0.068	0.6184			0.197	0.0752	0.207	0.0607				
Tnode7					-0.344	0.0215	-0.378	0.0027								
Tnode8					0.112	0.2778			0.234	0.0004	0.221	0.0007				
Tnode9					-0.269	0.051	-0.293	0.0088								
Tnode10					-0.026	0.8232										
Tnode11					0.322	0.0063	0.297	0.0007	0.448	<.0001	0.451	<.0001				
Tnode12					0.527	0.0004	0.451	0.0002	0.652	<.0001	0.625	<.0001				
Tnode13					-0.052	0.626										
Tnode14					0.751	<.0001	0.670	<.0001	0.846	<.0001	0.844	<.0001				
Tnode15					0.605	<.0001	0.573	<.0001	0.705	<.0001	0.712	<.0001				
Tnode16					-0.179	0.011	-0.191	0.0004								
Tnode17					0.092	0.3952										
Tnode18					0.674	0.0118	0.630	0.0165	0.731	0.0056	0.737	0.005				
Tnode19					0.372	0.0033	0.396	0.0006	0.447	0.0002	0.487	<.0001				
Tnode20					0.051	0.5882										
Tnode21					0.229	0.1291			0.299	0.0387	0.297	0.0394				
Tnode22					0.389	0.0074	0.367	0.0077	0.455	0.001	0.458	0.0009				
Tnode23					0.108	0.4589										
Tnode24					0.566	0.0003	0.510	0.0006	0.607	<.0001	0.615	<.0001				
Tnode25					0.000	.										
L1*L2															-0.152	0.0442
L1*L3													-0.132	<.0001	-0.137	<.0001
L1*L8															-0.229	0.0038
L2*L4															0.205	0.0054
L2*L7															0.124	0.0585
L2*L8															0.156	0.0465
L2*L9															0.162	0.027
L2*L10															0.154	0.0829
L4*L5													-0.390	0.0004	-0.348	0.0025
L4*L6															-0.263	0.0875
L4*L10													0.189	0.0372	0.210	0.0225
L5*L10															0.207	0.0614
L7*L9															0.175	0.0011
L7*L10															0.124	0.0934
L9*L10															0.211	0.0087
RadDist*L5															0.034	0.0798
RadDist*L6													0.136	<.0001	0.142	<.0001
RadDist*L7													0.042	0.0014	0.040	0.0026
RadDist*L8															-0.052	<.0001
RadDist*L9															0.051	0.0006
RadDist*L10													0.045	0.0086	0.041	0.0184
RadDist*Die Quad 1													-0.059	0.0045	-0.062	0.003
RadDist*Die Quad 2													-0.092	<.0001	-0.092	<.0001
RadDist*Die Quad 3													-0.029	0.1299	-0.030	0.1297
RadDist*Die Quad 4													0.000	.	0.000	.

* Note that the reduced model from including all two-way interactions was developed using the F-values from the Type III test for fixed effects, which gave a p-value of <0.0000 for RadDist.

Validation

The models were tested for validity by using a test set of data consisting of 11,445 dice with defects from 84 wafers. No outliers were removed from the test dataset. The model coefficients were used to determine prediction probabilities for each die. These predicted values were compared to the actual pass or fail outcomes, and measures of mean absolute deviation (MAD) and mean squared error (MSE) were calculated. The MAD and MSE values were also calculated at the wafer level by summing the expected probabilities for each wafer and comparing that value to the actual number of passing dice on the wafer in the test dataset. The charts showing the MAD and MSE values for each of the models used is shown for the die level in Figure 6.5, and the MAD and MSE values for each model at the wafer level is presented in Figure 6.6.

The MAD and MSE values for the die level in Figure 6.5 show that the differences between the models' predictive powers are very small. Also, recall from Chapter 4 that the main effects GLM model outperformed the existing semiconductor yield models significantly. Figure 4.6 compared the die-level MAD and MSE of GLM models against historical yield models, showing the die-level full nested, reduced nested, and full non-nested GLMs to have nearly the same amount of error from the actual results. (Note that the full, non-nested logit GLM shown in Figure 4.6 is the same as the model referred to as "Main Effects Only" in this study.) Figure 4.10 showed the wafer-level comparisons, with the die-level nested reduced GLM having the least amount of error. Figure 6.6 shows the wafer-level comparisons for the models from this study, furthering the work

of Chapter 4. At the die-level, all of the models in this study have nearly the same predictive power, with the best model in terms of MAD being the model containing only the main effect with a value of 0.3995. The worst MAD value was from the model that included the interactions taken from examining the CART tree and using them as predictors in the model, giving a value of 0.4240. One result to note here is that the use of the terminal nodes, either all of the terminal nodes or only those shown by CART to be better than the root node, with the main effects as predictors in the model outperformed the predictive ability of CART alone. This is true for the MSE values as well as the MAD values. The best MSE value came from the model that included all the two-way interactions and was then reduced (MSE=0.2048), but was followed closely by the main effects only reduced model, the main effects plus terminal nodes reduced model, and the main effects plus CART-selected terminal nodes full and reduced models, all with MSE=0.2049. The MSE values give more weight to larger errors because the values are squared, suggesting that the models with lower MSE values are closer to the predicted values more often.

As Figures 6.5 and 6.6 show, adding the terminal nodes from CART does not improve the predictive strength of the model, though this addition does not significantly diminish the predictive strength either. The advantage of including these terminal nodes lies in being able to determine which nodes are significant and can be most helpful in process improvement efforts. With CART able to produce many nodes in an optimal tree (i.e. Tree 4 in Figure 6.1), this can be of great value to practitioners.

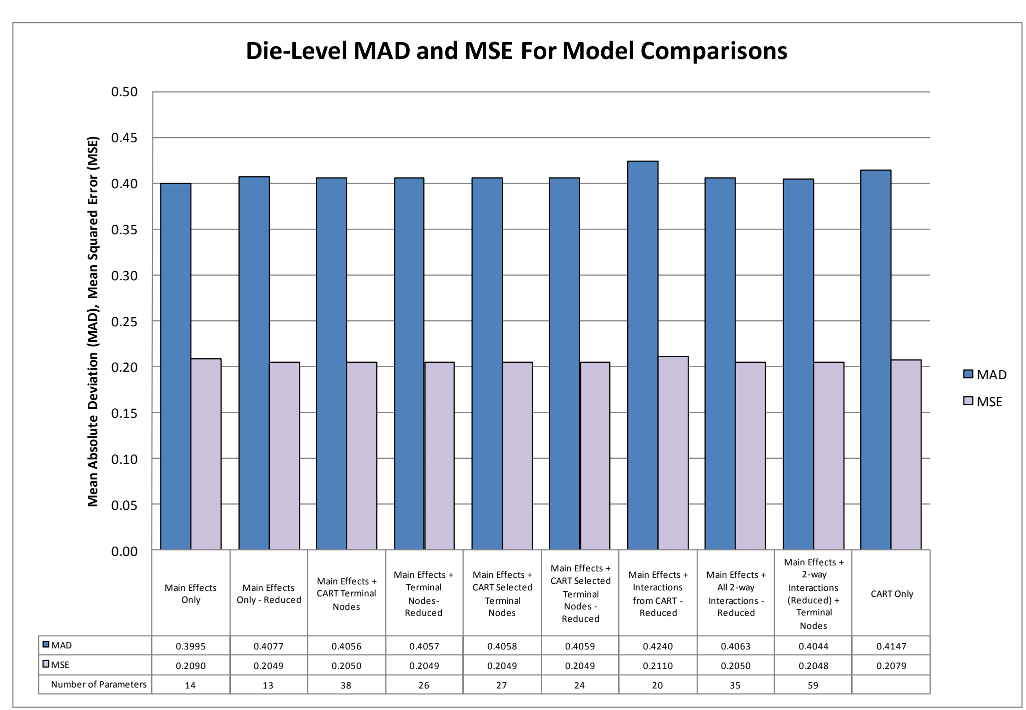

	Main Effects Only	Main Effects Only - Reduced	Main Effects + CART Terminal Nodes	Main Effects + Terminal Nodes- Reduced	Main Effects + CART Selected Terminal Nodes	Main Effects + CART Selected Terminal Nodes - Reduced	Main Effects + Interactions from CART - Reduced	Main Effects + All 2-way Interactions - Reduced	Main Effects + 2-way Interactions (Reduced) + Terminal Nodes	CART Only
MAD	0.3995	0.4077	0.4056	0.4057	0.4058	0.4059	0.4240	0.4063	0.4044	0.4147
MSE	0.2090	0.2049	0.2050	0.2049	0.2049	0.2049	0.2110	0.2050	0.2048	0.2079
Number of Parameters	14	13	38	26	27	24	20	35	59	

Figure 6.5. Die-level MAD and MSE for model comparisons. This chart shows that at the die-level, the MAD and MSE values for the models are all very similar.

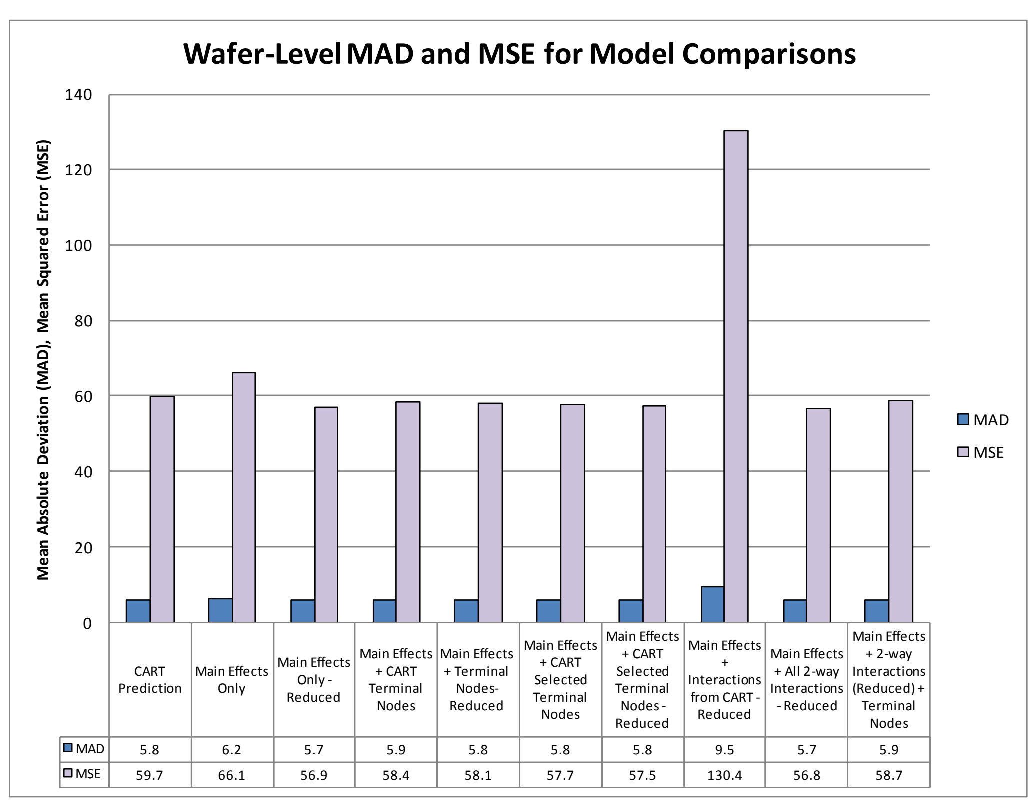

	CART Prediction	Main Effects Only	Main Effects Only - Reduced	Main Effects + CART Terminal Nodes	Main Effects + Terminal Nodes- Reduced	Main Effects + CART Selected Terminal Nodes	Main Effects + CART Selected Terminal Nodes - Reduced	Main Effects + Interactions from CART - Reduced	Main Effects + All 2-way Interactions - Reduced	Main Effects + 2-way Interactions (Reduced) + Terminal Nodes
MAD	5.8	6.2	5.7	5.9	5.8	5.8	5.8	9.5	5.7	5.9
MSE	59.7	66.1	56.9	58.4	58.1	57.7	57.5	130.4	56.8	58.7

Figure 6.6.Wafer-level MAD and MSE for model comparisons. This chart shows larger differences in the MAD and MSE values for the models at the wafer level.

The models can also be compared in terms of predictive power by examing charts of predicted vs. actual values of passing dice on a wafer using the test dataset. The models are all very close to one another, so the results of these charts are separated to retain clarity. Figure 6.7 shows the predictions using CART alone. The predicted values are very well clustered around the line for the actual passing dice. Figure 6.8 shows the full and reduced models for using only the main effects as predictors in the model. The reduced model produces slightly lower values than the full model, though both fit the actual data very well. Figure 6.9 shows the full and reduced models for using the main effects and the terminal nodes as predictors. Here, the reduce model predictions are nearly exactly the same as the full model's predicted values. The predictions also fit the actual data very well.

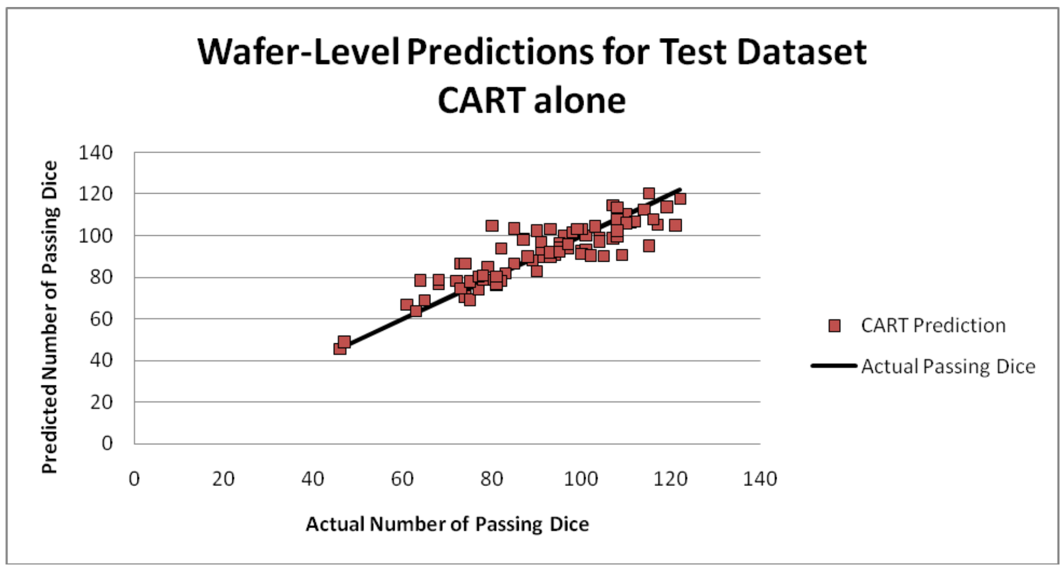

Figure 6.7. Wafer-level predictions for test dataset using CART alone.

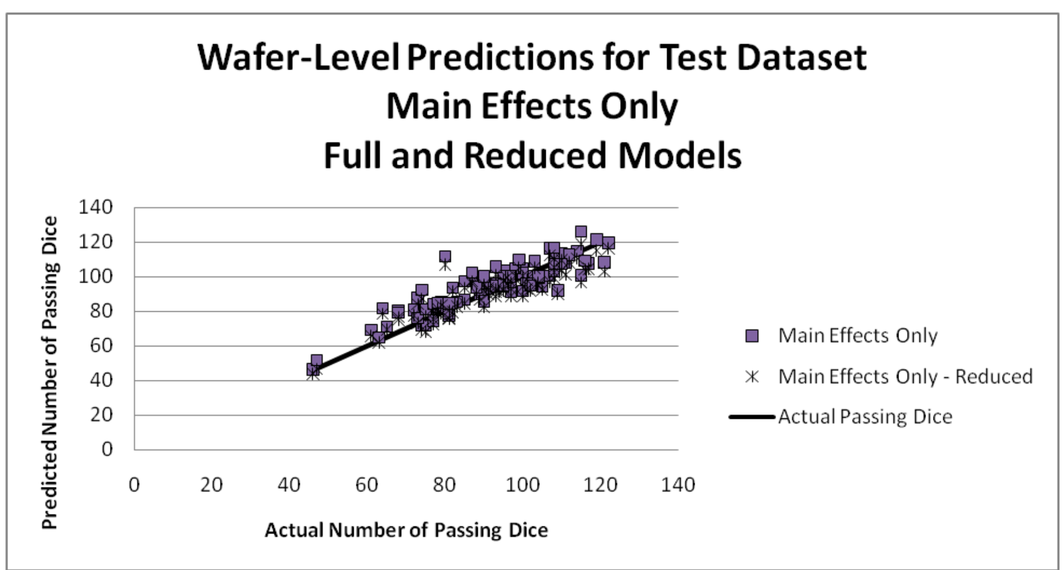

Figure 6.8. Wafer-level predictions for test dataset – Main effects only. This shows the preadicted values from using GLM full and reduced models with only the main effects as predictors.

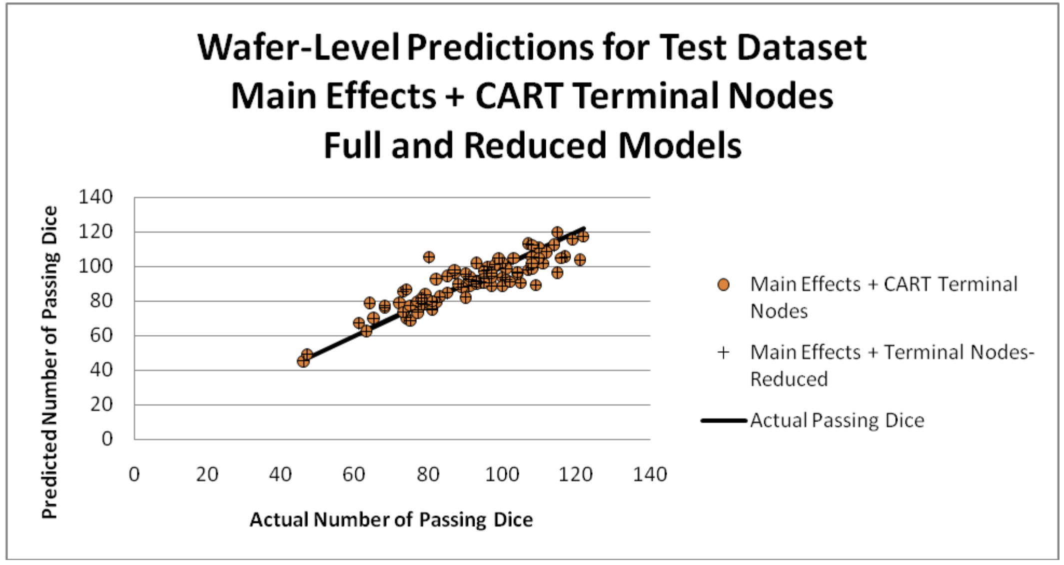

Figure 6.9. Wafer-level predictions for test dataset – Main effects plus CART terminal nodes. This shows the predicted values from using GLM full and reduced models with the main effects and the terminal nodes from CART as predictors.

Figure 6.10 displays the predictive power of the models containing the main effects plus the terminal nodes that CART identified as being better than the root node. Again, the reduced model points are centered on the full model points with both fittin the data well. Figure 6.11 shows the model that contains the main effects plus the interactions taken from the CART tree as predictors. This model consistently underestimates the actual yield of the wafer. It appears that it may be a better predictor for low-yield wafers (<70 wafers passing) than the other models, but at higher yields, this is the worst-performing model. The full and reduced models that included the main effects plus the two-way interactions is shown in Figure 6.12. Here again, the reduced model predictions are nearly the same as the full model, and there is no significant visual difference between these models and those in Figures 6.9 and 6.10. All of the models show strong predictive power with the exception of the models shown in Figure 6.11.

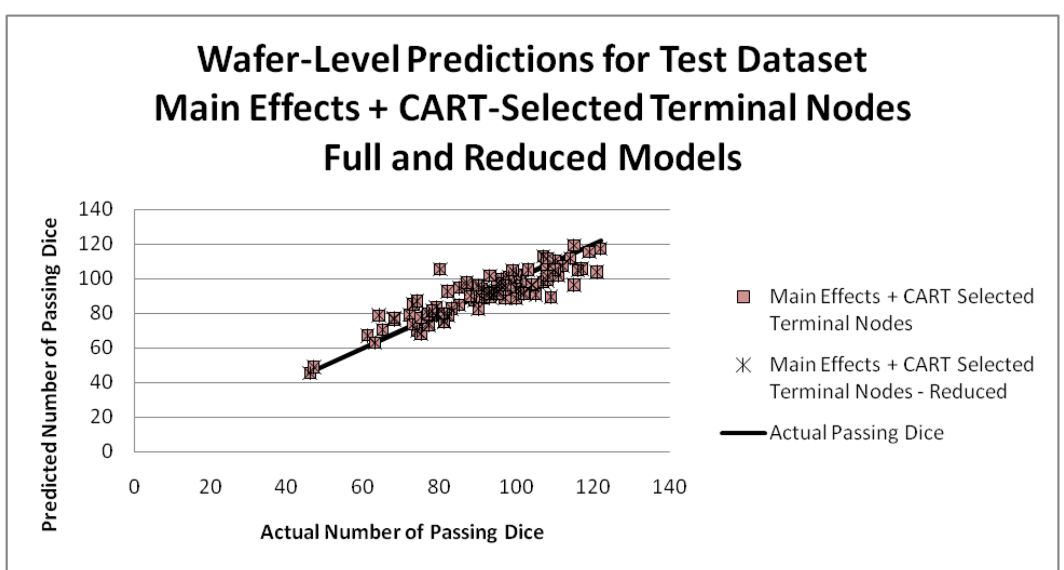

Figure 6.10. Wafer-level predictions for test dataset – Main effects plus CART-selected terminal nodes. This shows the preadicted values from using GLM full and reduced models with the main effects and the terminal nodes (selected by CART as being better than the root node) as predictors.

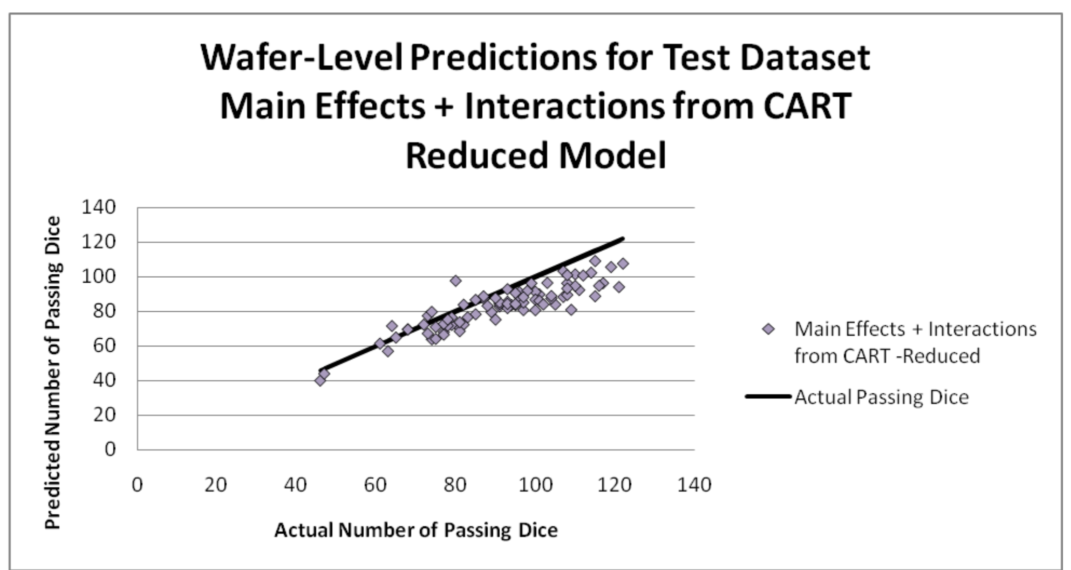

Figure 6.11. Wafer-level predictions for test dataset – Main effects plus interactions from CART. This shows the preadicted values from using a GLM reduced model with the main effects and the interactions identified from the CART tree as predictors.

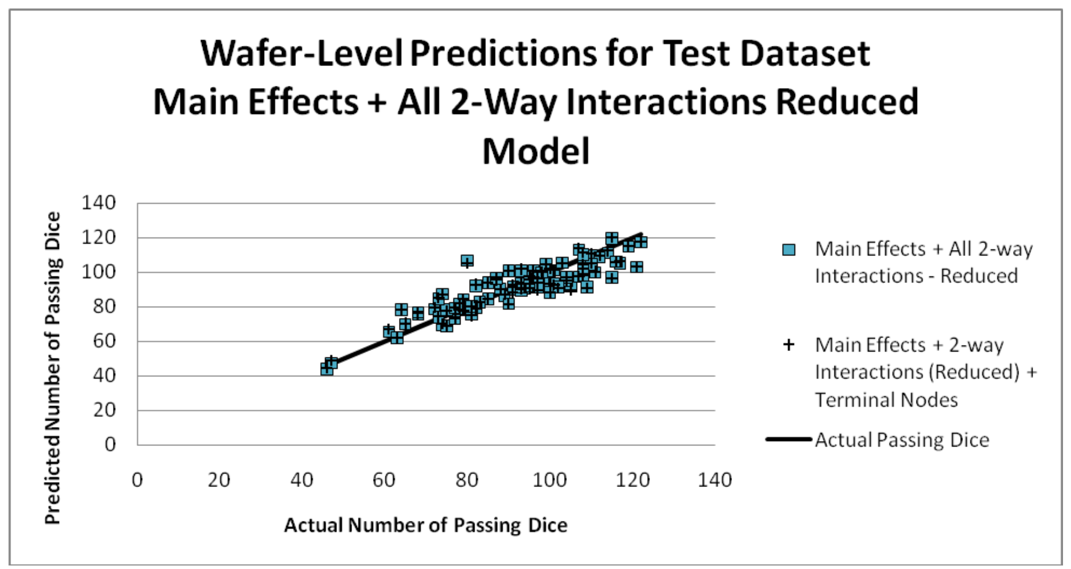

Figure 6.12. Wafer-level predictions for test dataset – Main effects plus all two-way interactions reduced model. This shows the preadicted values from using a GLM reduced model with the main effects and all the two-way interactions for the data as predictors. Another model with these predictors plus the 25 terminal nodes from CART used as predictors is also shown.

Terminal Nodes and Interactions

The reduced model that contained the main effects and the terminal node indicator variables from CART included 15 of the terminal nodes as statistically significant (α=0.1). Terminal nodes 1, 2, 4, 5, 7, 9, 11, 12, 14, 15, 16, 18, 19, 22, and 24 were included in the reduced model. These terminal nodes, their recipes, and the percent of passing dice that fall into the nodes in both the training and the test datasets are shown in Tables 6.5 and 6.6. Recall the main effects of radial distance and the defect counts of Layer 1 and Layer 5 were eliminated from the reduced model due to lack of significance. This indicates that the contribution of these factors may be well accounted for by the interactions contained in the terminal nodes. Indeed, Layer 1 occurs as part of the recipe in 14 of the 15 terminal nodes in the reduced model, and Layer 5 is present in seven of the 15 terminal nodes included in the reduced model.

Much can be learned by reading the tree from CART and should be considered when drawing conclusions about the results. Terminal Node 25 is selected when there are at least two layers with defects and at least three defects on the die. Of the dice falling into this node in the training dataset, only 49.4% pass. Thus, the terminal nodes in this tree focus on the occurrences where there are very few(less than three) defects present and can help focus improvement efforts for these areas. Practitioners may also be interested in learning more about the interactions present with these dice in Terminal Node 25. The data may be separated, and an additional tree or GLM could be constructed for this purpose.

Table 6.5. *Recipes and Classification Results for Terminal Nodes 1, 2, 4, 5, 7, 9, and 11*

Terminal Node from CART	1	2	4	5	7	9	11
Recipe for Node	TotLayWithDefs=1 L3=0 L1=0 TotDefPerDie=1 L5=0 L4=0 L10=0 L6=0 RadDist<=4.74 RadDist<=1.71	TotLayWithDefs=1 L3=0 L1=0 TotDefPerDie=1 L5=0 L4=0 L10=0 L6=0 RadDist<=4.74 RadDist>1.71	TotLayWithDefs=1 L3=0 L1=0 TotDefPerDie=1 L5=0 L4=0 L10=0 L6=0 RadDist>4.74 DieQuad=2 RadDist<=7.04 RadDist>5.52	TotLayWithDefs=1 L3=0 L1=0 TotDefPerDie=1 L5=0 L4=0 L10=0 L6=0 RadDist>4.74 DieQuad=2 RadDist>7.04	TotLayWithDefs=1 L3=0 L1=0 TotDefPerDie=1 L5=0 L4=0 L10=0 L6=0 RadDist>4.74 DieQuad=(1,3,4) RadDist<=6.2 RadDist>5.74	TotLayWithDefs=1 L3=0 L1=0 TotDefPerDie=1 L5=0 L4=0 L10=0 L6>0	TotLayWithDefs=1 L3=0 L1=0 TotDefPerDie=1 L5=0 L4>0
Percentage of Passing Dice in Node (Training Data)	62.5%	73.7%	70.9%	58.2%	61.4%	69.81%	76.4%
Percentage of Passing Dice in Node (Test Data)	67.35%	73.54%	72.39%	64.22%	60.8%	60.65%	74.54%

Table 6.6. *Recipes and Classification Results for Terminal Nodes 12, 14, 15, 16, 18, 19, 22, and 24*

Terminal Node from CART	12	14	15	16	18	19	22	24
Recipe for Node	TotLayWithDefs=1 L3=0 L1=0 TotDefPerDie=1 L5>0	TotLayWithDefs=1 L3=0 L1>0	TotLayWithDefs=1 L3>0	TotLayWithDefs>1 TotDefPerDie<3 L3=0 L1=0	TotLayWithDefs>1 TotDefPerDie<3 L3=0 L1>0 L4>0	TotLayWithDefs>1 TotDefPerDie<3 L3>0 L1=0 L10=0 RadDist>4.36 L7>0	TotLayWithDefs>1 TotDefPerDie<3 L3>0 L1=0 L10=0 RadDist<=4.36	TotLayWithDefs>1 TotDefPerDie<3 L3>0 L1>0
Percentage of Passing Dice in Node (Training Data)	81.2%	84.3%	80.1%	54.2%	78.7%	70.9%	71.0%	76.9%
Percentage of Passing Dice in Node (Test Data)	77.11%	80.17%	81.21%	57.98%	62.50%	63.74%	62.76%	76.73%

Terminal nodes 1-15 all have defects on only one layer while terminal nodes 16-25 have defects on at least 2 different layers. The interactions suggested by the recipes, then, have interesting interpretations. For example, the recipe for Terminal Node 1 includes dice that have only one defect that is on Layer 2, Layer 7, Layer 8, or Layer 9, and falls between the center of the wafer and a radial distance of 1.71. From the training data, only 62.5% of these dice pass. Because L1, L3, L4, L5, L6, and L10 are included in the recipe for Terminal Node 1, interactions between these effects may seem likely, but since the splits indicate that for this node, these layers all have zero defects, any interaction between them is difficult to interpret. One advantage is that the early processing layers (Layer 1 is the first layer of the die.) are part of the terminal node recipes, so it may be possible to predict yield earlier in the production process using only the data from these steps.

Another advantage may be in using the splitting criteria toward the bottom of the tree to learn more about potential processing issues. Figure 6.14 illustrates a wafer map showing the areas for the location of the dice for the first eight terminal nodes from the CART tree. The percentage of dice that passed in each of the nodes using the training dataset is also included. These nodes include radial distance in their branches and have only one defect on one layer and have no defects on Layers 1, 3, 4, 5, 6, and 10. This indicates that for dice with a defect on Layer 2, 7, 8, or 9, the position of the defect makes the largest impact on the resulting yield. The figure indicates that there may be processing issues that impact yield when a defect from these layers is found in the outer radius in

Quadrant 2 (Terminal Node 5, 58.2% passing) or in the center of the die (Terminal Node 1, 62.5% passing). There is also a small region in Quadrant 2 that has lower yield (Terminal Node 3, 60.9% passing) and in Quadrants 1, 3, and 4 (Terminal Node 7, 61.4% passing) that may be of help to process and defect metrology engineers in identifying potential causes for the problems. This type of analysis can be very constructive for practitioners.

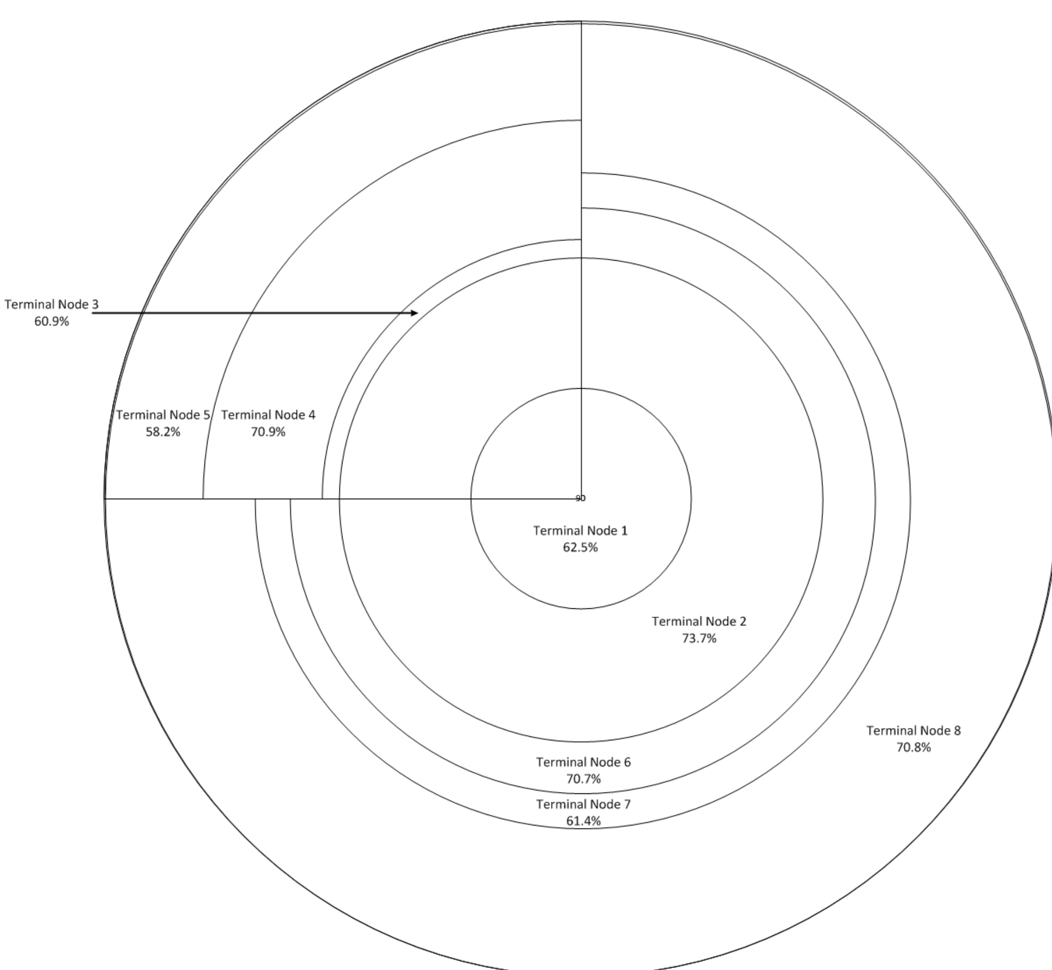

Figure 6.13. Wafer map showing the radial and quadrant regions that apply to terminal nodes 1-8 from the CART tree. These terminal nodes include dice that have only one defect occurring on layer 2, 7, 8, or 9. The percentages shown indicate the proportion of dice predicted to pass in that node.

Another interesting finding of this study is that the GLM model that used all the terminal nodes from CART and was then reduced identified different terminal nodes than the model that used the terminal nodes that CART identified as being better than the root node. While there was some consistency between the two, there were only 13 CART-identified nodes, compared to the 15 nodes reduced from the model that contained all 25. Both approaches identified Terminal Nodes 2, 4, 11, 12, 14, 15, 18, 19, 22, and 24 as significant. Differences include the reduced model from using all the terminal nodes identified Terminal Nodes 1, 5, 7, 9, and 16 as significant, while the CART-identified node model included Terminal Nodes 6, 8, and 21. These differences suggest it may be beneficial for practitioners to use GLMs to identify important terminal nodes instead of relying solely on CART's identification of the better terminal nodes.

Another interesting difference between the models is seen in comparing the model that was reduced after starting with all the two-factor interactions with those using CART terminal nodes. The interactions found to be statistically significant were not all described by the branching of the CART tree. Table 6.7 shows the interaction terms and the terminal nodes from CART that contain both of the factors in the interactions (not necessarily immediately following each other). Interactions containing L2, L8, and L9 are not included in the criteria for terminal nodes in the CART tree. This may indicate that these layers show important interactions with defects on other layers when there are more total defects on the die. Recall that any die with three or more defects was classified

into Terminal Node 25 without further splitting. This difference displays another advantage of using GLMs for yield modeling and process improvement.

Table 6.7. *Significant Interaction Terms and the Terminal Nodes that Contain Both Factors*

Interaction Terms	Terminal nodes from CART containing the combination of factors
L1*L2	None
L1*L3	1, 2, 3, 4, 5, 6, 7, 8, 9, 10, 11, 12, 13, 14, 16, 17, 18, 19, 20, 21, 22, 23, 24
L1*L8	None
L2*L4	None
L2*L7	None
L2*L8	None
L2*L9	None
L2*L10	None
L4*L5	1, 2, 3, 4, 5, 6, 7, 8, 9, 10, 11
L4*L6	1, 2, 3, 4, 5, 6, 7, 8, 9
L4*L10	1, 2, 3, 4, 5, 6, 7, 8, 9, 10
L5*L10	1, 2, 3, 4, 5, 6, 7, 8, 9, 10
L7*L9	None
L7*L10	19
L9*L10	None
RadDist*L5	1, 2, 3, 4, 5, 6, 7, 8
RadDist*L6	1, 2, 3, 4, 5, 6, 7, 8
RadDist*L7	20, 21, 22
RadDist*L8	None
RadDist*L9	None
RadDist*L10	1, 2, 3, 4, 5, 6, 7, 8, 19, 20, 21, 22
RadDist*DieQuad	3, 4, 5, 6, 7, 8, 20, 21

Summary

Using CART terminal nodes as predictors in the GLM model has not been proposed before. This approach uses two main steps: building an appropriate tree and then constructing the GLM model. This integrated use of CART and GLMs shows strong promise in both the areas of prediction and in improving process

understanding and root cause analysis for occurrences of interest. This technique does not have a significant impact on yield prediction, producing only slightly more error than the GLM with main effects alone, suggesting CART trees may be used well for prediction in this way.

Though the differences in prediction are minute between models including terminal nodes and those containing two-way interactions, the process implications and understanding can differ between these models and should be strongly considered when choosing a final approach. For example, if terminal node of interest is not split in the CART tree, interactions important for these observations will not be shown on the tree. If using two-way interactions directly in a model, it is best to include all possible interactions and then reduce the model rather than relying on CART branches to help identify important interactions. This latter approach resulted in the worst prediction errors seen in this study.

As shown in Chapter 4, the application of GLMs to semiconductor yield modeling is a much-improved approach over yield models of the past. The work shown in this chapter demonstrates other approaches that can produce nearly as accurate predictions while providing additional information critical to process improvement.

Chapter 7

CONCLUSIONS

This research contributes to the existing literature in a number of ways. This work uses generalized linear models, in different forms, to predict semiconductor yield based on defect count data, an approach to yield modeling that has not been explored before. This exploration has been done to understand how different GLM approaches can aid practitioners in problem solving and decision making. The validity of these GLM modeling strategies has been demonstrated by applying GLMs to a test dataset with success and by comparing the predicted values with those from models in the literature.

The use of fixed-effects GLM models showed an advantage in using die-level data to model yield, with this approach producing less forecasting error than both wafer-level models and historical models. The die-level models identified several fixed factors as significant, which could lead to better process understanding and improvement. The die-level modeling approach also allows the practitioner to consider the nested structure of the data, accurately reflecting the process of dice being produced together on a wafer, and wafers being processed together in a lot. Models built by trimming 5% of a training dataset as outliers produced the best goodness-of-fit results, but trimming 2.5% of the data produced very similar models. These models, created using 24 wafers as a training dataset and tested using 12 additional wafers of data, showed a 34.6% improvement in MSE and 31.1% improvement in MAD for the reduced, nested die-level GLM models compared to the best-performing historical model, Seeds'

model. These results demonstrate the potential of applying GLMs to these data for the purposes of accurate yield forecasting and process improvement.

While the GLM models account for the binomial response data, they assume all factors to be fixed. This assumption is not true for the random sampling that is commonly used in the fabrication process. A GLMM model allows a modeler to identify both random and fixed effects and to create models using a batch-specific or population-averaged approach, depending on the modeling objectives. GLMM models created using a large dataset of 168 wafers demonstrated this approach yields similar prediction error to the GLM models, even improving them under some conditions. The GLMM model results differ from the GLM results in a number of ways. First, different wafers are identified as significant, with the GLMM models identifying fewer wafers and including wafers with high yields as well as low yields. The GLM models selected more wafers as significant, but these were all lower-yield wafers. These GLM-identified wafers appeared to display some pattern defects, which may be helpful in process improvement and trouble-shooting, but the larger number of lots and wafers identified may also lead to false alarms by indicating a wafer to be significant when, in fact, it has no substantial problems.

The GLMM study showed differences between link functions used in the model (logit, probit, and complimentary log-log) to be very minor when all three link functions produced results. Convergence issued plagued the die-level study, and changing the degrees of freedom method may be useful in obtaining results if the default settings do not work. Also, if one link function doesn't return results

due to convergence concerns, another link function can be easily tried and trusted to produce meaningful output. As with the GLM study, the die-level GLMM models produced the best results in terms of prediction error, but they were closely followed by wafer-level adjusted models that account for the dice without defects on the wafer as well as the dice with defects that were considered in the model. Wafer-level models are consistent across model type (batch-specific or population-averaged; lot, wafer, or wafer(lot) modeled as a random effect) for large sample sizes over 150 wafers.

Finally, this research contributes to the literature by introducing a method for integrating CART with GLMs. This technique uses the terminal nodes from a classification tree as indicator variables for prediction in the GLM model. This approach adds value to the practitioner by providing prediction results nearly as good as those produced by the GLM alone while giving additional insight into potential process interactions that can be valuable in process improvement. This integrated approach takes advantage of both the easy-to-understand tree structure of the classification tree and the statistical analysis of the GLM to identify significant interactions and to construct an accurate yield forecasting model.

This work has potential use for practitioners and researchers alike. While this study showed the validity of these approaches by applying the methods to semiconductor yield modeling, these same techniques can be applied in other areas that also exhibit non-normal responses. The improvements in forecast accuracy and value in identifying key process factors may be important for many different applications.

Limitations

This study, which describes a modeling strategy using GLMs, does have limitations. In exploring and developing this strategy, data from only one semiconductor device were used to build and validate the models. This was a mature device, so this approach may not work well for new products without considering additional factors. The data for this device was from a four-month period and did not include information on defect size, defect type, or defect location on the die for the dice.

The response variable used for this work was the pass/fail result for each die (or proportion of passing dice for the wafer) and did not consider different types of failure modes. A similar approach may be employed to predict bin counts (counts of specific failure modes) using Poisson regression.

This research focused on using defect scan data for yield modeling and did not consider the process or parametric data for the wafers. Die failure can be due to non-defect related causes, but these were not considered in this modeling approach due to the limited corresponding data available.

Future Work

While this work illustrates the potential of using GLMs to model semiconductor yield, there are many ways this research can be extended. Using more or different predictor variables, such as defect type (killer or non-killer), defect size, and the location of the defect within a chip (within critical area or not), may improve the prediction capabilities of these models even more. These

predictors may add value to the models also in the process insight they could contribute by identifying which of these additional factors are critical in fabrication. In addition, the device studied in this research was a mature product. Evaluating these modeling strategies for newer products in early stages of their life cycles can provide more direction on how generally these techniques may be applied to forecast yield.

Models that focus on using only intermediate factors from early in the process (such as front-end processing layers) may also be of interest in guiding processing and scheduling decisions. For example, early prediction during the process can help practitioners to decide whether to continue processing wafers with a number of early defects or to instead start fabricating new wafers, to create forecasts designed more for planning purposes, and to reliably meet customer demand. These models may take into account process data recorded during fabrication as well as the defect counts detected on the front-end layers of the wafer.

Practitioners may also find useful a method that would identify at which prediction probabilities a die should be classified as “passing” or “failing” dice for prediction purposes. These cutoffs can be created based on the models described in this research. Different cutoff values could be compared using sensitivity and specificity measures and by comparing the areas under ROC curves (see Hosmer & Lemeshow, 2000). These cutoff values could be use to make decisions concerning continued processing for wafers that have already been impacted by defects.

Another area of future work may be in creating systems that can automate data collection, integration, and cleaning for the purposes of forming these types of models, making them more accessible to practitioners and more user-friendly. This automation could also be extended to include coding that would create the models (GLM, GLMM, CART, etc.) of interest to the user as well as model comparisons that could suggest the best performing models for the specific application. This coding may also include creating methods for integrating classification trees and GLMs (or GLMMs) in SAS or other software.

Another area of extention may be in using GLMs and GLMMs to detect special differences on wafers. Currently, gross failure defect patterns on wafers are often manually identified in industry, though research has been published that studies automating this process (Hansen, Nair, and Friedman, 1997; Fellows, Mastrangelo, and White, Jr., 2009). GLMMs may be used to consider the clustering of defects as random effects that can give more information about predicted yields as well as in automatically identifying these clusters that are usually caused by processing issues.

Finally, the actual yield and the yield values calculated from the dice with defects are different, as shown in Figure 7.1, suggesting that factors other than defects contribute to yield losses. Other types of data are recorded during wafer fabrication, including process data and parametric electrical test data. Integrating these process or parametric data with the defectivity data may produce even stronger and more useful GLM models for decision making. This integration may be done with a hierarchical approach, as suggested by Kumar (2006), or through

another method. As discussed, there are many opportunities for this work to be extended and advanced based on the results of this research and the needs of the semiconductor industry.

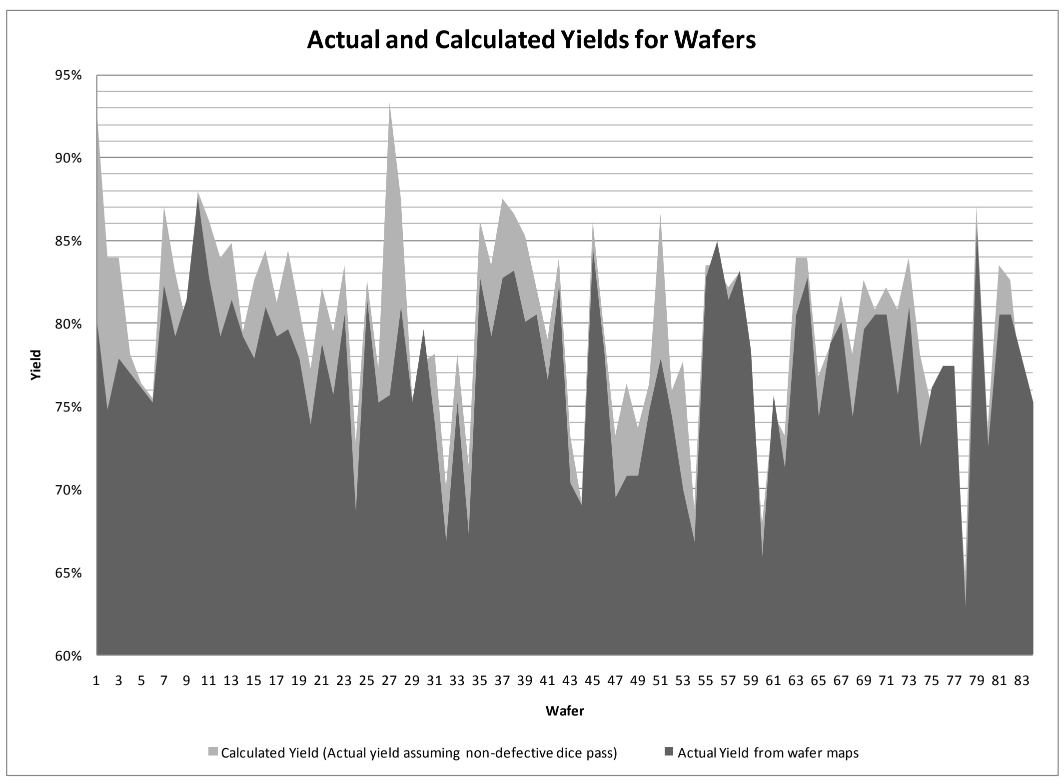

Figure 7.1. Actual and calculated yields for wafers. The actual yield values for the wafers in the test dataset are different from those calculated using only the information from the dice with defects. These differences account for some of the error in the GLM yield models.

REFERENCES

Agresti, A. (2002). Categorical data analysis (2nd ed.). Hoboken, New Jersey: John Wiley & Sons, Inc.

Anderson, K., Hill, E., & Mitchell, A. (2002). Spelunking in the data mine: On data mining as an analysis tool for the optimization of microprocessor speed. *IEEE/SEMI Advanced Semiconductor Manufacturing Conference*. 193-198.

Antonio, K. & Beirlant, J. (2007). Actuarial statistics with generalized linear mixed models. *Insurance: Mathematics and Economics, 40*, 58-76.

Bergeret, F., & Le Gall, C. (2003). Yield improvement using statistical analysis of process dates. *IEEE Transactions on Semiconductor Manufacturing, 16*, 535-542.

Berglund, C. N. (1996). Unified yield model incorporating both defect and parametric effects. *IEEE Transactions on Semiconductor Manufacturing, 9*, 447-454.

Braun, A. E. (2002). Yield management: no longer a closed system. *Semiconductor International, 25*(1), 49-54.

Braha, D. & Shmilovici, A. (2002). Data mining for improving a cleaning process in the semiconductor industry. *IEEE Transactions on Semiconductor Manufacturing, 15*(1), 91-101.

Breslow, N. E., & Clayton, D. G. (1993). Approximate inference in generalized linear mixed models. *Journal of the American Statistical Association, 88* (421), 9-25.

Brieman, L., Friedman, J., Olshen, R., & Stone, C. (1984). Classification and regression trees. Pacific Grove: Wadsworth.

Brown, D. E., Pittard, C. L., & Park, H. (1996). Classification trees with optimal multivariate decision nodes. *Pattern Recognition Letters, 17*, 699-703.

CART for Windows user’s guide (Version 5.0). (2002). San Diego, CA: Salford Systems.

Chandra, D. K., Ravi, V. & Bose, I. (2009). Failure prediction of dotcom companies using hybrid intelligent techniques. *Expert Systems with Applications, 36*, 4830-4837.

Chang, L. Y. & Chen, W. C. (2005). Data mining of tree-based models to analyze freeway accident frequency. *Journal of Safety Research, 36*, 365-375.

Chang, Y. C. (2010). Hierarchical approach to semiconductor yield modeling: Applications of generalized linear models. Ph.D. dissertation, University of Washington, United States -- Washington. Retrieved January 2, 2011, from Dissertations & Theses: Full Text.(Publication No. AAT 3421548).

Choi, M. & Lee, G. (2010). Decision tree for selecting retaining wall systems based on logistic regression analysis. *Automation in Construction, 19*, 917-928.

Costanza, M.C.; Paccaud, F. (2004). Binary classification of dyslipidemia from the waist-to-hip ratio and body mass index: a comparison of linear, logistic, and CART models. *BMC Medical Research Methodology, 4*(7). Retrieved January 2, 2011, from http://www.biomedcentral.com/1471-2288/4/7.

Cunningham, J. A. (1990). The use and evaluation of yield models in integrated circuit manufacturing. *IEEE Transactions on Semiconductor Manufacturing, 3*, 60-71.

Cunningham, S. P., Spanos, C. J., & Voros, K. (1995). Semiconductor yield improvement: results and best practices. *IEEE Transactions on Semiconductor Manufacturing, 8*, 103-9.

Czado, C. & Pfluger, C. (2008). Modeling dependencies between rating categories and their effects on prediction in a credit risk portfolio. *Applied Stochastic Models in Business and Industry, 24*, 237-259.

Dance, D. L., & Jarvis, R. (1992). Application of yield models for semiconductor yield improvement. *IEEE Transactions on Semiconductor Manufacturing, 5,* 41-46.

Davidson, R. A. (2009). Modeling postearthquake fire ignitions using generalized linear (mixed) models. *Journal of Infrastructure Systems, 15*(4), 351-360.

Dean, C. B. & Nielsen, J. D. (2007). Generalized linear mixed models: a review and some extensions. *Lifetime Data Analysis, 13*, 497-512.

Dingwall, A. G. F. (1968, October). High-yield-processed bipolor LSI arrays. Paper presented at the IEEE International Electron Devices Meeting, Washington, D.C.

Fellows, H. H., Mastrangelo, C. M., & and White, Jr., K. P. (2009). An empirical comparison of spatial randomness models for yield analysis. *IEEE Trans. on Electrononics Packaging Manufacturing*, *32*, 115-120.

Ferris-Prabhu, A. V. (1992). On the assumptions contained in semiconductor yield models. *IEEE Transactions on Computer-Aided Design, 11*(8), 966-975.

Fotouhi, A. R. (2008). Modelling overdispersion in longitudinal count data in clinical trials with application to epileptic data. *Contemporary Clinical Trials, 29,* 547-554.

Fu, C. Y. (2004). "Combining loglinear model with classification and regression tree (CART): an application to birth data". *Computational Statistics & Data Analysis, 45*, 865-874.

Gupta, S., Kulahci, M, Montgomery, D. C., & Borror, C. M. (2010). Analysis of signal-response systems using generalized linear mixed models. *Quality and Reliability Engineering International, 26*, 375-385.

Ham, W. E. (1978). Yield-area analysis. I. A diagnostic tool for fundamental integrated-circuit process problems. *RCA Review, 39*, 231-49.

Hansen, M. H., Nair, V. N., & Friedman, D. J. (1997). Monitoring wafer map data from integrated circuit fabrication processes for spatially clustered defects. *Technometrics, 39*(3), 241-253.

Hofstein, S. R., & Heiman, F. P. (1963). The silicon insulated-gate field-effect transistor. *Proceedings of the IEEE, 51*(9), 1190-1202.

Hosmer, D. W., & Lemeshow, S. (2000). *Applied logistic regression* (2nd ed.). Hoboken, New Jersey: John Wiley & Sons, Inc.

Hu, H. (2009) Supervised learning models in sort yield modeling. *2009 Advanced Semiconductor Manufacturing Conference Proceedings,* 133-136.

Hu, T. & Sung, S. Y. (2004). A trimmed mean approach to finding spatial outliers, *Intelligent Data Analysis*, *8*(1), 79-95.

Jearkpaporn, D., Borror, C. M., Runger, G. C., & Montgomery, D. C. (2007). Process monitoring for mean shifts for multiple stage processes. *International Journal of Production Research, 45*(23), 5547-5570.

Khoshgoftaar, T., M. & Allen, E. B. (2002). Predicting fault-prone software modules in embedded systems with classification trees. *International Journal of Reliability, Quality and Safety Engineering, 9*(1), 1-16.

Khoshgoftaar, T. M., Seliya, N. (2003). Fault prediction modeling for software quality estimation: Comparing commonly used techniques. *Empirical Software Engineering, 8*, 255-283.

Krueger, D. C., Montgomery, D. C., & Mastrangelo, C. M. (2011). Application of generalized linear models to predict semiconductor yield data using defect metrology data. *IEEE Transactions on Semiconductor Manufacturing, 24(1), 44-58*.

Kuhnert, P.M., Do, K.A., & McClure, R. (2000). Combining non-parametric models with logistic regression: an application to motor vehicle injury data. *Computational Statistics & Data Analysis, 34*, 371-386.

Kumar, N. (2006). Hierarchical modeling approach to improve factory operations in semiconductor manufacturing. (Doctoral dissertation, University of Washington). *Dissertation Abstracts International, 67*, 06.

Kumar, N., Kennedy, K., Gildersleeve, K., Abelson, R., Mastrangelo, C. M., & Montgomery, D. C. (2006). A review of yield modelling techniques for semiconductor manufacturing. *International Journal of Production Research, 44*(2), 5019-5036.

Kuo, W. & Kim, T. (1999). An overview of manufacturing yield and reliability modeling for semiconductor products. *Proceedings of the IEEE, 87*(8), 1329-1344.

Lee, J., & Pan, R. (2010). Analyzing step-stress accelerated life testing data using generalized linear models. *IIE Transactions, 42*, 589-598.

Lewis, S. L., Montgomery, D. C., & Myers, R. H. (2001). Examples of designed experiments with nonnormal responses. *Journal of Quality Technology, 33*(3), 265-278.

Lorenzo, A., Oter, D., Cruceta, S., Valtuena, J. F., Gonzalez, G., & Mata, C. (1999). Kill ratio calculation for in line yield prediction. *Proceedings of SPIE - The International Society for Optical Engineering, 3743*, 258-266.

Liu, H., Davidson, R. A., Apanasovich, T. V. (2007). Spatial generalized linear mixed models of electric power outages due to hurricanes and ice storms. *Reliability Engineering and System Safety, 93*, 875-890.

Madden, L. V., Turechek, W. W., Nita, M. (2002). Evaluation of generalized linear mixed models for analyzing disease incidence data obtained in designed experiments. *Plant Disease, 86*, 316-325.

McCullagh, P. & Nelder, J. A. (1989). *Generalized linear models* (2nd ed.). New York: Chapman and Hall.

Montgomery, D. C., Peck, E. A., & Vining, G. G. (2006). *Introduction to linear regression analysis* (4th ed.). Hoboken, New Jersey: John Wiley & Sons, Inc.

Moore, G. E. (1970). What level of LSI is best for you? *Electronics, 43*, 126-130.

Murphy, B. T. (1964). Cost-size optima of monolithic integrated circuits. *Proceedings of the IEEE, 52*(12), 1537-1545.

Murphy, B. T. (1971). Comments on "A new look at yield of integrated circuits". *Proceedings of the IEEE, 59*(7), 1128-1128.

Myers, R. H., Montgomery, D. C., Vining, G. G., and Robinson, T. J. (2010). *Generalized linear models with applications in engineering and the sciences* (2nd ed.). Hoboken, New Jersey: John Wiley & Sons, Inc.

Nag, P. K., Maly, W., & Jacobs, H. (1998). Advanced forecasting of cost and yield. *Semiconductor International, 21*, 163-70.

Nahar, R. K., (1993). The yield models and defect density monitors for integrated circuit diagnosis. *Microelectronics Reliability, 33*(14), 2153-2159.

Neagu, R. & Hoerl, R. (2005). A Six Sigma approach to predicting corporate defaults. *Quality and Reliability Engineering International, 21*, 293-309.

Nelder, J.A., & Wedderburn, R. W. M. (1972). Generalized linear models. *Journal of the Royal Statistical Society*. Series A (General), *135*(3), 370-384.

Nurani, R. K., Strojweas, A. J., Maly, W. P., Ouyang, C., Shindo, W., Akella, R., et al. (1998). In-line yield prediction methodologies using patterned wafer inspection information. *IEEE Transactions on Semiconductor Manufacturing, 11*(1), 40-47.

Okabe, T., Nagata, M., & Shimada, S. (1972). Analysis on yield of integrated circuits and a new expression for the yield. *Electrical Engineering in Japan, 92*, 135-41.

Price, J. E. (1970). A new look at yield of integrated circuits. *Proceedings of the IEEE, 58*(8), 1290-1291.

Raghavachari, M., Srinivasan, A. & Sullo, P. (1997) Poisson mixture yield models for integrated circuits: A critical review. *Microelectronics Reliability, 37*(4), 565-580.

Robinson, T. J., Myers, R. H., Montgomery, D. C. (2004). Analysis considerations in industrial split-plot experiments with non-normal responses. *Journal of Quality Technology, 36*(2), 180-192.

SAS. (2006, June). The GLIMMIX procedure. Retrieved January 31, 2011, from http://support.sas.com/rnd/app/papers/glimmix.pdf

Scheetz, L. J., Zhang, J. & Kolassa, J. (2009). Classification tree modeling to identify severe and moderate vehicular injuries in young and middle-aged adults. *Artificial Intelligence in Medicine, 45*, 1-10.

Seeds, R. B. (1967). Yield and cost analysis of bipolar LSI. *, International Electron Device Meeting Keynote Section*, (Abstract p. 12 of the meeting record).

Skinner, K. R., Montgomery, D. C., Runger, G. C., Fowler, J. W., McCarville, D. R., Rhoads, T. R., et al. (2002). Multivariate statistical methods for modeling and analysis of wafer probe test data, *IEEE Transactions on Semiconductor Manufacturing, 15*(4), 523-530.

Stapper, C. H. (1976). LSI yield modeling and process monitoring. IBM Journal of Research and Development, 20, 228-34.

Stapper, C. H. (1989). Fact and fiction in yield modeling. *Microelectronics Journal, 20*(1), 129-51.

Stapper, C. H., Armstrong, R.M., & Saji, K. (1983). Integrated circuit yield statistics. *Proceedings of the IEEE, 71*, 453-470.

Stapper, C. H. & Rosner, R. J. (1995). Integrated circuit yield management and yield analysis: Development and implementation. *IEEE Transactions on Semiconductor Manufacturing, 8*(2), 95-102.

Ture, M., Kurt, I., & Kurum, A. T. (2008). Comparing performances of logistic regression, classification and regression tree, and neural networks for predicting coronary artery disease. *Expert Systems with Applications, 34*, 366-374.

Ture, M., Kurt, I., Kurum, A. T., & Ozdamar, K. (2005). Comparing classification techniques for predicting essential hypertension. *Expert Systems with Applications, 29*, 583-588.

Wallmark, J. T. (1960). Design Considerations for Integrated Electronic Devices. Proceedings of the IRE, 48(3), 293-300.

Wang, C. H. (2008). Recognition of semiconductor defect patterns using spatial filtering and spectral clustering. *Expert Systems with Applications*, *34*, 1914-1923.

Weber, C. (2004). Yield learning and the sources of profitability in semiconductor manufacturing and process development. *IEEE Transactions on Semiconductor Manufacturing, 17*, 590-6.

White, Jr., K. P., Kundu, B., & Mastrangelo, C. M. (2008). Classification of defect clusters on semiconductor wafers via the Hough transformation. IEEE Transactions on Semiconductor Manufacturing, 21(2), 272-278.

Wolfinger, R. & O'Connell, M. (1993). Generealized linear models: A pseudo-likelihood approach. *Journal of Statistical Computation and Simulation, 48*, 233-243.

Yeh, C., Chen, C., Wu, F., & Chen, K. (2007). Validation and evaluation for defect-kill-rate and yield estimation models in semiconductor manufacturing. *International Journal of Production Research, 45*, 829-844.

Zhou, C., Ross, R., Vickery, C., Metteer, B., Gross, S. & Verret, D. (2002, August). Yield prediction using critical area analysis with inline defect data. Advanced Semiconductor Manufacturing IEEE/SEMI Conference and Workshop, 82-86.

APPENDIX A

SAS CODE

SAS CODE

SAS Code for Chapter 5

Die Level

GLM

```
ods html;
ods graphics on;
proc glimmix data=sasuser.thirtywafersdielevel method=RsPL
plots=(residualpanel(type=noblup unpack)
residualpanel(type=blup)
studentpanel(type=noblup));
*Method=RSPL for G-side, RMPL for R-side;
class WafID LotNo DieQuad;
model Pass =  LotNo WafID TotLayWithDefs RadDist DieQuad L1 L2 L3
L4 L5 L6 L7 L8 L9 L10/
dist=binomial link=probit solution;
run;
ods graphics off;
ods html close;
```

Nested GLM

```
ods html;
ods graphics on;
proc glimmix data=sasuser.thirtywafersdielevel method=RsPL
plots=(residualpanel(type=noblup unpack)
residualpanel(type=blup)
studentpanel(type=noblup));
*Method=RSPL for G-side, RMPL for R-side;
class WafID LotNo DieQuad;
model Pass =  WafID(LotNo) TotLayWithDefs RadDist DieQuad(WafID)
L1 L2 L3 L4 L5 L6 L7 L8 L9 L10/
dist=binomial link=logit solution;
run;
ods graphics off;
ods html close;
```

GLM with Overdispersion

```
ods html;
ods graphics on;
proc glimmix data=sasuser.thirtywafersdielevel method=RsPL
plots=(residualpanel(type=noblup unpack)
residualpanel(type=blup)
studentpanel(type=noblup));
*Method=RSPL for G-side, RMPL for R-side;
class WafID LotNo DieQuad;

model Pass =  LotNo WafID TotLayWithDefs RadDist DieQuad L1 L2 L3
L4 L5 L6 L7 L8 L9 L10/
dist=binomial link=logit solution;
random _residual_;
run;
ods graphics off;
ods html close;
```

Lot Random G

```
ods html;
ods graphics on;
proc glimmix data=sasuser.thirtywafersdielevel method=RsPL
plots=(residualpanel(type=noblup unpack)
residualpanel(type=blup)
studentpanel(type=noblup));
*Method=RSPL for G-side, RMPL for R-side;
class WafID LotNo DieQuad;
model Pass =  TotLayWithDefs RadDist DieQuad L1 L2 L3 L4 L5 L6 L7
L8 L9 L10/
dist=binomial link=probit solution ;
random int / subject = LotNo  g s;
run;
ods graphics off;
ods html close;
```

Lot Random with Overdispersion G

```
ods html;
ods graphics on;
proc glimmix data=sasuser.thirtywafersdielevel method=RsPL
plots=(residualpanel(type=noblup unpack)
residualpanel(type=blup)
studentpanel(type=noblup));
*Method=RSPL for G-side, RMPL for R-side;
class WafID LotNo DieQuad;
model Pass =  TotLayWithDefs RadDist DieQuad L1 L2 L3 L4 L5 L6 L7
L8 L9 L10/
dist=binomial link=cll solution ;
random int / subject = LotNo  g s;
random _residual_;
run;
ods graphics off;
ods html close;
```

Wafer(Lot) G

```
ods html;
ods graphics on;
proc glimmix data=sasuser.thirtywafersdielevel method=RsPL
plots=(residualpanel(type=noblup unpack)
residualpanel(type=blup)
studentpanel(type=noblup));
*Method=RSPL for G-side, RMPL for R-side;
class WafID LotNo DieQuad;
model Pass =  TotLayWithDefs RadDist DieQuad L1 L2 L3 L4 L5 L6 L7
L8 L9 L10/
dist=binomial link=logit solution ;
random int / subject =WafID(LotNo)  g s;
run;
ods graphics off;
ods html close;
```

Wafer(Lot) with Overdispersion G

```
ods html;
ods graphics on;
proc glimmix data=sasuser.thirtywafersdielevel method=RsPL
plots=(residualpanel(type=noblup unpack)
residualpanel(type=blup)
studentpanel(type=noblup));
*Method=RSPL for G-side, RMPL for R-side;
class WafID LotNo DieQuad;
model Pass =  TotLayWithDefs RadDist DieQuad L1 L2 L3 L4 L5 L6 L7
L8 L9 L10/
dist=binomial link=logit solution ;
random int / subject =WafID(LotNo)  g s;
random _residual_;
run;
ods graphics off;
ods html close;
```

Wafer G

```
ods html;
ods graphics on;
proc glimmix data=sasuser.thirtywafersdielevel method=RsPL
plots=(residualpanel(type=noblup unpack)
residualpanel(type=blup)
studentpanel(type=noblup));
*Method=RSPL for G-side, RMPL for R-side;
class WafID LotNo DieQuad;
model Pass =  TotLayWithDefs RadDist DieQuad L1 L2 L3 L4 L5 L6 L7
L8 L9 L10/
dist=binomial link=cll solution ;
random int / subject = WafID  g s;
run;
ods graphics off;
ods html close;
```

Wafer with Overdispersion G

```
ods html;
ods graphics on;
proc glimmix data=sasuser.thirtywafersdielevel method=RsPL
plots=(residualpanel(type=noblup unpack)
residualpanel(type=blup)
studentpanel(type=noblup));
*Method=RSPL for G-side, RMPL for R-side;
class WafID LotNo DieQuad;
model Pass =  TotLayWithDefs RadDist DieQuad L1 L2 L3 L4 L5 L6 L7
L8 L9 L10/
dist=binomial link=probit solution ;
random int / subject =WafID  g s;
random _residual_;
run;
ods graphics off;
ods html close;
```

Lot Random R

```
ods html;
ods graphics on;
proc glimmix data=sasuser.thirtywafersdielevel method=RmPL
plots=(residualpanel(type=noblup unpack)
residualpanel(type=blup)
studentpanel(type=noblup));
*Method=RSPL for G-side, RMPL for R-side;
class WafID LotNo DieQuad;
model Pass =   TotLayWithDefs RadDist DieQuad L1 L2 L3 L4 L5 L6
L7 L8 L9 L10/
dist=binomial link=logit solution ;
random _residual_ / sub=LotNo type=cs rside  cl s;
run;
ods graphics off;
ods html close;
```

Wafer(Lot) R

```
ods html;
ods graphics on;
proc glimmix data=sasuser.thirtywafersdielevel method=RmPL
plots=(residualpanel(type=noblup unpack)
residualpanel(type=blup)
studentpanel(type=noblup));
*Method=RSPL for G-side, RMPL for R-side;
class WafID LotNo DieQuad;
model Pass =   TotLayWithDefs RadDist DieQuad L1 L2 L3 L4 L5 L6
L7 L8 L9 L10/
dist=binomial link=logit solution ;
random _residual_ / sub=WafID(LotNo) type=cs rside  cl s;
run;
ods graphics off;
ods html close;
```

Wafer R

```
ods html;
ods graphics on;
proc glimmix data=sasuser.thirtywafersdielevel method=RmPL
plots=(residualpanel(type=noblup unpack)
residualpanel(type=blup)
studentpanel(type=noblup));
*Method=RSPL for G-side, RMPL for R-side;
class WafID LotNo DieQuad;
model Pass =   TotLayWithDefs RadDist DieQuad L1 L2 L3 L4 L5 L6
L7 L8 L9 L10/
dist=binomial link=logit solution ;
random _residual_ / sub=WafID type=cs rside  cl s;
run;
ods graphics off;
ods html close;
```

Wafer level

GLM

```
ods html;
ods graphics on;
proc glimmix data=waferleveltrainingdata310 method=RsPL
plots=(residualpanel(type=noblup unpack)
residualpanel(type=blup)
studentpanel(type=noblup));
class WafID LotNo;
PropPassed = PassingDice/DiceWithDef;
model PropPassed =  LotNo WafID TotLayWithDefs L1  L2 L3 L4 L5 l6
L7 L8 L9 L10/
dist=binomial link=probit solution ;
run;
ods graphics off;
ods html close;
```

Nested GLM

```
ods html;
ods graphics on;
proc glimmix data=waferleveltrainingdata310 method=RsPL
plots=(residualpanel(type=noblup unpack)
residualpanel(type=blup)
studentpanel(type=noblup));
class WafID LotNo;
PropPassed = PassingDice/DiceWithDef;
model PropPassed =  WafID(LotNo) TotLayWithDefs L1  L2 L3 L4 L5
l6 L7 L8 L9 L10/
dist=binomial link=logit solution ;
run;
ods graphics off;
ods html close;
```

GLM with OD:

```
ods html;
ods graphics on;
proc glimmix data=waferleveltrainingdata310 method=RsPL
plots=(residualpanel(type=noblup unpack)
residualpanel(type=blup)
studentpanel(type=noblup));
class WafID LotNo;
PropPassed = PassingDice/DiceWithDef;
model PropPassed =  LotNo WafID TotLayWithDefs L1  L2 L3 L4 L5 l6
L7 L8 L9 L10/
dist=binomial link=probit solution ;
random _residual_;
run;
ods graphics off;
ods html close;
```

Lot Random (G-side)

```
ods html;
ods graphics on;
proc glimmix data=waferleveltrainingdata310 method=RsPL
plots=(residualpanel(type=noblup unpack)
residualpanel(type=blup)
studentpanel(type=noblup));
class WafID LotNo;
PropPassed = PassingDice/DiceWithDef;
model PropPassed =   TotLayWithDefs L1  L2 L3 L4 L5 l6 L7 L8 L9
L10/
dist=binomial link=logit solution ;
random int / subject = LotNo g s;
run;
ods graphics off;
ods html close;
```

Lot Random (G-side) with Overdispersion

```
ods html;
ods graphics on;
proc glimmix data=waferleveltrainingdata310 method=RsPL
plots=(residualpanel(type=noblup unpack)
residualpanel(type=blup)
studentpanel(type=noblup));
class WafID LotNo;
PropPassed = PassingDice/DiceWithDef;
model PropPassed =   TotLayWithDefs L1  L2 L3 L4 L5 l6 L7 L8 L9
L10/
dist=binomial link=cll solution ;
random int / subject = LotNo g s;
random _residual_;
run;
ods graphics off;
ods html close;
```

Wafer(Lot) Random (G-side)

```
ods html;
ods graphics on;
proc glimmix data=waferleveltrainingdata310 method=RsPL
plots=(residualpanel(type=noblup unpack)
residualpanel(type=blup)
studentpanel(type=noblup));
class WafID LotNo;
PropPassed = PassingDice/DiceWithDef;
model PropPassed =   TotLayWithDefs L1  L2 L3 L4 L5 l6 L7 L8 L9
L10/
dist=binomial link=logit solution ;
random int / subject = WafID(LotNo) g s;
run;
ods graphics off;
ods html close;
```

Wafer(Lot) Random (G-side) with Overdispersion

```
ods html;
ods graphics on;
proc glimmix data=waferleveltrainingdata310 method=RsPL
plots=(residualpanel(type=noblup unpack)
residualpanel(type=blup)
studentpanel(type=noblup));
class WafID LotNo;
PropPassed = PassingDice/DiceWithDef;
model PropPassed =   TotLayWithDefs L1  L2 L3 L4 L5 l6 L7 L8 L9
L10/
dist=binomial link=logit solution ;
random int / subject = WafID(LotNo) g s;
random _residual_;
run;
ods graphics off;
ods html close;
```

Wafer Random (G-side)

```
ods html;
ods graphics on;
proc glimmix data=waferleveltrainingdata310 method=RsPL
plots=(residualpanel(type=noblup unpack)
residualpanel(type=blup)
studentpanel(type=noblup));
class WafID LotNo;
PropPassed = PassingDice/DiceWithDef;
model PropPassed =   TotLayWithDefs L1  L2 L3 L4 L5 l6 L7 L8 L9
L10/
dist=binomial link=logit solution ;
random int / subject = WafID g s;
run;
ods graphics off;
ods html close;
```

Wafer Random (G-side) with Overdispersion

```
ods html;
ods graphics on;
proc glimmix data=waferleveltrainingdata310 method=RsPL
plots=(residualpanel(type=noblup unpack)
residualpanel(type=blup)
studentpanel(type=noblup));
class WafID LotNo;
PropPassed = PassingDice/DiceWithDef;
model PropPassed =   TotLayWithDefs L1  L2 L3 L4 L5 l6 L7 L8 L9
L10/
dist=binomial link=logit solution ;
random int / subject = WafID g s;
random _residual_;
run;
ods graphics off;
ods html close;
```

Lot Random (R-side)

```
ods html;
ods graphics on;
proc glimmix data=waferleveltrainingdata310 method=RmPL
plots=(residualpanel(type=noblup unpack)
residualpanel(type=blup)
studentpanel(type=noblup));
class WafID LotNo;
PropPassed = PassingDice/DiceWithDef;
model PropPassed =   TotLayWithDefs L1  L2 L3 L4 L5 l6 L7 L8 L9
L10/
dist=binomial link=logit solution ;
random _residual_ / sub=LotNo type=cs rside  cl s;
run;
ods graphics off;
ods html close;
```

Wafer(Lot) Random (R-side)

```
ods html;
ods graphics on;
proc glimmix data=waferleveltrainingdata310 method=RmPL
plots=(residualpanel(type=noblup unpack)
residualpanel(type=blup)
studentpanel(type=noblup));
class WafID LotNo;
PropPassed = PassingDice/DiceWithDef;
model PropPassed =   TotLayWithDefs L1  L2 L3 L4 L5 l6 L7 L8 L9
L10/
dist=binomial link=logit solution ;
random _residual_ / sub=WAfID(LotNo) type=cs rside  cl s;
run;
ods graphics off;
ods html close;
```

Wafer Random (R-side)

```
ods html;
ods graphics on;
proc glimmix data=waferleveltrainingdata310 method=RmPL
plots=(residualpanel(type=noblup unpack)
residualpanel(type=blup)
studentpanel(type=noblup));
class WafID LotNo;
PropPassed = PassingDice/DiceWithDef;
model PropPassed =   TotLayWithDefs L1  L2 L3 L4 L5 l6 L7 L8 L9
L10/
dist=binomial link=cll solution ;
random _residual_ / sub=WAfID type=cs rside  cl s;
run;
ods graphics off;
ods html close;
```

SAS Code for Chapter 6

Die-Level Model with Fixed Effects and Terminal Nodes

```
ods html;
ods graphics on;
proc glimmix data=sasuser.cartdiedata method=RsPL
plots=(residualpanel(type=noblup unpack)
residualpanel(type=blup)
studentpanel(type=noblup));
*Method=RSPL for G-side, RMPL for R-side;
class WafID LotNo DieQuad;

model Pass1 =  TotalLayWithDefs RadDist DieQuad L1 L2 L3 L4 L5 L6
L7 L8 L9 L10
Tnode1 Tnode2 Tnode3 Tnode4 Tnode5 Tnode6 Tnode7 Tnode8 Tnode9
Tnode10 Tnode11 Tnode12 Tnode13 Tnode14
Tnode15 Tnode16 Tnode17 Tnode18 Tnode19 Tnode20 Tnode21 Tnode22
Tnode23 Tnode24 Tnode25
/ dist=binomial link=logit solution ddfm=kr;
run;
proc print data=glimmixout;
run;
ods graphics off;
ods html close;
```

Die-Level Full Model with Interactions from CART Tree 3

```
ods html;
ods graphics on;
proc glimmix data=sasuser.cartprobdiedata method=RsPL
plots=(residualpanel(type=noblup unpack)
residualpanel(type=blup)
studentpanel(type=noblup));
class WafID LotNo DieQuad;
model Pass1 =  TotalLayWithDefs RadDist  DieQuad L1 L2 L3 L4 L5
L6 L7 L8 L9 L10
 L1*L3 L4*L5 L4*L10 L10*L6 L6*RadDist  RadDist*DieQuad L1*L4
L1*L10 L10*RadDist L7*RadDist L7*DieQuad
/ dist=binomial link=logit solution ;

run;
ods graphics off;
ods html close;
```

Die-Level Reduced Model with Interactions from CART Tree 3

```
ods html;
ods graphics on;
proc glimmix data=sasuser.cartprobdiedata method=RsPL
plots=(residualpanel(type=noblup unpack)
residualpanel(type=blup)
studentpanel(type=noblup));
class WafID LotNo DieQuad;
model Pass1 =  TotalLayWithDefs RadDist  DieQuad L1 L2 L3 L4  L6
L7 L8 L9 L10
L1*L3 L4*L5 L4*L10 L6*RadDist RadDist*DieQuad L10*RadDist
L7*RadDist
/ dist=binomial link=logit solution ;

run;
ods graphics off;
ods html close;
```

Die-Level Model with All 2-way interactions

```
ods html;
ods graphics on;
proc glimmix data=sasuser.cartprobdiedata method=RsPL
plots=(residualpanel(type=noblup unpack)
residualpanel(type=blup)
studentpanel(type=noblup));
class WafID LotNo DieQuad;
model Pass1 =  TotalLayWithDefs RadDist  DieQuad L1 L2 L3 L4 L5
L6 L7 L8 L9 L10
L1*L2 L1*L3 L1*L4 L1*L5 L1*L6 L1*L7 L1*L8 L1*L9 L1*L10
L2*L3 L2*L4 L2*L5 L2*L6 L2*L7 L2*L8 L2*L9 L2*L10
L3*L4 L3*L5 L3*L6 L3*L7 L3*L8 L3*L9 L3*L10
L4*L5 L4*L6 L4*L7 L4*L8 L4*L9 L4*L10
L5*L6 L5*L7 L5*L8 L5*L9 L5*L10
L6*L7 L6*L8 L6*L9 L6*L10
L7*L8 L7*L9 L7*L10
L8*L9 L8*L10
L9*L10
RadDist*L1 RadDist*L2 RadDist*L3 RadDist*L4 RadDist*L5 RadDist*L6
RadDist*L7 RadDist*L8 RadDist*L9 RadDist*L10
DieQuad*RadDist DieQuad*L1 DieQuad*L2 DieQuad*L3 DieQuad*L4
DieQuad*L5 DieQuad*L6 DieQuad*L7 DieQuad*L8 DieQuad*L9
DieQuad*L10


/ dist=binomial link=logit solution ;

run;
ods graphics off;
ods html close;
```

Die-Level Reduced Model with Interactions

```
ods html;
ods graphics on;
proc glimmix data=sasuser.cartprobdiedata method=RsPL
plots=(residualpanel(type=noblup unpack)
residualpanel(type=blup)
studentpanel(type=noblup));
class WafID LotNo DieQuad;
model Pass1 =  TotalLayWithDefs RadDist  DieQuad L1 L2 L3 L4 L5
L6 L7  L9 L10
L1*L2 L1*L3 L1*L8 L2*L4 L2*L7 L2*L8 L2*L9 L2*L10 L4*L5 L4*L6
L4*L10 L5*L10 L7*L9 L7*L10 L9*L10
RadDist*L5 RadDist*L6 RadDist*L7 RadDist*L8 RadDist*L9
RadDist*L10 DieQuad*RadDist

/ dist=binomial link=logit solution ;


run;
ods graphics off;
ods html close;
```

BIOGRAPHICAL SKETCH

Dana Cheree Fritzemeier Krueger is a native of Stafford, KS. She earned her B.S. in chemical engineering from Kansas State University, Manhattan, KS in 1999 and worked for The Goodyear Tire & Rubber Co., Lincoln, NE for over five years as a development engineer for power transmission products. While with Goodyear, Mrs. Krueger was trained as a Six Sigma Black Belt, and she earned her M.S. in Industrial and Management Systems Engineering from the University of Nebraska – Lincoln in 2005 with an emphasis in engineering management. Her doctoral studies at Arizona State University, Tempe, AZ, focused on quality and reliability engineering. Mrs. Krueger is currently an instructor at Kansas State University in the Department of Management and resides with her husband and daughter in Manhattan, KS. Her research interests include applied statistics, designed experiments, and generalized linear models.

This document was generated using the Graduate College Format Advising tool. Please turn a copy of this page in when you submit your document to Graduate College format advising. You may discard this page once you have printed your final document. DO NOT TURN THIS PAGE IN WITH YOUR FINAL DOCUMENT!

181

181

181